2010

# Resistant-starch formation in high-amylose maize starch

Hongxin Jiang
*Iowa State University*, hxjiang@iastate.edu

**Resistant-starch formation in high-amylose maize starch**


By


**Hongxin Jiang**



A dissertation submitted to the graduate faculty

In partial fulfillment of the requirements for the degree of

DOCTOR OF PHILOSOPHY



Major: Food Science and Technology

Program of Study Committee:
Jay-lin Jane, Major Professor
Michael Blanco
Buddhi Lamsal
Paul Scott
Tong Wang



Iowa State University

Ames, Iowa

2010

# TABLE OF CONTENTS

v

## ABSTRACT

A new public high-amylose maize line, GEMS-0067, has been developed by USDA-ARS Germplasm Enhancement of Maize (GEM) Project. GEMS-0067 maize line is a homozygous mutant of *amylose-extender* (*ae*) gene and high-amylose modifier (HAM) gene(s). GEMS-0067 starches consist of 83.1-85.6% apparent amylose and 39.4%-43.2% resistant starch (RS), which are larger than the *ae* single-mutant starches (61.7-67.7% and 11.5%-19.1%, respectively) and normal maize starch (~30% and <1%, respectively). Maize *ae*-mutant starches consisted of spherical and elongated granules (up to 32%), which differed from normal maize starch, consisting of spherical and angular granules. The objectives of this study were to understand the mechanism of the RS formation in the maize *ae*-mutant starches, the crystalline structures of the maize *ae*-mutant starches, the formation of RS and elongated starch granules during the kernel development, and how dosage of the HAM gene(s) affected the structures and properties of endosperm starch of maize *ae*-mutant. We analyzed the structures and properties of the RS residues that remained after enzymatic hydrolysis of the maize *ae*-mutant starches at 95-100°C (AOAC method 991.43). The RS residues consisted of mainly partially hydrolyzed amylose and intermediate component (IC) and were more concentrated in the elongated starch granules and the outer layer of the spherical granules. The RS residues displayed the B-type polymorph and had gelatinization temperatures above 100°C. These results suggested that long-chain double-helical crystallites of amylose/IC were present in the native maize *ae*-mutant starches. The amylose/IC crystallites maintained the semi-crystalline structures at 95-100°C and were resistant to enzymatic hydrolysis at 95-100°C.

To understand the crystalline structures of the maize *ae*-mutant starches, we prepared Naegeli dextrins of the starches using sulfuric acid (15.3%, v/v) hydrolysis of the granular starch at 38°C for up to 102 days. The yields of the Naegeli dextrins ranged from 18.3 to 39.5%. The Naegeli dextrins displayed similar onset (45.1-51.4$^{o}$C), peak (113.9-122.2$^{o}$C), and conclusion (148.0-160.0$^{o}$C) gelatinization temperatures and had large enthalpy-changes (21.8-31.3 J/g) and percentage crystallinity (77.0-79.2%). The Naegeli dextrins showed unimodal molecular-size distributions with peak molecular-size at degree of polymerization (DP) 16. The molecular-size distributions of the Naegeli dextrins did not significantly change after debranching with isoamylase, indicating that the Naegeli dextrins are composed predominantly of linear molecules. The isoamylase-debranched Naegeli dextrins had average chain-lengths of DP 23.8-27.5 and large proportions of long chains (DP $\geq$ 25, 36.7-52.7%), resulting from hydrolysis of amylose double helices.

The RS contents and physicochemical properties of the *ae*-mutant maize (GEMS-0067) starches harvested at different kernel-developmental stages were analyzed. The RS content increased with kernel maturation and the increase in the amylose/IC content. The formation of long-chain double-helical crystallites of amylose/IC and the lipid content increased with kernel maturation and the increase in the amylose/IC content. These results suggested that the increase in the long-chain double-helical crystallites of amylose/IC and the increase in lipid content resulted in the increase in the RS content of the GEMS-0067 starch during the kernel development

The light and confocal laser-scanning micrographs of the physiologically mature GEMS-0067 starch granules showed that the arrangement of starch molecules varied between granules and within a granule. The transmission electron microscopic images of

GEMS-0067 endosperm tissues harvested at an early stage (20 days after pollination) of the kernel development showed that the elongated starch granules formed by fusion of small granules through amylose interaction in the amyloplast at the early stage of granule development.

To understand how dosage of the high-amylose modifier (HAM) gene affected the structures and properties of endosperm starch of maize *ae*-mutant, nine maize samples with HAM gene-dosage of 100%, 83.3%, 66.7%, 66.7%, 50%, 33.3%, 33.3%, 16.7%, and 0% were prepared in a generation-means analysis (GMA) study. An increase of HAM gene-dosage in maize *ae*-mutant resulted in higher amylose/IC content of the starch and significantly affected the molecular organization in the granule, granule morphology, starch crystallinity, and starch thermal properties. RS content of the starch was significantly correlated with HAM gene-dosage ($r = 0.81$, $P < 0.01$). The increase in HAM gene dosage in the endosperm of *ae*-mutant maize had little effect on the branch chain-length of the amylopectin and large molecular-weight IC but increased branch chain-length of the small molecular-weight IC. The HAM gene dosage also had little effect on the structure of amylose of the maize *ae*-mutant starch.

**GENERAL INTRODUCTION**

Starch, the second most abundant carbohydrate in nature next to cellulose, is synthesized in plant organs including seeds, stems, tubers, roots, leaves, and fruits. Starch is a large-producible, economical, and environmentally friendly ingredient for food and non-food applications, which serves as the major energy source in food and feed but also as a thickener, a binding agent, a texturizer, a filler, a film forming agent, and feedstock for fermentation to produce biomaterial and fuel. Normal starch consists of amylopectin and amylose molecules. Amylopectin consists of molecules of $\alpha1\rightarrow4$ linked D-glucopyranose units branch-linked by ~5% ($\alpha1\rightarrow6$) glycosidic bonds. Amylose molecules are primarily linear chains of ($\alpha1\rightarrow4$)-linked D-glucopyranose units; some amylose molecules possess a few branches. High-amylose maize starch also consists of intermediate component (IC) molecules, which have branched structures with molecular weights similar to amylose.

Starch is digested predominantly in the small intestine by digestive enzymes. A portion of starch, known as resistant starch (RS), resists enzymatic hydrolysis in the small intestine and passes to the large intestine for bacterial fermentation. RS provides many benefits to human health. When RS is used to replace rapidly digestible starch in food, it lowers the glycemic and insulin responses and reduces the risk for developing type II diabetes, obesity, and cardiovascular disease. RS lowers calorie content of foods and enhances lipid oxidation, which reduce body fat and impact body composition. Fermentation of RS in the colon promotes a healthy colon and reduces the risk of colon cancer.

RS is classified into five types. The type I RS is the physically inaccessible starch, resulting from starch granule entrapped in nondigestible plant tissue. The type II RS is raw starch granules such as potato, pea, or high-amylose maize starch, which has the B- or C-

type polymorphism. The type III RS is the retrograded amylose. The type IV RS is chemically modified starch. Type V RS is amylose-lipid complexed starch. RS can be readily applied in food products without changing of the qualities accepted by consumers as opposed to other dietary fibers such as cellulose, hemicelluloses, and lignin. The food industry has an increased interest in producing RS by enzymatic, chemical, and physical modifications of starch and plant breeding. In the past two decades, many methods have been developed to produce resistant starch. But all the RSs fall into the above five types.

A new line of high-amylose maize, GEMS-0067 (PI 643420), has been developed from the USDA-ARS Germplasm Enhancement of Maize (GEM) Project at Ames, IA, in collaboration with Truman State University in Kirksville, MO. The GEMS-0067 maize line is a homozygous mutant of amylose-extender (*ae*) and high-amylose modifier (HAM) gene(s). The maize *ae*-mutant is deficient in enzyme activity of SBEIIb in the endosperm, which results in starch having higher amylose content, larger amount of IC, and longer branch chain-length of amylopectin than normal maize starch. Preliminarily results showed that *sbeI* was part of HAM gene. The GEMS-0067 starches consist of 83.1-85.6% apparent-amylose, greater than the *ae* single-mutant starches of H99*ae*, OH43*ae*, B89*ae*, and B84*ae* (61.7-67.7%) and normal maize starch (~30%). The RS contents of the GEMS-0067 starches, determined using thermally stable α-amylase at 95-100 °C for 30 min (AOAC Method 991.43), are 39.4-43.2%, is much higher than that of the *ae* single-mutant starches (11.5-19.1%) and normal maize starch (< 1%). The GEMS-0067 starches consisted of up to 32% elongated starch granules, which were larger than *ae* single-mutant starches (~7%) and normal maize starch (0%). The objectives of this study were to understand the mechanism of the RS formation in the maize *ae*-mutant starches, the crystalline structures of the maize *ae*-

mutant starches, the formation of RS and elongated starch granules during the kernel

development of GEMS-0067 maize, and how dosage of the high-amylose modifier (HAM)

gene affected the structures and properties of endosperm starch of maize *ae*-mutant.

## DISSERTATION ORGANIZATION

This dissertation consists of six papers. This first paper, "Characterization of maize amylose-extender (*ae*) mutant starches: Part II. Structures and properties of starch properties of starch residues remaining after enzymatic hydrolysis at boiling-water temperature," has been published in the *Carbohydrate Polymers*. The second paper, "Characterization of maize amylose-extender (*ae*) mutant starches: Part III. Structures and properties of the Naegeli dextrins," has been accepted by the *Carbohydrate polymers*. The third paper, "Resistant-starch formation in high-amylose maize starch during kernel development," has been submitted to the *Journal of Agricultural and Food Chemistry*. The fourth paper, "Formation of elongated starch granules in high-amylose maize," has been published in the *Carbohydrate Polymers*. The fifth paper, "Variations in starch physicochemical properties from a generation-means analysis study using amylomaize V and VII parents," has been accepted by the *Journal of Agricultural and Food Chemistry*. The sixth paper, "Dosage effect of high-amylose modifier (HAM) gene on the starch structure of amylose-extender (*ae*) mutant maize," follows the format of the *Journal of Cereal Science* for submission to the *Journal of Cereal Science*. The six papers are preceded by a General Introduction and a Literature Review and followed by a General Conclusion and Acknowledgements. The Literature Cited in the Literature Review is listed in the alphabetical order of the first author's last name.

## LITERATURE REVIEW

**Structure of starch granule**

Starch is the second most abundant carbohydrate in nature next to cellulose. Native starch is in form of white and semi-crystalline granules, which are synthesized in chloroplasts or amyloplasts of plant organs including seeds, stems, tubers, roots, leaves, and fruits (Robyt, 1998). Starch has characteristic features varying in molecular structure, molecular organization of granule, morphological properties, gelatinization and pasting properties, starch polymorphs and percentage crystallinity, and enzyme digestibility (Jane, 2004).

*Molecular structure*

Normal starch consists of two polysaccharides: amylopectin and amylose. Amylopectin has a highly branched structure consisting of chains of ($\alpha$1, 4)-linked D-glucopyranose units, which are branch-linked by ~5% ($\alpha$1, 6) glycosidic bonds (French, 1984). Amylose is an essentially linear polymer of ($\alpha$1, 4)-linked D-glucopyranose units (Takeda et al., 1989a; Takeda et al., 1986; Takeda et al., 1993b). High-amylose maize starch also contains intermediate-component (IC) molecules, which have branched structures but molecular weights are smaller than amylopectin molecules and similar to amylose (Baba & Arai, 1984; Klucinec & Thompson, 1998; Li et al., 2008; Wang et al., 1993). The IC molecules display the iodine-binding capacity and $\beta$-amylolysis limit between amylopectin and amylose molecules (Kasemsuwan et al., 1995).

Normal starch consists of 15-30% amylose, depending on the botanical origin, degree of maturity, growing condition, and the method used for determination (Chung et al., 2009;

Hasjim et al., 2009; Jane et al., 1999; Jane et al., 1996; Li et al., 2007; Lu et al., 1996; Ono et al., 1998; Reddy & Seib, 1999; Srichuwong et al., 2005a, 2005b; Wang & Wang, 2001; Wu et al., 2007; Yoo et al., 2009). Waxy starch contains only amylopectin (Yoo & Jane, 2002b), whereas high-amylose starch usually consists of more than 50% amylose (Campbell et al., 2007; Li et al., 2008; Regina et al., 2006; Shi et al., 1998).

Amylose molecules can be separated from amylopectin using either gel-permeation chromatography (Jane & Chen, 1992; Li et al., 2008) or n-amyl alcohol fractionation (Kasemsuwan et al., 1995; Li et al., 2008; Schoch, 1942; Takeda et al., 1989a). Amylose molecules in high-amylose maize starch also can be separated from amylopectin and IC molecules using normal-butanol fractionation because the amylopectin and IC molecules cannot be precipitated with normal-butanol (Li et al., 2008). After amylopectin, IC, and amylose are isolated and purified, their characteristics have been analyzed using chemical, physical, and enzymatic methods.

The molecular-weights and gyration radii of amylopectins isolated from different starches vary from $7.0 \times 10^7$ to $5.7 \times 10^9$ g/mol and 191 to 782 nm, respectively (Yoo & Jane, 2002a). The amylopectin molecular-weights of waxy starches are substantially larger than that of the normal starch counterparts. The high-amylose maizes have smaller sizes of amylopectins than normal maize (Li et al., 2008; Yoo & Jane, 2002a). The average molecular-weights of IC molecules of high-amylose maize starches range from $1.5 \times 10^5$ to $10.4 \times 10^5$ g/mol (Li et al., 2008). The average molecular-sizes of amylose molecules vary between degrees of polymerization (DP) ~500 of high-amylose maize starch and DP ~6000 of potato starch (Jane, 2004).

Branch chains of amylopectin are designated as A, B, and C chains, which are arranged in clusters (Hizukuri, 1986). The A chains are chains whose reducing ends attach to B or C chains but do not carry any other chains. The B chains have reducing ends attached to B or C chains and also carry A or other B chains. The C chain possesses a reducing end and carries A or B chains. The A chains are generally short and extend within one cluster. The B chains are further classified into B1, B2, and B3 chains, extending through one, two, and three clusters, respectively (Hizukuri, 1986). Amylose molecules are essentially linear molecules (Takeda et al., 1989a; Takeda et al., 1989b)

*Organization of starch granule*

In normal starch, amylopectin and amylose molecules are synthesized side by side from the hilum (growth center) to the granule surface (Jane, 2007). The amylopectin and amylose molecules are organized in semi-crystalline structures of double helices, which comprise of crystalline and non-crystalline lamellas. The thickness of a crystalline and an amorphous lamella is 9-10 nm as determined using small angle X-ray scattering (Jenkins et al 1993). The branch chains of amylopectin molecules form double helices and contribute to the starch crystallinity. Amylose molecules in normal starch are in an amorphous form, which are interspersed and intertwined with amylopectin molecules because of the low concentration of amylose (Jane et al., 1992; Kasemsuwan & Jane, 1994). The entanglement between amylose molecules and amylopectin holds the integrity of starch granule (Debet & Gidley, 2007; Jane, 2006). The amylose molecules are more concentrated at the periphery of the granule. The starch molecules around the hilum are loosely packed (Gray & BeMiller, 2004; Huber & BeMiller, 2001; Jane & Shen, 1993; Li et al., 2007; Pan & Jane, 2000). The

amylopectin molecules at the center of the granule have greater proportions of the long B-chains than those at the periphery of the granule (Pan and Jane 2000).

Cereal starches contain approximately 0.2-1% lipids (Jiang et al., 2010b; Morrison, 1992, , 1993, , 1995; Morrison et al., 1993a). Amylose molecules can form amylose-lipid complex in the starch granules, which are not homogenously distributed in starch granule and are more concentrated at the periphery of the granule (Morrison et al., 1993a; Morrison et al., 1993b). This is in agreement with more amylose molecules being present at the periphery of the granule (Li et al., 2007; Jane and Shen, 1993). Two forms of amylose-lipid complex, amorphous and crystalline amylose-lipid complexes, have been reported (Biliaderis & Galloway, 1989; Biliaderis & Seneviratne, 1990; Tufvesson et al., 2003a, 2003b). Amorphous amylose-lipid complex has lower dissociation temperature (<100°C) than the crystalline amylose-lipid complex (> 100°C). The crystalline amylose-lipid complex displays a V-type X-ray diffraction pattern with $2\theta$ peaks at 8°, 13°, and 20° (Zobel, 1988; Zobel et al., 1967).

Although starch exists in various plant organs, all the starches have one of the three X-ray diffraction patterns for the packing of the double helices in the granules, designated as A-, B-, and C-types (Jane, 2004). The A-type polymorph has a monoclinic unit cell, and the B-type polymorph has a hexagonal unit cell (Buleon et al., 1998a; Wu & Sarko, 1978). The C-type polymorph has a combination of the A- and B-type polymorphs. The A polymorph is located essentially in the outer part of the granule of the C-type polymorph starch granule, whereas the B-type polymorph is found mostly at the center (Buleon et al., 1998b). The branch chain-length of amylopectin has been found to be a key factor in determining the crystalline polymorphs (Hizukuri et al., 1983). The B-type polymorph starches, such as

potato, amylomaize V, and amylomaize VII, consist of amylopectin molecules with long average branch-chain lengths. The A-type polymorph starches, such as normal maize, waxy maize, wheat, and barley, consist of amylopectin molecules with shorter average branch-chain lengths (Jane, 2004). It has been reported that the branch linkages of amylopectin in the B-type polymorph starch are mostly located in the amorphous region, whereas the branching points of amylopectin in the A-type polymorph starch are located in both amorphous and crystalline regions (Jane et al., 1997). The crystallinity of starch is due to the packing of the starch molecules in the granules, which also are affected by water content, temperature, and the presence of other solutes and solvents. The crystalline region is more resistant to acid and amylase hydrolyses than the amorphous region because of its stable double helical structure (Svensson & Eliasson, 1995).

**Starch gelatinization**

Starch gelatinization is an irreversible change from a semi-crystalline structure to an amorphous structure with the presence of sufficient water at high temperature, which is associated with the dissociation of the double helices, loss of birefringence when viewed under a polarized light, and disruption of granular structure (Jane, 2004). The gelatinization temperature and enthalpy change of starch are commonly measured using a differential scanning calorimeter (DSC). It is essential to have two times (by weight) or more water present with the starch to assure a reproducible gelatinization temperature. The gelatinization properties are affected by the starch structures and minor components present in the starch granules, which are determined by the botanical origin of starch (Jane, 2004). It has been reported that starch consisting of phosphate-monoester groups attached to the amylopectin

displays a lower gelatinization temperature because of the repulsion force between the negative charges of the phosphate-monoester groups (Jane et al., 1999). Starch consisting of a larger proportion of the short branch-chains (DP 6-12) of amylopectin shows a lower gelatinization temperature because the short branch-chains create more defects in the crystalline structure of the granule (Jane et al., 1997; Jane et al., 1999). It has been reported that the peak and the conclusion gelatinization-temperatures increase with the increase of the amylose content in the high-amylose maize starches (Li et al., 2008; Jiang et al., 2010a). This is attributed to the double-helical crystallites formed by the amylose molecules and the long branch-chains of amylopectin/IC.

**Biosynthesis of starch**

The building block of starch, glucose, is synthesized in the chloroplast of green plants by photosynthesis. Photosynthesis occurs in two stages: light and dark reactions (Robyt, 1998). The light reaction produces a source of reducing power (electrons) in the form of reduced nicotinamide adenine dinucleotide phosphate (NADPH) and a source of high energy in the form of adenosine triphosphate (ATP) molecules. The dark reaction of photosynthesis is the fixation of carbon dioxide to produce glucose, which is driven by the NADPH and ATP produced in the light reaction. The fixation of carbon dioxide is a cyclic process (Calvin Cycle) starting from ribulose 1, 5-diphosphate in $C_3$ plants, or with phosphoenol pyruvate in $C_4$ or tropical plants.

Glucose produced by photosynthesis is converted to sucrose and starch in leaves. In storage organs such as the potato tubers and the cereal endosperms, starch is synthesized

from sucrose transported from the leaves (James et al., 2003; Morell & Myers, 2005; Myers et al., 2000; Smith, 2001).

Starch molecules are cooperatively synthesized in the chloroplast or amyloplast by four classes of core enzymes including ADP-glucose pyrophosphorylase, starch synthases, starch-branching enzymes, and starch-debranching enzymes (James et al., 2003; Morell & Myers, 2005; Myers et al., 2000; Smith, 2001). Other enzymes including starch phosphorylases, disproportionating enzymes, and glucan-water dikinases also show minor functions in starch biosynthesis (James et al., 2003; Morell & Myers, 2005; Myers et al., 2000; Smith, 2001).

ADP-glucose pyrophosphorylase is a heterotetrameric enzyme consisting of two large and two small subunits, which synthesizes ADP-glucose from glucose-1-phosphate and ATP in the first committed step of the starch biosynthetic pathway. ADP-glucose is the substrate for starch synthases in elongation of starch chains. ADP-glucose pyrophosphorylase occurs both in the cytoplasm (85-95%) and inside the amyloplast of maize endosperm (Denyer et al., 1996). The maize mutants of *brittle 2* (*bt2*) and *shrunken 2* (*sh2*) contain around 25% of the starch of normal maize because they have less enzyme activity of ADP-glucose pyrophosphorylase in their endosperm tissues. The *bt2* maize contains reduced levels of the small subunits of the ADP-glucose pyrophosphorylase in the endosperm and *sh2* maize has reduced levels of the large subunits (James et al., 2003; Morell & Myers, 2005; Myers et al., 2000; Smith, 2001).

Starch synthases (SSs) utilize ADP-glucose to elongate the linear chains of amylose and amylopectin molecules by adding glucose units with α-1, 4 linkages. Cereal endosperms contain SSs including Granular-bound SSI (GBSSI), SSI, SSIIa, SSIII, and SSIV (Ball et al.,

1998; James et al., 2003; Morell & Myers, 2005; Smith, 2001; Smith et al., 2001). The

GBSSI is responsible for the biosynthesis of amylose molecules and extra-long chains of

amylopectin in cereal endosperms (Hanashiro et al., 2008; Yoo & Jane, 2002b). The enzyme

activity of GBSSI is missing in the endosperms of waxy maize, rice, sorghum, and wheat.

Lack of GBSSI enzyme activity has little effect on the yield of starch in waxy mutants. The

SSI, SSIIa, SSIII, and SSIV have been found to be responsible for the elongation of branch

chains of amylopectin molecules in cereal endosperms (Ball et al., 1998; James et al., 2003;

Morell & Myers, 2005; Smith, 2001; Smith et al., 2001; Zhang et al., 2004). The SSI is

involved in the biosynthesis of the branch chains of DP 6-11. The SSIIa is needed for the

biosynthesis of the branch chains of DP 12-25. The SSIII elongates the branch chains longer

than DP 25. The *sugary 2* (*su2*) maize starch is a result of the loss of the SSIIa enzyme

activity in the endosperm (Zhang et al., 2004). In the *su2* maize starch, the level of

amylopectin is reduced and the amylose level increases to ~35% (Jobling, 2004). The

amylopectin of *su2* maize starch contains more short branch-chains (DP 6-12) than

amylopectins of normal and waxy maize starches (Perera et al., 2001). The *dull1* (*du1*) gene

has been reported to encode the SSIII enzyme in the maize endosperm (Gao et al., 1998).

During starch biosynthesis, starch branching enzymes catalyze the formation of $\alpha$-1,6

branch-linkages between linear chains (James et al., 2003; Morell & Myers, 2005; Smith,

2001). In normal-maize endosperm, three isoforms of starch branching enzyme (SBEI,

SBEIIa, and SBEIIb) are involved in the biosynthesis of amylopectin. SBEIIa and SBEIIb

prefer to cleave and transfer shorter chains and catalyze the formation of $\alpha1\rightarrow6$ glycosidic

bonds *in vitro*, whereas SBEI prefers transferring longer chains (Guan & Preiss, 1993).

SBEIIb plays a major role in the biosynthesis of amylopectin molecules in maize endosperm

rather than SBEI and SBEIIa (James et al., 2003). Maize *amylose extender* (*ae*) mutant is deficient in enzyme activity of SBEIIb in the endosperm, which results in starch having higher amylose content, larger amount of IC, and longer branch chain-length of amylopectin than normal maize starch (Jane et al., 1999; Li et al., 2008; Shi & Seib, 1995; Yuan et al., 1993). Mutational analysis of SBEIIa gene in maize endosperm shows that loss of SBEIIa alone has no affect on the composition of endosperm starch and the fine structure of amylopectin (James et al 2003). The lack of SBEI enzyme activity in the endosperm of maize *sbeI* single-mutant has no or little impact on the starch structure (Blauth et al., 2001; Yao et al., 2004).

Starch debranching enzymes hydrolyze the $\alpha1$, 6 branch-linkages of amylopectin. Two starch debranching enzymes, isoamylase and pullulanase, have been identified in maize (James et al., 2003; Morell & Myers, 2005; Smith, 2001). The *sugary1* (*su1*) mutant of maize, a basis of sweet corn, shows the lack of isoamylase activity in the endosperm. The starch accumulation is low in the s*u1* mutant, but a highly branched phytoglycogen accumulates instead of the starch (James et al., 2003; Morell & Myers, 2005; Schultz & Juvik, 2004; Smith, 2001). The *zpu1* gene of maize encodes pullulanase in the endosperm (Beatty et al., 1999).

During the biosynthesis of amylopectin, it is known that the branch chains are elongated by SSs. Elongation of branch chains is in a radial order from the hilum to the granule surface. The elongated branch-chains are branched by starch branching enzymes. The debranching enzymes that hydrolyze $\alpha$-1, 6-branches are unable to debranch the branch linkages located inside the starch granule (Myers et al., 2000). The hydrolyzed molecules are used as substrates for SSs, and the biosynthetic processes continue to synthesize amylopectin.

The oligosaccharides produced from debranching reactions may also serve as the primer for the GBSSI to synthesize amylose (Ball et al., 1998).

**High-amylose maize**

Normal maize starch contains ~30% amylose (Hasjim et al., 2009). High-amylose maize starches with amylose contents of 50, 70, and 80% have been commercialized and designated as amylomaize V, VII, and VIII, respectively. High-amylose maize starch with 90% amylose also has been reported (Li et al., 2008; Shi et al., 1998). The development of high-amylose maize was initiated in the 1940s both at Purdue University, West Lafayette, IN and the Northern Regional Research Laboratory, ARS, USDA (BeMiller, 2009). The breakthrough of breeding the high-amylose maize is the discovery of maize *ae* mutant, which produces starch with ~50% apparent amylose (Kramer et al., 1958; Kramer et al., 1956; Vineyard et al., 1958a, 1958b). Hybrid *ae*-mutant maize possessing both high starch yield and amylose content was commercialized in 1958 and known as amylomaize V (BeMiller, 2009). In 1988, Stinard and Robertson reported a dominant *Amylose-extender* mutant (*Ae-5180*) in a mutator population, which produces starch with ~55% apparent-amylose content (Kasemsuwan et al., 1995).

Commercialized high-amylose maize starch with ~50% amylose is maize *ae* single-mutant starch. And the high-amylose maize starches with amylose contents of 70, 80, and 90% are results of high-amylose modifier (HAM) genes in the maize *ae*-mutants. Sidebottom et al (1998) reported that the amylomaize VII starch contained ~70% amylose content, which could the result of loss of SBEI enzyme activity in addition to the *ae* mutation. A low amylopectin starch has been reported to have an even higher amylose level than amylomaize

VII starch because of an additional loss of SBEIIa enzyme activity (Sidebottom et al., 1998).

A new public USDA line of high-amylose maize, GEMS-0067, has been developed by M.

Campbell at Truman State University nursery in Kirksville, MO, working cooperatively with

the USDA-ARS Germplasm Enhancement of Maize (GEM) project in Ames, IA (Campbell

et al., 2007). GEMS-0067 maize line is a homozygous mutant of the recessive *ae* gene and

HAM gene(s) (Campbell et al., 2007; Wu et al., 2009). Preliminary results showed that the

*sbeI* might be partial or exclusive HAM gene (Campbell et al., 2007). The GEMS-0067

starches have greater apparent-amylose contents (83.1-85.6%) than maize *ae* single-mutant

starches (61.7-67.7%) (Li et al., 2008). Lightner et al. (1999) reported that maize *ae* mutants

could have amylose levels elevated to 90% when they were genetically transformed with

antisense constructs for SBEI.

The structures of maize *ae*-mutant starches have been widely studied (Baba & Arai,

1984; Baba et al., 1982; Jane et al., 1999; Jiang et al., 2010b; Jiang et al., 2010c; Li et al.,

2008; Shi & Seib, 1995; Takeda et al., 1989a; Takeda et al., 1993a; Wang et al., 1993; Yuan

et al., 1993). Maize *ae*-mutant starches have higher apparent and absolute amylose contents,

larger amount of IC, and longer branch chain-length of amylopectin than normal maize starch.

The IC of maize *ae* single-mutant starch has average molecular-sizes DP 250-300, with four

or five branches and average chain lengths of DP ~50 (Baba and Arai, 1984). After

introducing the HAM gene to the maize *ae*-mutant, the starch has higher apparent and

absolute amylose content and longer branch chain-length of IC molecules but shorter branch

chain-length of amylopectin molecules than maize *ae* single-mutant starch (Li et al., 2008).

The apparent-amylose content of the starch is measured on the basis of iodine bound to the

starch molecules. The long branch-chains of the amylopectin and IC molecules also bind

iodine. Thus, the apparent-amylose content of the maize *ae*-mutant starch is substantially

larger than the absolute amylose content, in which the iodine bound by amylopectin and IC is

subtracted from the total iodine bound by the starch (Jane et al., 1999).

Maize *ae*-mutant starches display the B-type X-ray diffraction pattern (Li et al., 2008;

Shi et al., 1998), which differs from the normal and waxy maize starches (A-type) (Jane et al.,

1997). It has been reported that the B-type polymorph in maize *ae*-mutant starches is a result

of the long branch-chains of the amylopectin (Hizukuri et al., 1983; Jane et al., 1999).

Studies have shown that starch with a larger amylose content has less susceptibility to

enzyme hydrolysis (Jane et al., 2003; Li et al., 2008). Maize *ae*-mutant starches have high

conclusion gelatinization-temperatures (100.5-130°C), which increase with amylose contents

of the starches (Li et al., 2008; Shi et al., 1998).

Maize endosperm is a triploid tissue resulting from fusion of two maternal nuclei and

one paternal nucleus during fertilization (Birchler, 1993). Increasing doses of the recessive *ae*

allele proportionally decrease the enzyme activity of SBEIIb (Hedman & Boyer, 1982).

Although an increase in amylose content has been reported in *Aeaeae* when compared to

*AeAeAe* endosperm genotypes (Fergason et al., 1966), there is no significant difference

between *AeAeAe* and *AeAeae*.


**Starch digestion and resistant starch**

Hydrolysis of starch to glucose is important for plant and animal growth and ethanol

production. The digestion of starch occurs partially in the mouth and predominantly in the

small intestine where pancreatic α-amylase is released and dextrinase, amyloglucosidase, α-

glucosidase, and maltase are embedded in the brush border of the intestinal wall (Sang &

Seib, 2006). In general, starch in food is consumed after the food is processed. Starch is

gelatinized at a temperature above the gelatinization temperature of the starch and in the

presence of excess water during processing. The enzymatic hydrolysis of gelatinized starch

molecules is much faster than that of raw starch granules (Tester et al., 2006). High branch

densities of amylopectin and great degrees of chemical modification to the starch molecules

have been reported to reduce the enzymatic hydrolysis of the gelatinized starch molecules.

Enzymes of different sources display different hydrolysis rates of gelatinized starch

molecules (Han & BeMiller, 2007; He et al., 2008; Robyt & French, 1967; Zhang et al.,

2008).

The enzymatic hydrolysis of raw starch granules is a complex process, including the

binding of the enzyme to the starch granule and hydrolysis (Lehmann & Robin, 2007). A

number of factors have been reported to impact the enzymatic hydrolysis of the raw starch

granules, which include the granular size, the polymorphism, the structure of the amylopectin,

the amylose content, the lipid content, the surface feature, and the sources of the enzymes.

These factors relate to the botanical origins of the starch granules, which determine the starch

granule structures (Lehmann & Robin, 2007; Tester et al., 2006). Larger starch granules are

generally digested at a slower rate than smaller starch granules because of the smaller relative

surface area of the larger starch granules for the enzymatic hydrolysis (Tester et al., 2006).

The A-type polymorph starches, such as normal and waxy maize starches, are more

easily hydrolyzed by enzymes than the B- and C-type polymorph starches, such as potato,

green banana, and high-amylose maize starches (Jane et al., 2003). This difference is

attributed to the chain lengths of the branch-chain double helices and the packing of the

double helices in the starch granules. The longer chains of B-type polymorph starch form

longer and more stable double helices when compared with the A-type polymorph starch (Jane et al., 1999). Shorter double helices of the A-type polymorph starch granules are more readily digestible compared to the B-type starch granules. The branching linkages of the amylopectin in the A-type polymorph starches are scattered in both the amorphous and crystalline regions, whereas those of the B-type polymorph starches are mostly in the amorphous region (Jane et al., 1997). The amylopectin of the A-type polymorph starch has a larger proportion of branch chains of DP 6-12 than that of B-type polymorph starch (Jane et al., 1999). Thus, the packing of the double helices in the A-type polymorph starch granules generates weak points in the crystalline region, which are susceptible for the enzymatic hydrolysis. The A-type polymorph starch granules contain peripheral pores and channels resulting from the endogenous amylase hydrolysis (Fannon et al., 1993; Jane et al., 2003; Li et al., 2007), which increase the surface area of the starch granules and facilitate enzymatic hydrolysis of the starch molecules. The A-type polymorph starch granules have more voids than that of the B-type counterparts that have homogenous internal structure (Jane, 2006; Jane, 2007), which results in the A-type polymorph starch granules more susceptible for the enzymatic hydrolysis. The A-type polymorph starch granules are digested from the surface to the hilum and have many pin holes after digestion. Amylase then can hydrolyze starch granules from the inside out. B-type polymorph starch granules are digested by erosion of starch granules starting from the surface (Robyt, 1998).

The increase in amylose content in the starch granules decreases the enzymatic digestibility of the starch granules (Jane, 2006; Jane, 2007; Li et al., 2008). This could be attributed to the amylose molecules interacting with amylopectin, which restricts the starch swelling and reduces the enzyme's accessibility to hydrolyze starch molecules (Case et al.,

1998; Jiang et al., 2010b; Shi et al., 1998). Lipids present in the starch granules also retard the enzymatic hydrolysis (Jiang et al., 2010b). This could be attributed to the amylose-lipid complex, which is resistant to amylase hydrolysis (Jane & Robyt, 1984), restricts starch swelling and then reduces the enzymatic hydrolysis of the starch granules (Morrison, 2000; Morrison et al., 1993c). The lipids present on the surface of the granules may result in less accessibility of the enzyme to the starch molecules (Morrison, 1981, 1995).

Starch has different physiological effects to human health depending on its rate and extent of digestion. Resistant starch (RS) resists human digestive enzymes and passes to the large intestine as a prebiotic for bacterial fermentation (Englyst & Cummings, 1985; Englyst & Macfarlane, 1986). RS provides many health benefits, including reductions in glycemic and insulin responses, colon cancer, type II diabetes, obesity, and cardiovascular diseases (Behall et al., 2006a; Behall et al., 2006b; Dronamraju et al., 2009; Robertson et al., 2005; Robertson et al., 2003; Van Munster et al., 1994; Zhang et al., 2007).

On the basis of mechanisms of RS formation, five types of RS have been proposed (Englyst et al., 1992; Jane et al., 2009; Sang et al., 2007; Woo & Seib, 2002). Type 1 RS is starch entrapped in cell wall, protein, and other materials. Type 2 RS is uncooked potato, pea, green banana, or high-amylose maize starch, which has the B- or C-type polymorph. Type 3 RS is the retrograded amylose, which has semi-crystalline structures with a melting temperature above 120°C and is resistant to most food processing. Type 4 RS is starch modified chemically by esterifications of starch granules using acetic anhydride, propylene oxide, or octenyl succinic anhydride and by crosslinking of starch granules with sodium trimetaphosphae, phosphous oxychoride, or citric acid. The hydrophobic groups attached to starch molecules increase the water insolubility of the starch granules and decrease the

accessibility of the enzymes to the starch molecules, and also prevent the starch molecules from being bound by enzymes. Type 5 RS is amylose-lipid complexed starch. The amylose-lipid complex has a high dissociation temperature and restricts starch granules swelling, which is stable to most food processing. The amylose-lipid complex is resistant to amylase hydrolysis (Jane & Robyt, 1984).

Many methods, including Englyst's method (Englyst et al., 1992), AOAC 2002.02/AACC 32-40 method, and AOAC method 991.43, have been used for analyzing RS contents of different food products or raw materials. For human consumption, starch is usually cooked. Thus, starch residues that can't be hydrolyzed by thermally stable α-amylase at 95-100°C for 30 min and subsequent glucoamylase hydrolysis (AOAC method 991.43) are true RS according to the AACC Dietary Fiber Definition Committee Report (AACC, 2001). High-amylose maize starches consist of a large proportion of RS (11.5-43.2%) determined using AOAC method 991.43 for total dietary fiber (Li et al., 2008; Shi et al., 1998; Shi & Jeffcoat, 2001).

RS can be readily applied in food products without changing the qualities acceptable by consumers when compared to other dietary fibers such as cellulose, hemicelluloses, and lignin. The food industry has an increased interest in producing RS by enzymatic, chemical, and physical modifications of starch and modifications made by plant breeding. In the past two decades, many methods have been developed to produce resistant starch. But all the RSs fall into the above five types of RS.

**Roles of starch structures on the RS content of native high-amylose maize starch**

Although high-amylose maize starch has been selectively bred for about 60 years, the interest for RS in high-amylose maize starches has recently attracted the attention of the consumers in the past two decades because of the healthy eating trend. Because high-amylose maize starches are highly resistant to enzymatic hydrolysis and consist of large proportions of RS, the structure and properties of the starches and their RS residues have been widely studied in order to understand the mechanism of the RS formation in the starches (Evans & Thompson, 2004; Jiang et al., 2010a; Jiang et al., 2010b; Li et al., 2008; Shi et al., 1998; Shi & Jeffcoat, 2001).

It has been proposed that both molecular structures and molecular organization of the starch molecules in high-amylose maize starch granules contribute to the resistance of starch molecules to pancreatic α-amylase hydrolysis at 37°C (Evans & Thompson, 2004; Shi & Jeffcoat, 2001). This is evidenced by broad molecular-weight distributions of the RS residues obtained after pancreatic α-amylase hydrolysis of high-amylose maize starches at 37°C and by the branch chain-length profiles of the RS residues similar to the native high-amylose maize starches.

Li et al. (2008) characterized high-amylose maize starches including GEMS-0067 and *ae* single-mutants of H99*ae*, OH43*ae*, B89*ae*, and B84*ae*. GEMS-0067 starches have larger RS contents (39.4-43.2%) than maize *ae* single-mutant starches (11.5-19.1%), determined using thermally stable α-amylase at 95-100°C (AOAC method 991.43). The RS content is negatively correlated with amylopectin content of the maize *ae*-mutant starch, indicating that amylopectin has no or little contributions to the RS formation in the maize *ae*-mutant starches. Li et al. (2008) also observed that the GEMS-0067 starches contain 36.1-45.0% IC higher than most of the *ae* single-mutant starches (22.4-27.0 %) except OH43*ae* starch

(52.0 %) (Li et al., 2008). Li et al. (2008) further separated the IC molecules into large

molecular-weight IC and small molecular-weight IC using Sepharose CL-2B gel-permeation

chromatography. The average branch-chain lengths of the small molecular-weight IC

molecules (DP 38.7-50.6) are longer than that of large molecular-weight IC (DP 31.6-38.5)

and amylopectin molecules (DP 32.0-37.6) (Li et al., 2008). The RS content of the maize *ae*-

mutant starch increases with the increase in amylose/IC content. These findings suggested

that the amylose/IC molecules contributed to the RS formation in the starch. The conclusion

gelatinization-temperatures of the maize *ae*-mutant starches were between 100.5 and 130°C.

Thus, Li et al. (2008) proposed that the semi-crystalline structures of the maize *ae*-mutant

starch were retained after enzymatic hydrolysis at 95-100°C.

**Elongated starch granules in high-amylose maize**

Starch granules vary in shape, size, and submicroscopic structure. The sizes of

normal-maize starch granules range between 5 and 20 μm. High-amylose maize starches

have even a narrower size range: 4 to 18 microns (Hegenbart 1996). Normal-maize starch

contains starch granules with spherical and angular shapes (Perera et al., 2001;

Wongsagonsup et al., 2008). High-amylose maize (*ae*-mutant) starches consist of mainly

spherical granules and elongated granules that include the shapes rod, filament, triangle,

socks, etc (Boyer et al., 1976; Jiang et al., 2010b; Mercier et al., 1970; Shi & Jeffcoat, 2001;

Sidebottom et al., 1998; Wolf et al., 1964). The elongated starch granules mainly locate in

the center part of the kernel of *ae*-mutant maize (Boyer et al., 1976).

Amylopectin and amylose are organized into semi-crystalline structure of double

helices. Thus, the birefringence pattern of a starch granule when viewed under a polarized

light reflects the arrangement of starch molecules in the starch granule (French, 1984).

Normal-maize starch granules display a typical birefringence pattern showing a Maltese-cross (Wongsagonsup et al., 2008), reflecting the fact that the starch molecules are aligned in a radial order centered at the hilum and are perpendicular to the granule surface. The center of the Maltese-cross is the hilum where biosynthesis of the starch granule initiates (Jane, 2004). Most spherical granules of high-amylose maize starch exhibit bright Maltese-crosses (Wolf et al., 1964), which are consistent with the confocal laser-scanning microscope (CLSM) images of the 8-amino-1,3,6-pyrenetrisulfonic acid (APTS)-stained spherical granules showing bright color around one hilum (Glaring et al., 2006). These findings indicate that the spherical granule is developed from one single granule. The elongated starch granules display three types of birefringence pattern (Wolf et al, 1964). The type 1 birefringence pattern displays several Maltese-crosses overlapping in one granule. The type 2 birefringence pattern shows combinations of one or more Maltese-crosses and weak to no birefringence on other parts of the granule. And the type 3 birefringence pattern exhibits no birefringence or only weak birefringence along the edge of the elongated granules. The different birefringence patterns of the elongated starch granules indicate that the arrangement of starch molecules varies between elongated granules and within an elongated granule, which is consistent with CLSM images of the APTS-stained elongated granules revealing multiple regions with different intensities of fluorescence in one elongated granule (Glaring et al., 2006).

**References**

Baba, T., & Arai, Y. (1984). Structural features of amylomaize Starch .3. Structural

characterization of amylopectin and intermediate material in amylomaize starch granules. *Agricultural and Biological Chemistry, 48*, 1763-1775.

Baba, T., Arai, Y., Yamamoto, T., & Itoh, T. (1982). Some structural features of amylomaize starch. *Phytochemistry, 21*, 2291-2296.

Ball, S. G., van de Wal, M. H. B. J., & Visser, R. G. F. (1998). Progress in understanding the biosynthesis of amylose. *Trends in Plant Science, 3*, 462-467.

Beatty, M. K., Rahman, A., Cao, H., Woodman, W., Lee, M., Myers, A. M., & James, M. G. (1999). Purification and molecular genetic characterization of ZPU1, a pullulanase-type starch-debranching enzyme from maize. *Plant Physiology, 119*, 255-266.

Behall, K. M., Scholfield, D. J., & Hallfrisch, J. G. (2006a). Barley [beta]-glucan reduces plasma glucose and insulin responses compared with resistant starch in men. *Nutrition Research, 26*, 644-650.

Behall, K. M., Scholfield, D. J., Hallfrisch, J. G., & Liljeberg-Elmstaahl, H. G. M. (2006b). Consumption of both resistant starch and beta -glucan improves postprandial plasma glucose and insulin in women. *Diabetes Care, 29*, 976-981.

BeMiller, J. N. (2009). One hundred years of commercial food carbohydrates in the United States. *Journal of Agricultural and Food Chemistry, 57*, 8125-8129.

Biliaderis, C. G., & Galloway, G. (1989). Crystallization behavior of amylose-V complexes: structure-property relationships. *Carbohydrate Research, 189*, 31-48.

Biliaderis, C. G., & Seneviratne, H. D. (1990). Solute effects on the thermal stability of glyceryl monostearate-amylose complex superstructures. *Carbohydrate Research, 208*, 199-213.

Birchler, J. A. (1993). Dosage analysis of maize endosperm development. *Annual Review of Genetics, 27*, 181-204.

Blauth, S. L., Kim, K., Klucinec, J. D., Shannon, J. C., Thompson, D. B., & Guiltnan, M. J. (2001). Identification of Mutator insertional mutants of starch-branching enzyme 1 (sbe1) in Zea mays L. *Plant Molecular Biology, 48*, 287-297.

Boyer, C. D., Daniels, R. R., & Shannon, J. C. (1976). Abnormal starch granule formation in Zea-Mays-L endosperms possessing amylose-extender mutant. *Crop Science, 16*, 298-301.

Buleon, A., Colonna, P., Planchot, V., & Ball, S. (1998a). Starch granules: structure and biosynthesis. *International Journal of Biological Macromolecules, 23*, 85-112.

Buleon, A., Gerard, C., Riekel, C., Vuong, R., & Chanzy, H. (1998b). Details of the Crystalline Ultrastructure of C-Starch Granules Revealed by Synchrotron Microfocus Mapping. *Macromolecules, 31*, 6605-6610.

Campbell, M. R., Jane, J., Pollak, L., Blanco, M., & O'Brien, A. (2007). Registration of maize germplasm line GEMS-0067. *Journal of Plant Registrations, 1*, 60-61.

Case, S. E., Capitani, T., Whaley, J. K., Shi, Y. C., Trzasko, P., Jeffcoat, R., & Goldfarb, H. B. (1998). Physical Properties and Gelation Behavior of a Low-Amylopectin Maize Starch and Other High-Amylose Maize Starches. *Journal of Cereal Science, 27*, 301-314.

Chung, H.-J., Liu, Q., & Hoover, R. (2009). Impact of annealing and heat-moisture treatment on rapidly digestible, slowly digestible and resistant starch levels in native and gelatinized corn, pea and lentil starches. *Carbohydrate Polymers, 75*, 436-447.

Debet, M. R., & Gidley, M. J. (2007). Why do gelatinized starch granules not dissolve

completely? Roles for amylose, protein, and lipid in granule "ghost" integrity. *Journal of Agricultural and Food Chemistry, 55*, 4752-4760.

Denyer, K., Dunlap, F., Thorbjornsen, T., Keeling, P., & Smith, A. M. (1996). The major form of ADP-glucose pyrophosphorylase in maize endosperm is extra-plastidial. *Plant Physiology, 112*, 779-785.

Dronamraju, S. S., Coxhead, J. M., Kelly, S. B., Burn, J., & Mathers, J. C. (2009). Cell kinetics and gene expression changes in colorectal cancer patients given resistant starch: a randomised controlled trial. *Gut, 58*, 413-420.

Englyst, H. N., & Cummings, J. H. (1985). Digestion of the polysaccharides of some cereal food in the human small intestine. *American Journal of Clinical Nutrition, 42*, 778-787.

Englyst, H. N., Kingman, S. M., & Cummings, J. H. (1992). Classification and measurement of nutritionally important starch fractions. *European Journal of Clinical Nutrition, 46 Suppl 2*, S33-50.

Englyst, H. N., & Macfarlane, G. T. (1986). Breakdown of resistant and readily digestible starch by human gut bacteria. *Journal of the Science of Food and Agriculture, 37*, 699-706.

Evans, A., & Thompson, D. B. (2004). Resistance to a-amylase digestion in four native high-amylose maize starches. *Cereal Chemistry, 81*, 31-37.

Fannon, J. E., Shull, J. M., & Bemiller, J. N. (1993). Interior Channels of Starch Granules. *Cereal Chemistry, 70*, 611-613.

French, D. (1984). Organization of starch granules. In R. L. Whistler, J. N. BeMiller, & E.

F. Paschall. *Starch: Chemistry and Technology,* pp. 183-247). New York: Academic Press.

Gao, M., Wanat, J., Stinard, P. S., James, M. G., & Myers, A. M. (1998). Characterization of dull1, a maize gene coding for a novel starch synthase. *Plant Cell, 10*, 399-412.

Gray, J. A., & BeMiller, J. N. (2004). Development and utilization of reflectance confocal laser scanning microscopy to locate reaction sites in modified starch granules. *Cereal Chemistry, 81*, 278-286.

Guan, H. P., & Preiss, J. (1993). Differentiation of the properties of the branching isoenzymes from maize (Zea mays). *Plant Physiology, 102*, 1269-1273.

Han, J.-A., & BeMiller, J. N. (2007). Preparation and physical characteristics of slowly digesting modified food starches. *Carbohydrate Polymers, 67*, 366-374.

Hanashiro, I., Itoh, K., Kuratomi, Y., Yamazaki, M., Igarashi, T., Matsugasako, J.-i., & Takeda, Y. (2008). Granule-bound starch synthase I is responsible for biosynthesis of extra-long unit chains of amylopectin in rice. *Plant and Cell Physiology, 49*, 925-933.

Hasjim, J., Srichuwong, S., Scott, M. P., & Jane, J.-l. (2009). Kernel composition, starch structure, and enzyme digestibility of opaque-2 maize and quality protein maize. *Journal of Agricultural and Food Chemistry, 57*, 2049-2055.

He, J., Liu, J., & Zhang, G. (2008). Slowly digestible waxy maize starch prepared by octenyl succinic anhydride esterification and heat-moisture treatment: Glycemic response and mechanism. *Biomacromolecules, 9*, 175-184.

Hedman, K. D., & Boyer, C. D. (1982). Gene dosage at the amylose-extender locus of

maize: Effects on the levels of starch branching enzymes. *Biochemical genetics, 20*, 483-492.

Hizukuri, S. (1986). Polymodal distribution of the chain lengths of amylopectins and its significance. *Cabohydrate Research, 147*, 342.

Hizukuri, S., Kaneko, T., & Takeda, Y. (1983). Measurement of the chain-length of amylopectin and its relevance to the origin of crystalline polymorphism of starch granules. *Biochimica et Biophysica Acta, 760*, 188-191.

Huber, K. C., & BeMiller, J. N. (2001). Location of sites of reaction within starch granules. *Cereal Chemistry, 78*, 173-180.

James, M. G., Denyer, K., & Myers, A. M. (2003). Starch synthesis in the cereal endosperm. *Current Opinion in Plant Biology, 6*, 215-222.

Jane, J.-l. (2004). Starch: structure and properties. In P. Tomasik. *Chemical and Functional Properties of Food Saccharides* pp. 81-101). New York: CRC Press.

Jane, J.-l. (2006). Current understanding on starch granule structures. *Journal of Applied Glycoscience, 53*, 205-213.

Jane, J.-l., Ao, Z., Duvick, S. A., Wiklund, M., Yoo, S.-H., Wong, K.-S., & Gardner, C. (2003). Structures of amylopectin and starch granules: How are they synthesized? *Journal of Applied Glycoscience, 50*, 167-172.

Jane, J.-L., Hasjim, J., Birt, D., & Zhao, Y. (2009). Resistant food starches and methods related thereto. (p. 29pp). Application: WO. Iowa State University Research Foundation, USA.

Jane, J.-l., Wong, K.-s., & McPherson, A. E. (1997). Branch-structure difference in

starches of A- and B-type x-ray patterns revealed by their Naegeli dextrins.
*Carbohydrate Research, 300*, 219-227.

Jane, J. (2007). Structure of starch granules. *The Japanese Society of Applied Glycoscience, 54*, 31-36.

Jane, J., Chen, Y. Y., Lee, L. F., McPherson, A. E., Wong, K. S., Radosavljevic, M., & Kasemsuwan, T. (1999). Effects of amylopectin branch chain length and amylose content on the gelatinization and pasting properties of starch. *Cereal Chemistry, 76*, 629-637.

Jane, J., Kasemsuwan, T., Chen, J. F., & Juliano, B. O. (1996). Phosphorus in rice and other starches. *Cereal Foods World, 41*, 827-832.

Jane, J., Xu, A., Radosavljevic, M., & Seib, P. A. (1992). Location of amylose in normal starch granules. I. Susceptibility of amylose and amylopectin to cross-linking reagents. *Cereal Chemistry, 69*, 405-409.

Jane, J. L., & Chen, J. F. (1992). Effect of amylose molecular size and amylopectin branch chain length on paste properties of starch. *Cereal Chemistry, 69*, 60-65.

Jane, J. L., & Robyt, J. F. (1984). Structure studies of amylose-V complexes and retrograded amylose by action of alpha amylases, and a new method for preparing amylodextrins. *Carbohydrate Research, 132*, 105-118.

Jane, J. L., & Shen, J. J. (1993). Internal structure of the potato starch granule revealed by chemical gelatinization. *Carbohydrate Research, 247*, 279-290.

Jiang, H., Campbell, M., Blanco, M., & Jane, J.-l. (2010b). Characterization of maize

amylose-extender (ae) mutant starches. Part II: Structures and properties of starch residues remaining after enzymatic hydrolysis at boiling-water temperature. *Carbohydrate Polymers*, 80(1), 1-12.

Jiang, H., Horner, H. T., Pepper, T. M., Blanco, M., Campbell, M., & Jane, J. (2010c). Formation of elongated starch granules in high-amylose maize. *Carbohydrate Polymers*, 80(2), 534-539.

Jobling, S. (2004). Improving starch for food and industrial applications. *Current Opinion in Plant Biology, 7*, 210-218.

Kasemsuwan, T., & Jane, J. (1994). Location of amylose in normal starch granules. II. Locations of phosphodiester crosslinking revealed by phosphorus-31 nuclear magnetic resonance. *Cereal Chemistry, 71*, 282-287.

Kasemsuwan, T., Jane, J., Schnable, P., Stinard, P., & Robertson, D. (1995). Characterization of the dominant mutant amylose-extender (Ae1-5180) maize starch. *Cereal Chemistry, 72*, 457-464.

Klucinec, J. D., & Thompson, D. B. (1998). Fractionation of high-amylose maize starches by differential alcohol precipitation and chromatography of the fractions. *Cereal Chemistry, 75*, 887-896.

Kramer, H. H., Bear, R. P., & Zuber, M. S. (1958). Designation of high amylose gene loci in maize. *Agronomy Journal, 50*, 229.

Kramer, H. H., Whistler, R. L., & Anderson, E. G. (1956). A new gene interaction in the endosperm of maize. *Agronomy Journal, 48*, 170-172.

Lehmann, U., & Robin, F. (2007). Slowly digestible starch - its structure and health implications: a review. *Trends in Food Science & Technology, 18*, 346-355.

Li, L., Blanco, M., & Jane, J.-l. (2007). Physicochemical properties of endosperm and pericarp starches during maize development. *Carbohydrate Polymers, 67*, 630-639.

Li, L., Jiang, H., Campbell, M., Blanco, M., & Jane, J.-l. (2008). Characterization of maize amylose-extender (ae) mutant starches. Part I: Relationship between resistant starch contents and molecular structures. *Carbohydrate Polymers, 74*, 396-404.

Lightner, J., Broglie, K., Cressman, R., Hines, C., & Hubbard, N. (1999). Production of a very-high amylose corn starch by inactivation of starch branching enzyme I in an amylose-extender mutant background. *Maize Genetics Conference*. Lake Geneva, WI.

Lu, T.-j., Jane, J.-l., Keeling, P. L., & Singletary, G. W. (1996). Maize starch fine structures affected by ear developmental temperature. *Carbohydrate Research, 282*, 157-170.

Mercier, C., Charbonniere, R., Gallant, D., & Guilbot, A. (1970). Development of some characteristics of starches extracted from normal corn and amylomaize grains during their formation. *Staerke, 22*, 9-16.

Morell, M. K., & Myers, A. M. (2005). Towards the rational design of cereal starches. *Current Opinion in Plant Biology, 8*, 204-210.

Morrison, W. R. (1981). Starch lipids: a reappraisal. *Starch/Staerke, 33*, 408-410.

Morrison, W. R. (1992). Analysis of cereal starches. *Modern Methods of Plant Analysis, 14*, 199-215.

Morrison, W. R. (1993). Barley lipids. *Barley*, 199-246.

Morrison, W. R. (1995). Starch lipids and how they relate to starch granule structure and functionality. *Cereal Foods World, 40*, 437-438, 440-431, 443-436.

Morrison, W. R. (2000). Starch lipids, starch granule structure and properties. *Special*

*Publication - Royal Society of Chemistry, 212*, 261-270.

Morrison, W. R., Law, R. V., & Snape, C. E. (1993a). Evidence for inclusion complexes of lipids with V-amylose in maize, rice and oat starches. *Journal of Cereal Science, 18*, 107-109.

Morrison, W. R., Tester, R. F., Gidley, M. J., & Karkalas, J. (1993b). Resistance to acid hydrolysis of lipid-complexed amylose and lipid-free amylose in lintnerized waxy and non-waxy barley starches. *Carbohydrate Research, 245*, 289-302.

Morrison, W. R., Tester, R. F., Snape, C. E., Law, R., & Gidley, M. J. (1993c). Swelling and gelatinization of cereal starches. IV. Some effects of lipid-complexed amylose and free amylose in waxy and normal barley starches. *Cereal Chemistry, 70*, 385-391.

Myers, A. M., Morell, M. K., James, M. G., & Ball, S. G. (2000). Recent progress toward understanding biosynthesis of the amylopectin crystal. *Plant Physiology, 122*, 989-997.

Ono, K., Seib, P. A., & Takahashi, S. (1998). Properties of hydroxypropylated wheat starches. *Nippon Kasei Gakkaishi, 49*, 985-992.

Pan, D. D., & Jane, J. l. (2000). Internal Structure of Normal Maize Starch Granules Revealed by Chemical Surface Gelatinization. *Biomacromolecules, 1*, 126-132.

Perera, C., Lu, Z., Sell, J., & Jane, J. (2001). Comparison of physicochemical properties and structures of sugary-2 cornstarch with normal and waxy cultivars. *Cereal Chemistry, 78*, 249-256.

Reddy, I., & Seib, P. A. (1999). Paste properties of modified starches from partial waxy wheats. *Cereal Chemistry, 76*, 341-349.

Regina, A., Bird, A., Topping, D., Bowden, S., Freeman, J., Barsby, T., Kosar-Hashemi,

B., Li, Z. Y., Rahman, S., & Morell, M. (2006). High-amylose wheat generated by RNA interference improves indices of large-bowel health in rats. *Proceedings of the National Academy of Sciences of the United States of America, 103*, 3546-3551.

Robertson, M. D., Bickerton, A. S., Dennis, A. L., Vidal, H., & Frayn, K. N. (2005). Insulin-sensitizing effects of dietary resistant starch and effects on skeletal muscle and adipose tissue metabolism. *American Journal of Clinical Nutrition, 82*, 559-567.

Robertson, M. D., Currie, J. M., Morgan, L. M., Jewell, D. P., & Frayn, K. N. (2003). Prior short-term consumption of resistant starch enhances postprandial insulin sensitivity in healthy subjects. *Diabetologia, 46*, 659-665.

Robyt, J. F. (1998). *Essentials of Carbohydrate Chemistry*, Springer-Verlag, New York.

Robyt, J. F., & French, D. (1967). Multiple attack hypothesis of alpha -amylase action. Action of porcine pancreatic, human salivary, and Aspergillus oryzae alpha -amylases. *Archives of Biochemistry and Biophysics, 122*, 8-16.

Sang, Y., Prakash, O., & Seib, P. A. (2007). Characterization of phosphorylated cross-linked resistant starch by 31P nuclear magnetic resonance (31P NMR) spectroscopy. *Carbohydrate Polymers, 67*, 201-212.

Sang, Y., & Seib, P. A. (2006). Resistant starches from amylose mutants of corn by simultaneous heat-moisture treatment and phosphorylation. *Carbohydrate Polymers, 63*, 167-175.

Schoch, T. J. (1942). Fractionation of starch by selective precipitation with butanol. *Journal of the American Chemical Society, 64*, 2957-2961.

Schultz, J., & Juvik, J. A. (2004). Current models for starch synthesis and the sugary

enhancer1 (*se1*) mutation in *Zea mays*. *Plant Physiology and Biochemistry, 42*, 457-464.

Shi, Y.-C., Capitani, T., Trzasko, P., & Jeffcoat, R. (1998). Molecular structure of a low-amylopectin starch and other high-amylose maize starches. *Journal of Cereal Science, 27*, 289-299.

Shi, Y.-C., & Jeffcoat, R. (2001). Structural features of resistant starch In B. McCleary, & L. Prosky. *Advanced Dietary Fibre Technology* pp. 430-439). Oxford, UK: Wiley-Blackwell.

Shi, Y.-C., & Seib, P. A. (1995). Fine structure of maize starches from four wx-containing genotypes of the W64A inbred line in relation to gelatinization and retrogradation. *Carbohydrate Polymers, 26*, 141-147.

Sidebottom, C., Kirkland, M., Strongitharm, B., & Jeffcoat, R. (1998). Characterization of the difference of starch branching enzyme activities in normal and low-amylopectin maize during kernel development. *Journal of Cereal Science, 27*, 279-287.

Smith, A. M. (2001). The Biosynthesis of Starch Granules. *Biomacromolecules, 2*, 335-341.

Smith, A. M., Zeeman, S. C., & Denyer, K. (2001). The synthesis of amylose. *Special Publication - Royal Society of Chemistry, 271*, 150-163.

Srichuwong, S., Sunarti, T. C., Mishima, T., Isono, N., & Hisamatsu, M. (2005a). Starches from different botanical sources I: Contribution of amylopectin fine structure to thermal properties and enzyme digestibility. *Carbohydrate Polymers, 60*, 529-538.

Srichuwong, S., Sunarti, T. C., Mishima, T., Isono, N., & Hisamatsu, M. (2005b).

Starches from different botanical sources II: Contribution of starch structure to swelling and pasting properties. *Carbohydrate Polymers, 62*, 25-34.

Svensson, E., & Eliasson, A. (1995). Crystalline changes in native wheat and potato starches at intermediate water levels during gelatinization. *Carbohydrate Polymers, 26*, 171-176.

Takeda, C, Takeda, Y., & Hizukuri, S. (1989a). Structure of amylomaize amylose. *Cereal Chemistry, 66*, 22-25.

Takeda, C., Takeda, Y., & Hizukuri, S. (1993a). Structure of the amylopectin fraction of amylomaize. *Carbohydrate Research, 246*, 273-281.

Takeda, Y., Hizukuri, S., & Juliano, B. O. (1986). Purification and structure of amylose from rice starch. *Carbohydrate Research, 148*, 299-308.

Takeda, Y., Hizukuri, S., & Juliano, B. O. (1989b). Structures and amounts of branched molecules in rice amyloses. *Carbohydrate Research, 186*, 163-166.

Takeda, Y., Tomooka, S., & Hizukuri, S. (1993b). Structures of branched and linear-molecules of rice amylose. *Carbohydrate Research, 246*, 267-272.

Tester, R. F., Qi, X., & Karkalas, J. (2006). Hydrolysis of native starches with amylases. *Animal Feed Science and Technology, 130*, 39-54.

Tufvesson, F., Wahlgren, M., & Eliasson, A.-C. (2003a). Formation of amylose-lipid complexes and effects of temperature treatment. Part 1. Monoglycerides. *Starch/Staerke, 55*, 61-71.

Tufvesson, F., Wahlgren, M., & Eliasson, A.-C. (2003b). Formation of amylose-lipid complexes and effects of temperature treatment. Part 2. Fatty acids. *Starch/Staerke, 55*, 138-149.

Van Munster, I. P., Tangerman, A., & Nagengast, F. M. (1994). Effect of resistant starch on colonic fermentation, bile acid metabolism, and mucosal proliferation. *Digestive Diseases and Sciences, 39*, 834-842.

Vineyard, M. L., Bear, R. P., MacMasters, M. M., & Deatherage, W. L. (1958a). Development of "amylomaize"—corn hybrids with high amylose starch. I. Genetic considerations. *Agronomy Journal, 50*.

Vineyard, M. L., Bear, R. P., MacMasters, M. M., & Deatherage, W. L. (1958b). Development of "amylomaize"—corn hybrids with high amylose starch. II. Results of breeding efforts. *Agronomy Journal, 58*, 598-602.

Wang, L., & Wang, Y.-J. (2001). Structures and physicochemical properties of acid-thinned corn, potato and rice starches. *Starch/Staerke, 53*, 570-576.

Wang, Y. J., White, P., Pollak, L., & Jane, J. (1993). Amylopectin and intermediate materials in starches from mutant genotypes of the Oh43 inbred line. *Cereal Chemistry, 70*, 521-525.

Wolf, M. J., Seckinger, H. L., & Dimler, R. J. (1964). Microscopic characteristics of high-amylose corn starches. *Staerke, 16*, 377-382.

Wongsagonsup, R., Varavinit, S., & BeMiller, J. N. (2008). Increasing slowly digestible starch content of normal and waxy maize starches and properties of starch products. *Cereal Chemistry, 85*, 738-745.

Woo, K. S., & Seib, P. A. (2002). Cross-linked resistant starch: preparation and properties. *Cereal Chemistry, 79*, 819-825.

Wu, H. C. H., & Sarko, A. (1978). The double-helical molecular structure of crystalline A-amylose. *Cabohydrate Research, 61*, 27-40.

Wu, X., Zhao, R., Bean, S. R., Seib, P. A., McLaren, J. S., Madl, R. L., Tuinstra, M., Lenz, M. C., & Wang, D. (2007). Factors impacting ethanol production from grain sorghum in the dry-grind process. *Cereal Chemistry, 84*, 130-136.

Wu, Y., Campbell, M., Yen, Y., Wicks, Z., III, & Ibrahim, A. M. H. (2009). Genetic analysis of high amylose content in maize (Zea mays L.) using a triploid endosperm model. *Euphytica, 166*, 155-164.

Yao, Y., Thompson, D. B., & Guiltinan, M. J. (2004). Maize starch-branching enzyme isoforms and amylopectin structure. In the absence of starch-branching enzyme IIb, the further absence of starch-branching enzyme Ia leads to increased branching. *Plant Physiology, 136*, 3515-3523.

Yoo, S.-H., & Jane, J.-l. (2002a). Molecular weights and gyration radii of amylopectins determined by high-performance size-exclusion chromatography equipped with multi-angle laser-light scattering and refractive index detectors. *Carbohydrate Polymers, 49*, 307-314.

Yoo, S.-H., & Jane, J.-l. (2002b). Structural and physical characteristics of waxy and other wheat starches. *Carbohydrate Polymers, 49*, 297-305.

Yoo, S.-H., Perera, C., Shen, J., Ye, L., Suh, D.-S., & Jane, J.-L. (2009). Molecular Structure of Selected Tuber and Root Starches and Effect of Amylopectin Structure on Their Physical Properties. *Journal of Agricultural and Food Chemistry, 57*, 1556-1564.

Yuan, R. C., Thompson, D. B., & Boyer, C. D. (1993). Fine structure of amylopectin in relation to gelatinization and retrogradation behavior of maize starches from three wx-containing genotypes in two inbred lines. *Cereal Chemistry, 70*, 81-89.

Zhang, G., Sofyan, M., & Hamaker, B. R. (2008). Slowly Digestible State of Starch: Mechanism of Slow Digestion Property of Gelatinized Maize Starch. *J. Agric. Food Chem., 56*, 4695-4702.

Zhang, W., Wang, H., Zhang, Y., & Yang, Y. (2007). Effects of resistant starch on insulin resistance of type 2 mellitus patients. *Chinese J. Prev. Med., 41*, 101-104.

Zhang, X., Colleoni, C., Ratushna, V., Sirghie-Colleoni, M., James, M. G., & Myers, A. M. (2004). Molecular characterization demonstrates that the Zea mays gene sugary2 codes for the starch synthase isoform SSIIa. *Plant Molecular Biology, 54*, 865-879.

Zobel, H. F. (1988). Starch crystal transformations and their industrial importance. *Starch/Staerke, 40*, 1-7.

Zobel, H. F., French, A. D., & Hinkle, M. E. (1967). X-ray diffraction of oriented amylose fibers. II. Structure of V-amyloses. *Biopolymers, 5*, 837-845.

# CHAPTER 1. CHARACTERIZATION OF MAIZE AMYLOSE-EXTENDER (*ae*) MUTANT STARCHES: PART II. STRUCTURES AND PROPERTIES OF STARCH RESIDUES REMAINING AFTER ENZYMATIC HYDROLYSIS AT BOILING-WATER TEMPERATURE

A paper published in the *Carbohydrate polymers*

Hongxin Jiang [a], Mark Campbell [b], Mike Blanco [c], Jay-lin Jane [a,*]

[a] Department of Food Science and Human Nutrition, Iowa State University, Ames, IA 50011, USA

[b] Truman State University, Kirksville, MO 63501, USA

[c] USDA-ARS/Plant Introduction Research Unit, Ames, IA 50011, USA

*Corresponding author. Tel: +1 515 294 9892. Fax: +1 515 294 8181. E-mail address: jjane@iastate.edu (J. Jane).

## Abstract

GEMS-0067 maize *ae*-line starches developed by the Germplasm Enhancement of Maize (GEM) project consist of 39.4%-43.2% resistant-starch (RS), which is larger than the existing *ae*-line starches of H99*ae*, OH43*ae*, B89*ae*, and B84*ae* (11.5%-19.1%) as reported in part I of the study. The objective of this study was to understand the mechanism of the RS formation in the GEMS-0067 *ae*-line starch. In the current study, we analyzed the structures and properties of the RS residues that remained after enzymatic hydrolysis of the *ae*-line starches at 95-100°C. The RS residues consisted of two major components: large starch molecules of average degrees of polymerization (DP) 840-951 with a few branches and small starch molecules (average DP 59-74) with mostly linear chains. All the RS residues had a semi-crystalline structure with the B-type polymorph and displayed high onset (100.7-107.7°C), peak (118.6-121.4°C), and conclusion (139.7-158.8°C) gelatinization-temperatures.

After the maize *ae*-mutant starches were defatted with methanol, the RS contents decreased

to 27.8-28.9% for the GEMS-0067 *ae*-line starches and 9.0-11.0% for the existing *ae*-line

starches. The RS residues were attributed to the presence of long-chain double-helical

crystallites derived from amylose and the intermediate component (IC). These crystallites

present in native *ae*-line starches had gelatinization temperatures above 100°C and

maintained the semi-crystalline structures after enzymatic hydrolysis at 95-100°C.

**Keywords:** Resistant starch; Starch structure; Amylose-extender mutant; High-amylose

maize starch; Long-chain double-helical crystallite

## 1. Introduction

This paper reports a continuing study on characterization of maize *ae*-mutant starches.

Part I of the study reported molecular structures and properties of selected maize *ae*-mutant

starches, which included three new lines derived from GEMS-0067 *ae*-line, designated as

GSOH 1, GSOH 2, and GSOH 3, and four additional *ae*-lines, H99*ae*, OH43*ae*, B84*ae*, and

B89*ae,* designated as "existing *ae*-lines" (Li et al., 2008). GEMS-0067 was developed by M.

Campbell at Truman State University nursery in Kirksville, MO, working cooperatively with

the GEM project in Ames, IA. GEMS-0067 was derived from an exotic tropical breeding

cross designated as GUAT209:S13 with the accession Guatemala 209 crossed to a stiff-stalk

line (S13) (Campbell et al., 2007). GEMS-0067 is homozygous for the *ae* gene and is also

known to have modifier genes for enhancing the level of amylose (Campbell et al., 2007).

The starches of GEMS-0067 *ae*-lines displayed significantly larger RS contents (39.4-

43.2%) than that of the existing *ae*-lines (11.5-19.1%) determined using AOAC method

991.43 for total dietary fiber (Li et al., 2008). RS contents of the starch samples, determined

using Englyst's method (Englyst et al., 1992) after cooking the starch at 100°C for 30min,

also showed that GEMS-0067 *ae*-line starches had more RS (30.9-34.3%) than did the

existing *ae*-line starches (18.6-20.9%) (Li et al., 2008). The GEMS-0067 *ae*-line starches had

greater apparent-amylose contents (83.1-85.6%) and less amylopectin contents (10.7-13.9%)

than did the existing *ae*-line starches (61.7-67.7% and 25.4-33.5%, respectively) (Li et al.,

2008). The RS content was positively correlated with the apparent-amylose content of the

maize *ae*-mutant starch (r = 0.99) (Li et al., 2008). The GEMS-0067 *ae*-line starches

contained 36.1-45.0% IC, which were higher than the IC contents of most of the existing *ae*-

line starches (22.4-27.0 %) except OH43*ae* starch (52.0 %) (Li et al., 2008). The average

branch-chain lengths of the IC molecules isolated from the maize *ae*-mutant starches varied

from DP 31.6 to 50.6 (Li et al., 2008). The GEMS-0067 *ae*-line starches displayed higher

conclusion gelatinization-temperatures (122.0-130.0°C) than did the existing *ae*-line starches

(100.5-105.3°C) (Li et al., 2008). The authors proposed that the semi-crystalline structure of

the GEMS-0067 *ae*-line starches remained after digesting with thermally stable α-amylase at

95-100°C. Consequently, the GEMS-0067 *ae*-line starches displayed greater RS contents (Li

et al., 2008).

Structures of RS obtained after enzymatic hydrolysis of high-amylose maize starches

using pancreatic α-amylase at 37°C have been reported (Evans & Thompson, 2004; Shi &

Jeffcoat, 2001). On the basis of broad molecular-weight distributions of the RS residue, Shi

and Jeffcoat (2001) concluded that both molecular structures and the granular structure of

high-amylose maize starch granules contributed to the resistance of starch molecules to

pancreatic α-amylase hydrolysis (Shi & Jeffcoat, 2001). Evans and Thompson (2004) reported that the RS residue had similar branch chain-length profiles to the native high-amylose maize starch and proposed that the molecular organization in the high-amylose maize starch granule was the primary factor resulting in the enzyme resistance of starch (Evans & Thompson, 2004).

In the current study, we aimed to identify which starch components (amylose, IC, or amylopectin) remained in the RS residues, where they were located in the starch granule, and what types of physical structures they had by analyzing the chemical, physical, and morphological structures of the RS residues remaining after the thermal and enzymatic treatments. We also investigated how lipids in the starch affected the enzymatic hydrolysis of the starch. On the basis of these results, we proposed a mechanism of RS formation in the *ae*-line starches.

## 2. Materials and methods

### 2.1. Materials

Maize kernels of three new lines (F6 generation) derived from GEMS-0067 *ae*-lines, including GUAT209:S13×(OH43*ae*×H99*ae*) B-B-4-1-2-1-1 (GSOH 1), GUAT209:S13×(OH43*ae*×H99*ae*) B-B-4-4-2-1-1 (GSOH 2), and GUAT209:S13×(OH43*ae*×H99*ae*) B-B-4-4-2-1-2 (GSOH 3), and four existing *ae*-lines H99*ae*, OH43*ae*, B89*ae*, and B84*ae* were produced at the Truman State University Farm (Kirksville, MO). All chemicals were reagent grade, obtained from Sigma-Aldrich Co. (St. Louis, MO) or Fisher Scientific (Pittsburgh, PA), and were used as received. Crystalline *Pseudomonas* isoamylase (EC 3.2.1.68) with specific activity about 66,000 units per

milligram of protein was purchased from Hayashibara Biochemical Laboratories, Inc.

(Okayama, Japan) and was used without further purification.

## 2.2. Starch isolation

Starch was isolated from maize kernels using the method reported by Li et al. (2008).

## 2.3. Removal of lipid

The lipid was removed according to the method reported by Schoch (1942). Starch (5.0 g)

was placed in a Whatman Cellulose Extraction Thimble (22 mm I.D. × 80 mm) and was

defatted using methanol in a Soxhlet extractor for 24 h. The methanol of the extraction

solution was removed using a rotary evaporator (Büchi/Brinkmann Rotavapor-R). The lipid

residue was dried at 105°C overnight. The content of the removed lipid was calculated as the

amount of the dried lipid residue divided by the dry weight of the native starch. The defatted

starches were dried at 37°C for 24 h.

## 2.4. RS content

RS content was determined using AOAC Official Method 991.43 for total dietary fiber

(AOAC, 2003) following the procedure reported by Li et al. (2008).

## 2.5. Starch morphology

Scanning electron microscopy (SEM) images of starch samples were taken using a

scanning electron microscope (JEOL JSM-35, Tokyo, Japan) at the Microscopy and

NanoImaging Facility, Iowa State University. The starch samples were coated with gold-palladium (60:40), and the SEM images were taken at 10 kV (Ao & Jane, 2007).

The percentage of rod/filamentous starch granules was determined using the number of rod/filamentous starch granules divided by the total number of starch granules shown on SEM images. At least 900 total starch granules were used for the calculation of the percentage. The short (S) and the long (L) axes of starch granules were measured using SIS Pro software (Soft Imaging System Inc., Lakewood, CO), and the L/S ratios were calculated. Starch granules were considered as rod/filamentous granules when the L/S ratios were larger than 1.3.

2.6. Molecular-weight distributions of the RS residues

Molecular-weight distributions of the RS residues obtained after enzymatic hydrolysis of native ae-line starches at 95-100°C (AOAC Method 991.43) were analyzed using a high-performance size-exclusion chromatography (HPSEC) equipped with a refractive-index (RI) detector. The RS residue (20mg) was wetted with water (0.2 mL), dispersed in dimethyl sulfoxide (DMSO) (1.8 mL) at 100°C for 1 h and kept at room temperature with gentle mechanical stir for 16 h, precipitated using ethanol (20 X), collected, and then redissolved in boiling water with mechanical stir in a boiling-water bath for 30 min. An aliquot (100 μL) of the dispersion was filtered through a nylon membrane (5 μm pore size) following the method of Yoo and Jane (2002) with modifications. The HPSEC-RI system consisted of an isocratic pump (HP 1050, Hewlett Packard, Valley Forge, PA), an injection valve (100 μl sample loop, Model 7725, Rheodyne), and an RI detector (G1362A, Agilent, Santa Clara, CA). SB-806 and SB-804 analytical columns with a Shodex OH pak SB-G guard column (Showa Denko

K.K., Tokyo, Japan) were used to analyze the molecular weights of the RS residues. Milli-Q

water (18 Ω) filtered through a membrane with a pore size of 0.02 μm (Cat. No. 6809-5002,

Whatman) was used as the eluent. Pullulan standards (P-5, P10, P20, P50, P100, P200, and

P400, Showa Denko K.K., Tokyo, Japan) were used as references for the determination of

molecular weights of the RS residues.

The molecular-weight distributions of the RS residues were also analyzed using

Sepharose CL-2B gel permeation chromatography (GPC), following the method of Jane and

Chen (1992). Three peaks, designated as large (F1), medium (F2), and small (F3) molecular-

weight fractions, were collected separately for further structural analysis of each of the RS

molecules.


*2.7. Molecular structures of the RS residues collected in the F2 fraction*

The F2 fraction of the RS residue was collected and debranched following the method

described by Li et al. (2008). The samples with and without debranching reaction were

dispersed in DMSO (90%) at 100°C, precipitated using ethanol (20 X), collected, and then

redissolved in hot water with stirring in a boiling-water bath for 30 min. An aliquot (20 μL)

of the dispersion was filtered through a nylon membrane (5 μm pore size) and analyzed using

a HPSEC equipped with an RI detector (HPSEC-RI). The HPSEC-RI system consisted of a

pump (Prostar 210, Varian, Walnut Creek, CA), an injection valve (20 μl sample loop, Model

7725, Rheodyne), and an RI detector (Prostar 355, Varian, Walnut Creek, CA). A SB-803

analytical column with a Shodex OH pak SB-G guard column (Showa Denko K.K., Tokyo,

Japan) was used to determine the molecular weights of the samples. The temperature of the

columns was maintained at 50.0°C using a column oven (Model 510, varian, Walnut Creek,

CA). The temperature of the RI detector was set at 35.0°C. The eluent was distilled-deionized water filtered through a membrane with pore size of 0.45 µm. Maltopentaose, maltohexaose, maltoheptaose, and the same pullulan standards described in *2.6* were used for molecular-weight calibration.

*2.8. Molecular structures and chain-length distributions of the RS residues collected in the F3 fraction*

The molecular-weight distributions of the RS residues collected in the F3 fraction, before and after isoamylase-debranching, were determined using a GPC column packed with Bio-Gel P-30 gel (1.5 I.D. × 50 cm) (Bio-Rad Laboratories, Richmond, CA). The eluent was a sodium-chloride aqueous solution (25mM) containing sodium hydroxide (pH adjusted to 9.8). The column was run in a descending mode with a flow rate of 18 mL/hr. Fractions of 2.0 mL each were collected and analyzed for total carbohydrate content using the phenol-sulfuric acid method (Dubois et al., 1956).

The isoamylase-debranched F3 starch was also analyzed for the chain-length distribution using a fluorophore-assisted capillary-electrophoresis (FACE) following the procedure of Morell, Samuel, and O'shea (1998) with modifications. The debranched sample was adjusted to pH 7, boiled for 15 min, and filtered through a membrane filter (1.2 µm pore size). The filtrate (80 µL, 2mg/mL) was dried at 45°C using a centrifugal vacuum evaporator for 3 h. Two µL of 8-aminopyrene-1,3,6-trisulfonic acid (APTS, Cat. No. 09341, Sigma, St. Louis, MO) solution (0.2M APTS in 15% acetic acid) and 2 µL of sodium cyanoborohydride (1M in tetrahydrofuran, Cat. No. 296813, Sigma, St. Louis, MO) were added to the dried sample.

The mixture was incubated at 40°C for 16 h. The APTS-labeled sample was injected into the FACE system (P/ACE MDQ, Beckman Coulter, Fullerton, CA) at 0.5 psi for 5 seconds. A N-CHO coated capillary tubing (50 μm I.D., 50cm length, Cat. No. 477601, Beckman Coulter, Fullerton, CA) was used to separate APTS-labeled molecules. The separation was performed at 23.5 kV at 25°C.

*2.9. Starch crystallinity*

Starch samples were equilibrated in a chamber with 100% relative humidity at 25°C for 24 hours. X-ray diffraction patterns of the starch samples were determined using a diffractometer (D-500, Siemens, Madison, WI) with copper $K_\alpha$ radiation (Ao & Jane, 2007). Crystallinity of the starch was calculated using the following equation. Crystallinity (%) = $100A_c/(A_c + A_a)$, where $A_c$ is the crystalline area on the X-ray diffractogram and $A_a$ is the amorphous area.

*2.10. Thermal properties of the RS residues*

Thermal properties of the RS residues were analyzed using a differential scanning calorimeter (DSC) (DSC-7, Perkin-Elmer, Norwalk, CT) (Kasemsuwan et al., 1995). Starch (~6.0 mg, dry basis) was precisely weighed in a stainless steel pan, mixed with ~18μL of distilled water. The pan was sealed, equilibrated at room temperature for 1 h, and then heated at a rate of 10°C/min from 10 to 180°C. A sealed empty pan was used as the reference. Onset ($T_o$), peak ($T_p$), and conclusion ($T_c$) temperatures and enthalpy change ($\Delta H$) of starch gelatinization were calculated using Pyris software (Perkin-Elmer, Norwalk, CT).

## 3. Results and discussion

### 3.1. Morphology of native maize ae-mutant starches and their RS residues

SEM images of native maize *ae*-mutant starches are shown in Fig. 1. All the native *ae*-mutant starches consisted of mainly two types of starch granules: spherical granules and rod/filamentous granules. The rod/filamentous granules displayed shapes of rod, filament, triangle, socks, etc (Figs.1A-1G). Some filamentous granules were more than 50 μm long (Fig. 1B). Starches of the GEMS-0067 *ae*-lines consisted of substantially larger proportions of rod/filamentous granules (22.6-32.0%) (Table 1 and Figs. 1A-1C) than that of the existing *ae*-lines (5.2-7.7%) (Table 1 and Figs. 1D-1G). The proportion of rod/filamentous granules increased with the increase in apparent-amylose content of the maize *ae*-mutant starch (r = 0.98, $p < 0.05$). Apparent-amylose contents are 83.1-85.6% for the GEMS-0067 *ae*-line and 61.7-67.7% for the existing *ae*-line starches reported by Li et al. (2008). Many studies have reported the presence of rod/filamentous granules in maize *ae*-mutant starches, but none have shown such large proportions as observed in the GEMS-0067 *ae*-line starches (Boyer et al., 1976; Mercier et al., 1970; Shi & Jeffcoat, 2001; Sidebottom et al., 1998; Wolf et al., 1964).

Representative SEM images of the RS residues collected after α-amylase hydrolysis of the starches at 95-100°C (AOAC Method 991.43) are shown in Fig. 2. Fragmented, hallowed, and half-shell-like granules and granules retaining the original shape were observed in the RS residues of GEMS-0067 *ae*-line starches (Figs 2A & 2B). Granules that retained the native shape were mostly rod/filamentous starch granules, and there were many such granules observed in the RS residues of GEMS-0067 *ae*-line starches (Figs. 2A & 2B). There was little or no gel-like starch in the RS residues of GEMS-0067 *ae*-line starches. The RS

residues of the existing *ae*-line starches, however, were mostly in a gel-like form (Figs. 2C & 2D).

The hollowed and half-shell-like granules observed in the RS residues of GEMS-0067 *ae*-lines (Figs. 2A & 2B) and the gel-like starch in the RS residues of the existing *ae*-lines (Figs. 2C & 2D) were likely the remnants of the outer layer of spherical granules, which consisted of more amylose as reported previously (Jane & Shen, 1993; Li et al., 2007; Pan & Jane, 2000). It is plausible that starch molecules around the hilum were promptly gelatinized and hydrolyzed because the starch molecules around the hilum were loosely packed and had less amylose (Gray & BeMiller, 2004; Huber & BeMiller, 2001; Jane & Shen, 1993; Li et al., 2007; Pan & Jane, 2000). All the SEM results (Figs. 2A-2D) showed that the RS was more concentrated in rod/filamentous starch granules and at the outer layer of the spherical starch granule.

*3.2. Effect of lipid on the RS content*

The amounts of lipids extracted from the native starch samples using methanol were 0.59-0.69% (dry starch basis, dsb) for GEMS-0067 *ae*-line starches and 0.23-0.41% (dsb) for the existing *ae*-line starches (Table 1). The RS contents of the methanol-defatted starches of the GEMS-0067 *ae*-lines (27.8-28.9%) were substantially less than that of the native starches without defatting (37.3-43.4%) (Table 1). The RS contents of the existing *ae*-line starches after defatting (9.0-11.0%) were also decreased from that of the native starches (10.6-14.9%) (Table 1). These results showed that lipids in the native maize *ae*-mutant starches reduced enzymatic digestibility of starch at 95-100°C.

*3.3. Molecular-weight distributions of the RS residues*

Molecular-weight distributions of the RS residues remaining after the thermal treatment at 95-100°C and enzymatic hydrolysis, analyzed using HPSEC-RI, are shown in Fig. 3. The amylopectin molecules (peak eluted between 18.4-22.4 min) were hydrolyzed to smaller molecules, and the amylopectin peak disappeared after the thermal and enzymatic treatments (Fig. 3). The residual RS showed three peaks in the chromatograms, which were divided and designated as F1 (average DP ~ $3.47 \times 10^5$), F2 (average DP 840-951), and F3 (average DP 59-74) (Fig. 3 and Table 2). The ratios of F1:F2:F3 are summarized in Table 2. All the RS residues contained small amounts of F1 starch (2.3-5.5%), which were likely partially hydrolyzed amylopectin. The RS residues obtained from the GEMS-0067 *ae*-line starches consisted of larger proportions of F2 starch (30.8-37.9%) than those obtained from the existing *ae*-line starches (14.7-20.2%).

Sepharose CL-2B chromatograms of the RS residues were similar to the HPSEC-RI chromatograms of the RS residues shown in Fig. 3. Thus, the chromatograms of the Sepharose CL-2B are not shown. F1, F2, and F3 fractions separated by the Sepharose CL-2B column were collected separately and used for the structural analysis of starch molecules.

*3.4. Molecular structures of the RS residues collected in the F2 fraction*

Molecules collected in the F2 fraction separated by the Sepharose CL-2B column were debranched to determine the branch structures of the F2 starch molecules. The molecular-weight distributions of the F2 starch molecules, before and after isoamylase debranching, are shown in Fig. 4. Before the debranching reaction, the F2 starch molecules showed one major peak and some minor peaks of molecular weights larger than DP 2827 (eluted before 15 min)

with an exception of B84*ae*. After the isoamylase-debranching reaction of the F2 starch, the minor peaks of large molecules (> DP 2827) disappeared, suggesting those large molecules being highly branched partially hydrolyzed amylopectin and IC molecules. The chromatograms showed two major peaks, designated as P1 and P2 (Fig. 4). The average molecular weights of the P1 and P2 of the GEMS-0067 *ae*-lines (DP 547-675 and DP 57-60, respectively) were larger than that of the H99*ae*, OH43*ae*, and B89*ae* (DP 411-491 and DP 47-53, respectively) and B84*ae* (DP 98 and 17, respectively) (Table 2). The large linear-molecules of the P1 obtained from GEMS-0067 *ae*-line starches and the majority of the existing *ae*-line starches resembled the structures of amylose molecules.

The debranched F2 starch of the B84*ae* RS residue consisted of mainly short-chain molecules of DP 98 and 17 for P1 and P2, respectively (Fig. 4G and Table 2). The lack of large amylose-like molecules in the debranched F2 starch of the B84*ae* RS residue (Table 2) coincided with the lowest RS content (10.6%) (Table 1) and the lowest conclusion gelatinization-temperature ($T_c$ = 100.5 °C) of the B84*ae* starch among all the *ae*-line starch samples tested (Li et al., 2008). Therefore, the B84*ae* starch was considered to have a different structure from others and would be discussed separately.

The average molecular weights (DP 864-951) of the F2 starches obtained from all the samples except B84*ae* (Table 2) were similar to that of the amyloses isolated from GEMS-0067 *ae*-line and H99*ae* starches (DP 817 and DP 756, respectively) and from other high-amylose maize starches (DP 690-740) (Jane & Chen, 1992; Takeda et al., 1989). The average molecular-weights of the P1 and P2 of the debranched F2 starches (Table 2), however, were smaller than that of the two major peaks of debranched amyloses isolated from the GEMS-0067 *ae*-line starch (DP 1359 and 143, respectively) and from the H99*ae* starch (DP 1200

and 156, respectively). These results suggested presence of partially hydrolyzed amylose, IC, or amylopectin molecules in the F2 fraction. The presence of partially hydrolyzed amylose molecules was evident by the average molecular-weights of the P1 linear molecules (DP 411-675) smaller than that of the major peak of the debranched amyloses of GEMS-0067 *ae*-line (DP 1359) and H99*ae* (DP 1200). The presence of the partially hydrolyzed IC and amylopectin molecules in the F2 starches was evident by the disappearance of the minor peak (DP > 2827) of the F2 starches after the isoamylase-debranching reaction (Fig. 4) and the average molecular-weights of the P2 (DP 47-60) of the debranched F2 starches (Table 2). The presence of the partially hydrolyzed amylose, IC, and amylopectin molecules in the F2 fraction could be resulted from the fact that amylose and some IC and amylopectin molecules formed long-chain double-helical crystallites having gelatinization temperature above 95-100°C. These long-chain double-helical crystallites formed a block and protected the bulk of the amylose and parts of IC and amylopectin molecules from enzymatic hydrolysis at 95-100°C.

*3.5. Molecular structures and chain-length distributions of the RS residues collected in the F3 fraction*

The molecular-weight distributions of starch molecules in the F3 fraction determined using GPC, with and without isoamylase-debranching, are shown in Fig. 5. Most of the F3 starch molecules were linear and could not be debranched except some large F3 starch molecules (DP > ~73) that were debranched by isoamylase and produced smaller linear-molecules (Fig. 5). The chain-length distribution of the debranched F3 starch was also determined using FACE (Fig. 6). FACE is powerful in determining the molecular-weight

distribution of individual small linear-molecules, but it has a limited maximum detectable chain-length at about DP 80. The chain-length distributions of the debrached F3 starch molecules, both on molar and mass bases, are summarized in Table 3. The debranched F3 starches showed larger proportions of chains with DP > 25 (77.0-90.6%, mass-based) (Table 3 and Fig. 6) than did the debranched amylopectins (50.4-55.5%), large molecular-weight IC (52.8-65.0%), and most small molecular-weight IC (67.8-89.3%) (Li et al., 2008). These results suggested that the F3 starch molecules could consist of the residues of amylose, IC, and amylopectin molecules resulting from enzymatic hydrolysis of semi-crystalline amylose and branch-chains of IC and amylopectin. The remaining fragments of crystalline amylose after B. subtilis $\alpha$-amylase hydrolysis have average molecular weight of DP 50 ranging from DP 45 to 65 (Jane & Robyt, 1984).

*3.6. Thermal properties of the RS residues*

Despite the large differences in the contents of the RS residues remaining after enzymatic hydrolysis of the maize *ae*-line starches (Table 1), all the RS residues displayed similar gelatinization temperatures (100.7-107.7°C, 118.6-121.4°C, and 139.7-158.8°C for $T_o$, $T_p$, and $T_c$, respectively) (Table 4), which were higher than their native starch counterparts (Li et al., 2008), but lower than the RS residues obtained from retrograded amylose (120.4-125.5°C, 148.1-157.7°C, and 166.5-177.0°C, respectively) reported by Sievert and Pomeranz (1990). The high onset gelatinization-temperatures of the RS residues (above 100.7°C) (Table 4) indicated the presence of long-chain double-helical crystallites in the RS residues. These long-chain double-helical crystallites retained semi-crystalline structures after heating at 95-100°C and enzymatic hydrolysis.

The significant increase in the $T_o$ from ~65$^o$C of the native starches to > 100$^o$C of the RS residues was attributed to the gelatinization and hydrolysis of amylopectin that had a low gelatinization temperature. The increase in the $T_c$ from ~100$^o$C (existing *ae*-lines) or ~125$^o$C (GEMS-0067 *ae*-lines) of the native starches to ~145$^o$C of the RS residues could be the result of removal of non-resistant starch. It was plausible that RS crystallites were present in the native starch but at low concentrations, which were below the threshold of the DSC detector. To test this hypothesis, we ran DSC thermograms of mixtures of the native starch and RS residue. The gelatinization thermogram of a mixture of 90% GEMS-0067 *ae*-line starch and 10% RS residue appeared similar to that of the native starch (Data not shown). More studies will be conducted to further understand the increase in the conclusion gelatinization-temperature of the RS residues.

*3.7. Crystalline structures and RS formation*

All the native maize *ae*-mutant starches displayed the B-type X-ray diffraction pattern (Fig. 7A), which was in agreement with the results reported by Shi et al. (1998). Although the amylopectin contents were 10.7-13.9% for the GEMS-0067 *ae*-line starches (Li et al., 2008), the percentage crystallinity of those starches were 22.8-26.1% (Fig. 7A). These results clearly indicated that some amylose/IC molecules of the GEMS-0067 *ae*-line starches were also present in the double-helical crystalline-structure in the starch granules, which contributed to the total percentage crystallinity. In normal starch granules, it is known that amylopectin molecules are in the crystalline structure, whereas amylose molecules are present in amorphous (French, 1984; Jane et al., 1992). It was likely that amylose molecules, the dominant component in the granule of the *ae*-line starch, were not separated by

amylopectin molecules and, thus, interacted with one another and formed the double-helical crystalline structure during the development of the starch granule. This finding was supported by the presence of partially preserved amylose molecules in the F2 fraction of the RS residues (Table 2 and Fig. 4), mostly linear chains up to > DP ~73 in the F3 fraction of the RS residues (Fig. 5), and the high conclusion gelatinization-temperatures (100.5-130.0°C) for the *ae*-line starches (Li et al., 2008).

Because RS content decreases with the increase in the amylopectin content of *ae*-line starch (Li et al. 2008), it is likely that the long-chain double-helical crystallites were mainly derived from amylose and IC, which had gelatinization temperatures above 100°C (Table 4). These long-chain double-helical crystallites retained the semi-crystalline structures at 95-100°C and were resistant to the enzymatic hydrolysis during the thermal treatment.

All the RS residues also displayed the B-type X-ray diffraction pattern with percentage crystallinity ranging from 21.9 to 24.1% for the GEMS-0067 *ae*-lines and 15.0-16.0% for the existing *ae*-lines (Fig. 7B). The decrease in the percentage crystallinity of the existing *ae*-line RS residues, from 27.5-33.0% of the native starches (Fig. 7A) to 15.0-16.0% of the RS residues (Fig. 7B), could be attributed to the hydrolysis of amylopectin in the starch granule. The existing *ae*-line starch consisted of substantially more amylopectin (25.4-33.5%) than the GEMS-0067 *ae*-line starch (10.7-13.9%) (Li et al., 2008). The percentages of crystallinity observed for the RS residues of the GEMS-0067 *ae*-line starch and the existing *ae*-line starch agreed with the SEM images of the RS residues. The RS residue of the existing *ae*-line starch displayed gel-like structure (Fig. 2C), which appeared amorphous, whereas that of the GEMS-0067 *ae*-line starch retained the granular structure (Fig. 2A), which had similar percentages of crystallinity to the native GEMS-0067 *ae*-line starches.

Although all the RS residues displayed the B-type X-ray diffraction pattern, the sharpness of the peaks at 14.5°, 21.9°, and 23.7° was reduced (Fig. 7B). This could be the result of the decrease in the crystallite size and distortion of the arrangement of the smaller starch-crystallites in the granule during enzymatic hydrolysis at 95-100°C. The absence of the V-type X-ray diffraction patterns with 2θ peaks at 8°, 13°, and 20° in the native starch and the RS residue (Zobel, 1988; Zobel et al., 1967) showed that lipids present in the starch granule were not in a crystalline amylose-lipid complex.

## 4. Conclusions

The GEMS-0067 *ae*-line starches had substantially larger proportions of rod/filamentous starch granules (22.6-32.0%) than did the existing *ae*-line starches (5.2-7.7%). The rod/filamentous starch granules and the outer layer of the spherical starch granules were more resistant to enzymatic hydrolysis at 95-100°C and remained in the RS residues. All the RS residues displayed the B-type polymorph and had gelatinization temperatures above 100°C. All the RS residues consisted of two major components: large molecules (average DP 840-951) of mostly partially-preserved amylose and IC molecules, and small molecules (average DP 59-74) of mostly linear chains resulting from enzymatic hydrolysis of semi-crystalline amylose, IC, and amylopectin molecules at 95-100°C. The long-chain double-helical crystallites of amylose/IC molecules in the native *ae*-line starches, which had gelatinization-temperature above 100°C, retained the semi-crystalline structures and were resistant to the enzymatic hydrolysis at 95-100°C. Lipids present in the granule also protected starch from enzymatic hydrolysis at 95-100°C.

**Acknowledgement**

The authors thank the USDA-ARS GEM project for the support on this research, Microscopy and NanoImaging Facility at Iowa State University for the microscopic study, and Dr. Schlorholtz for help on X-ray analysis.

**References**

Ao, Z., & Jane, J. (2007). Characterization and modeling of the A- and B-granule starches of wheat, triticale, and barley. *Carbohydrate Polymers, 67*, 46-55.

AOAC (2003). Association of Official Analytical Chemists (AOAC) Official Method 991.43. Total, soluble, and insoluble dietary fiber in foods. In W. Horwithz. *Official methods of analysis of the AOAC international*. Gaithersburg, Maryland: AOAC International.

Boyer, C. D., Daniels, R. R., & Shannon, J. C. (1976). Abnormal starch granule formation in Zea-Mays-L endosperms possessing amylose-extender mutant. *Crop Science, 16*, 298-301.

Campbell, M. R., Jane, J., Pollak, L., Blanco, M., & O'Brien, A. (2007). Registration of maize germplasm line GEMS-0067. *Journal of Plant Registrations, 1*, 60-61.

Dubois, M., Gilles, K. A., Hamilton, J. K., Rebers, P. A., & Smith, F. (1956). Colorimetric method for determination of sugars and related substances. *Analytical Chemistry, 28*, 350-356.

Englyst, H. N., Kingman, S. M., & Cummings, J. H. (1992). Classification and

measurement of nutritionally important starch fractions. *European Journal of Clinical Nutrition, 46 Suppl 2*, S33-50.

Evans, A., & Thompson, D. B. (2004). Resistance to a-amylase digestion in four native high-amylose maize starches. *Cereal Chemistry, 81*, 31-37.

French, D. (1984). Organization of starch granules. In R. L. Whistler, J. N. Bemiller, & E. F. Paschall. *Starch: Chemistry and Technology* (pp. 183-247). New York: Academic Press.

Gray, J. A., & BeMiller, J. N. (2004). Development and utilization of reflectance confocal laser scanning microscopy to locate reaction sites in modified starch granules. *Cereal Chemistry, 81*, 278-286.

Huber, K. C., & BeMiller, J. N. (2001). Location of sites of reaction within starch granules. *Cereal Chemistry, 78*, 173-180.

Jane, J., Xu, A., Radosavljevic, M., & Seib, P. A. (1992). Location of amylose in normal starch granules. I. Susceptibility of amylose and amylopectin to cross-linking reagents. *Cereal Chemistry, 69*, 405-409.

Jane, J., & Chen, J. F. (1992). Effect of amylose molecular size and amylopectin branch chain length on paste properties of starch. *Cereal Chemistry, 69*, 60-65.

Jane, J., & Robyt, J. F. (1984). Structure studies of amylose-V complexes and retrograded amylose by action of alpha amylases, and a new method for preparing amylodextrins. *Carbohydrate Research, 132*, 105-118.

Jane, J., & Shen, J. J. (1993). Internal structure of the potato starch granule revealed by chemical gelatinization. *Carbohydrate Research, 247*, 279-290.

Kasemsuwan, T., Jane, J., Schnable, P., Stinard, P., & Robertson, D. (1995).

Characterization of the dominant mutant amylose-extender (Ae1-5180) maize starch. *Cereal Chemistry, 72*, 457-464.

Li, L., Blanco, M., & Jane, J. (2007). Physicochemical properties of endosperm and pericarp starches during maize development. *Carbohydrate Polymers, 67*, 630-639.

Li, L., Jiang, H., Campbell, M., Blanco, M., & Jane, J. (2008). Characterization of maize amylose-extender (ae) mutant starches. Part I: Relationship between resistant starch contents and molecular structures. *Carbohydrate Polymers, 74*, 396-404.

Mercier, C., Charbonniere, R., Gallant, D., & Guilbot, A. (1970). Development of some characteristics of starches extracted from normal corn and amylomaize grains during their formation. *Staerke, 22*, 9-16.

Morell, M. K., Samuel, M. S., & O'Shea, M. G. (1998). Analysis of starch structure using fluorophore-assisted carbohydrate electrophoresis. *Electrophoresis, 19*, 2603-2611.

Pan, D. D., & Jane, J. (2000). Internal structure of normal maize starch granules revealed by chemical surface gelatinization. *Biomacromolecules, 1*, 126-132.

Schoch, T. J. (1942). Noncarbohydrate substances in the cereal starches. *Journal of the American Chemical Society, 64*, 2954-2956.

Shi, Y.-C., Capitani, T., Trzasko, P., & Jeffcoat, R. (1998). Molecular structure of a low-amylopectin starch and other high-amylose maize starches. *Journal of Cereal Science, 27*, 289-299.

Shi, Y.-C., & Jeffcoat, R. (2001). Structural features of resistant starch. In B. McCleary, & L. Prosky. *Advanced Dietary Fibre Technology* (pp. 430-439). Oxford, UK: Wiley-Blackwell.

Sidebottom, C., Kirkland, M., Strongitharm, B., & Jeffcoat, R. (1998). Characterization

of the difference of starch branching enzyme activities in normal and low-amylopectin maize during kernel development. *Journal of Cereal Science, 27*, 279-287.

Sievert, D., & Pomeranz, Y. (1990). Enzyme-resistant starch. II. Differential scanning calorimetry studies on heat-treated starches and enzyme-resistant starch residues. *Cereal Chemistry, 67*, 217-221.

Takeda, C., Takeda, Y., & Hizukuri, S. (1989). Structure of amylomaize amylose. *Cereal Chemistry, 66*, 22-25.

Wolf, M. J., Seckinger, H. L., & Dimler, R. J. (1964). Microscopic characteristics of high-amylose corn starches. *Staerke, 16*, 377-382.

Yoo, S.-H., & Jane, J. (2002). Molecular weights and gyration radii of amylopectins determined by high-performance size-exclusion chromatography equipped with multi-angle laser-light scattering and refractive index detectors. *Carbohydrate Polymers, 49*, 307-314.

Zobel, H. F. (1988). Starch crystal transformations and their industrial importance. *Starch/Staerke, 40*, 1-7.

Zobel, H. F., French, A. D., & Hinkle, M. E. (1967). X-ray diffraction of oriented amylose fibers. II. Structure of V-amyloses. *Biopolymers, 5*, 837-845.

Table 1
Proportions of rod/filamentous granules, lipid extracted, and RS content in maize *ae*-mutant starches

| Sample | Proportions of rod/filamentous granules (%) | Lipid extracted[a] (%) | RS (%)[b] | |
|---|---|---|---|---|
| | | | Before defatting | After defatting[a] |
| GSOH 1 | $32.0 \pm 0.0$ | $0.69 \pm 0.05$ | $41.5 \pm 2.0$ | $28.9 \pm 0.4$ |
| GSOH 2 | $30.2 \pm 2.4$ | $0.59 \pm 0.03$ | $43.4 \pm 3.2$ | $27.8 \pm 2.8$ |
| GSOH 3 | $22.6 \pm 1.0$ | $0.64 \pm 0.03$ | $37.3 \pm 0.7$ | $27.8 \pm 0.2$ |
| H99*ae* | $7.7 \pm 0.6$ | $0.38 \pm 0.03$ | $13.0 \pm 0.3$ | $11.0 \pm 0.9$ |
| OH43*ae* | $5.6 \pm 0.4$ | $0.41 \pm 0.02$ | $14.0 \pm 0.5$ | $10.9 \pm 0.3$ |
| B89*ae* | $7.5 \pm 0.8$ | $0.23 \pm 0.02$ | $14.9 \pm 0.4$ | $9.3 \pm 0.3$ |
| B84*ae* | $5.2 \pm 0.9$ | $0.41 \pm 0.01$ | $10.6 \pm 1.4$ | $9.0 \pm 0.7$ |

[a] Extraction of lipids was done using methanol in a soxhlet extractor for 24h.
[b] The RS content was determined using AOAC Method 991.43 for total dietary fiber.

Table 2
Average molecular weights (MW) of the RS residues collected in the F2 and F3 fractions[a, b,]

| Sample | Ratio (%) | | | MW of F2 (DP) | | | MW of F3 |
| | | | | Before debranching | After debranching | | (DP) |
| | F1 | F2 | F3 | | P1 | P2 | |
| --- | --- | --- | --- | --- | --- | --- | --- |
| GOSH 1 | 5.5 | 36.9 | 57.6 | 951 | 547 | 57 | 72 |
| GOSH 2 | 5.2 | 37.9 | 56.9 | 944 | 648 | 60 | 74 |
| GOSH 3 | 5.0 | 30.8 | 64.2 | 864 | 675 | 59 | 69 |
| H99*ae* | 2.9 | 20.2 | 76.9 | 870 | 491 | 53 | 61 |
| OH43*ae* | 2.3 | 19.2 | 78.4 | 870 | 422 | 47 | 63 |
| B89*ae* | 4.3 | 18.2 | 77.5 | 883 | 411 | 47 | 62 |
| B84*ae* | 3.9 | 14.7 | 81.4 | 840 | 98 | 17 | 59 |

[a] F1, F2, and F3 were large, medium, and small molecular-weight fractions of RS residues, respectively.
[b] DP = degree of polymerization; P1 and P2 are two peaks of debranched F2 starch.

Table 3
Molar-based chain-length distributions of the debranched RS residues collected in the F3 fraction[a]

| Sample | Average CL (DP)[b] | DP≤12 (%) | DP13-24 (%) | DP25-36 (%) | DP≥37 (%) |
|---|---|---|---|---|---|
| GSOH 1 | 40.3 (50.7) | 4.5 ± 0.2 (1.1)[c] | 22.1 ± 0.2 (10.4) | 22.5 ± 1.1 (17.0) | 50.8 ± 1.2 (71.5) |
| GSOH 2 | 41.9 (51.2) | 2.9 ± 0.2 (0.7) | 19.0 ± 0.2 (8.7) | 22.4 ± 0.7 (16.3) | 55.5 ± 0.6 (74.3) |
| GSOH 3 | 39.2 (49.5) | 3.4 ± 0.0 (0.9) | 25.7 ± 0.6 (12.4) | 23.0 ± 0.6 (17.8) | 47.6 ± 1.6 (68.9) |
| H99*ae* | 31.8 (41.1) | 7.7 ± 0.1 (2.3) | 35.1 ± 0.1 (20.7) | 24.7 ± 0.5 (23.3) | 32.5 ± 0.3 (53.7) |
| OH43*ae* | 34.4 (43.7) | 5.4 ± 0.2 (1.5) | 30.7 ± 0.2 (16.9) | 25.9 ± 0.4 (22.7) | 38.0 ± 0.0 (58.9) |
| B89*ae* | 35.7 (44.2) | 6.6 ± 0.5 (1.7) | 23.4 ± 1.2 (12.4) | 26.9 ± 0.3 (22.9) | 43.1 ± 2.0 (63.0) |
| B84*ae* | 40.2 (49.8) | 5.6 ± 0.1 (1.3) | 20.1 ± 0.1 (9.4) | 20.0 ± 0.6 (15.2) | 54.3 ± 0.6 (74.1) |

[a] Molar-based chain-length distribution of the debranched RS residue was analyzed using FACE.

[b] DP = degree of polymerization.

[c] The number in the parenthesis is mass-based percentage of chain-lengths of the debranched RS residue.

Table 4
Thermal properties of the RS residues[a]

| Sample | Gelatinization | | | |
|---|---|---|---|---|
| | $T_o$ (°C) | $T_p$ (°C) | $T_c$ (°C) | $\Delta H$ (J/g) |
| GOSH 1 | 107.7 ± 0.3 | 120.5 ± 0.3 | 148.5 ± 0.7 | 14.4 ± 1.2 |
| GOSH 2 | 107.1 ± 1.1 | 119.3 ± 0.5 | 139.7 ± 2.8 | 15.6 ± 1.5 |
| GOSH 3 | 107.3 ± 1.6 | 121.3 ± 0.8 | 143.5 ± 0.7 | 16.6 ± 1.2 |
| H99*ae* | 101.2 ± 1.2 | 119.6 ± 1.7 | 145.8 ± 2.4 | 14.3 ± 1.5 |
| OH43*ae* | 102.9 ± 2.2 | 118.6 ± 2.0 | 142.7 ± 0.8 | 12.2 ± 1.4 |
| B89*ae* | 100.7 ± 0.2 | 121.4 ± 1.5 | 158.8 ± 1.6 | 25.7 ± 0.1 |
| B84*ae* | 100.8 ± 0.4 | 121.1 ± 0.1 | 145.6 ± 1.9 | 22.0 ± 0.0 |

[a] $T_o$, $T_p$, $T_c$, and $\Delta H$ are onset temperature, peak temperature, conclusion temperature, and enthalpy change, respectively.
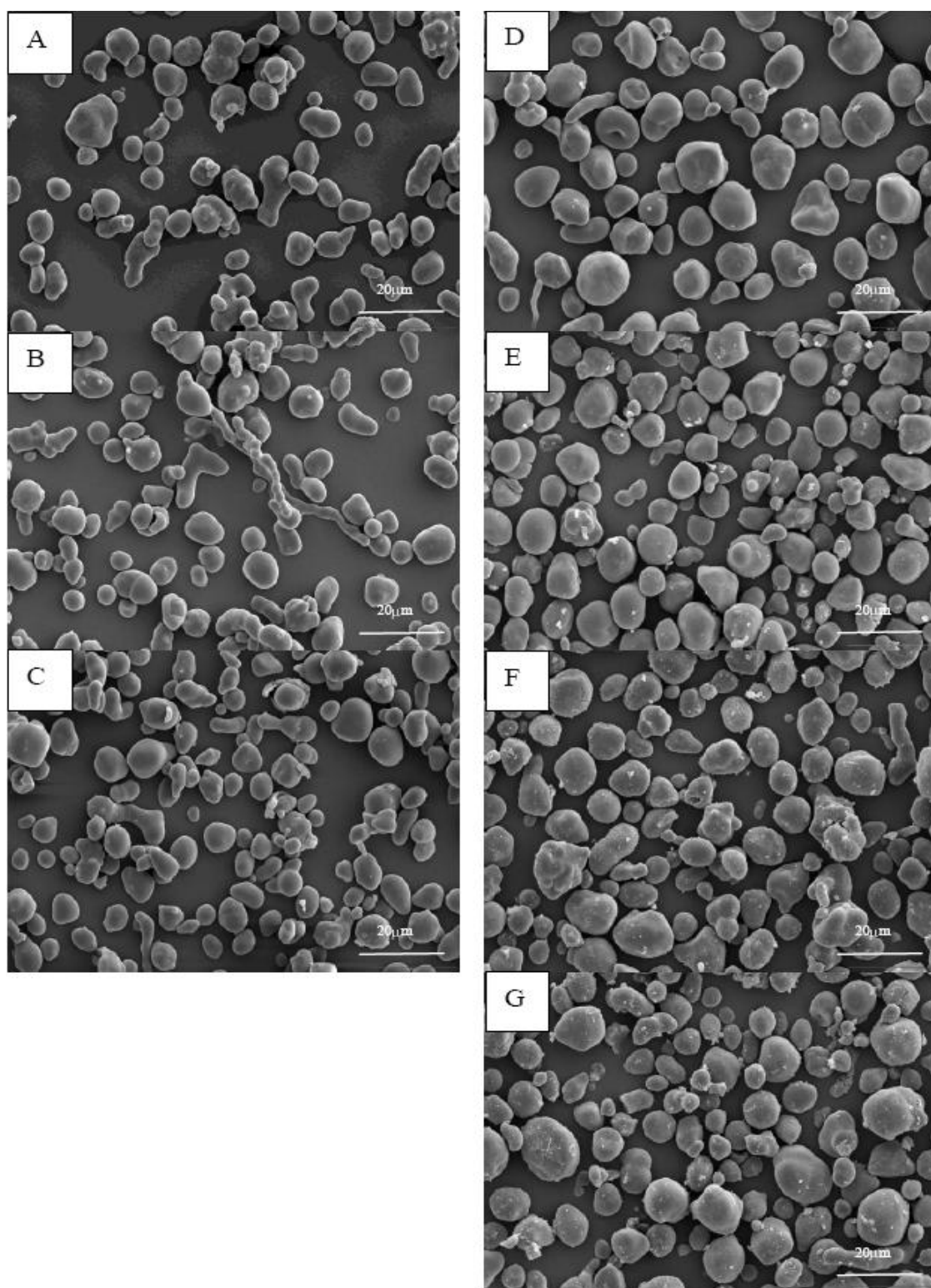
Fig. 1. SEM images of native maize *ae*-mutant starches. A: GSOH 1, B: GSOH 2, C: GSOH 3, D: H99*ae*, E: OH43*ae*, F: B89*ae*, and G: B84*ae*.
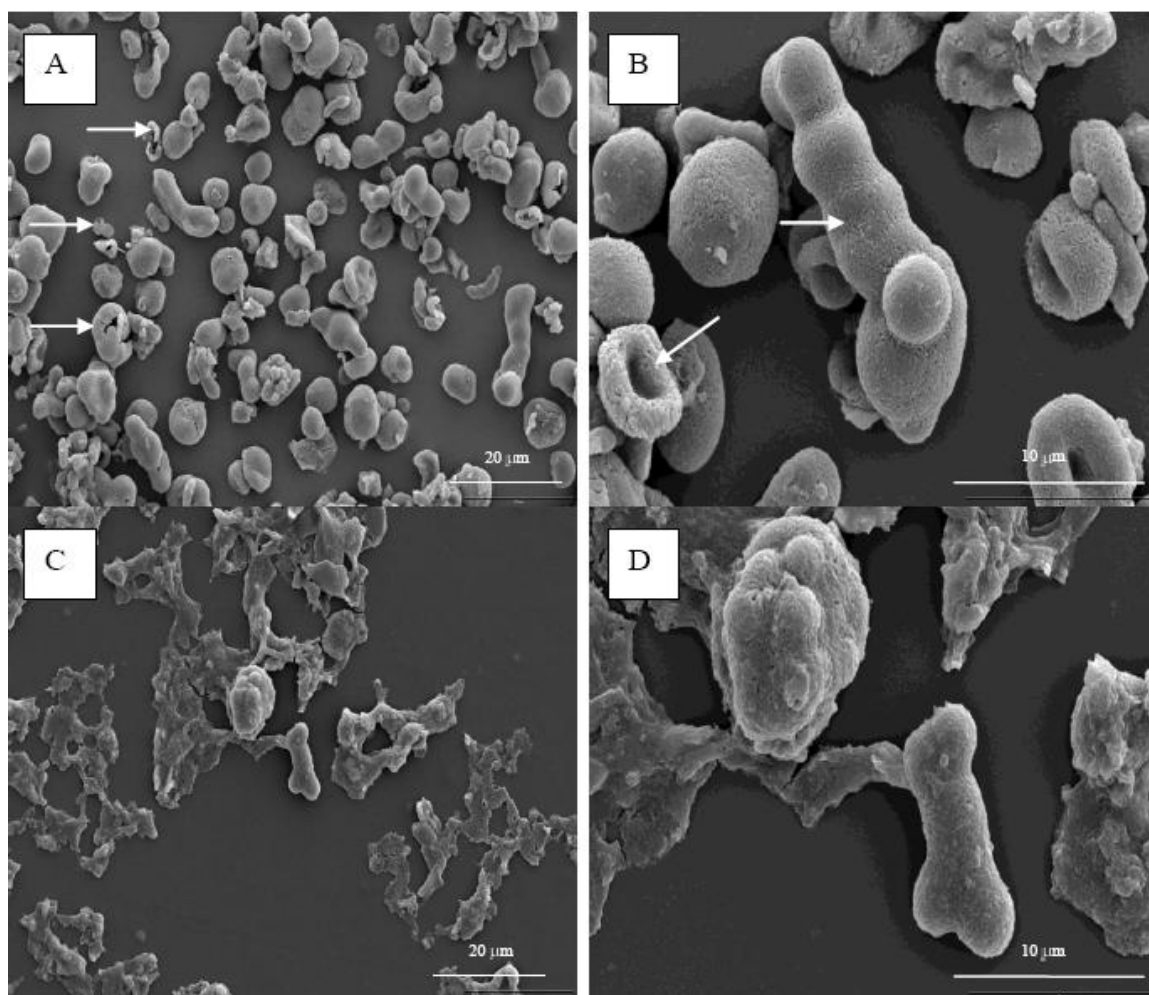
Fig. 2. Selected SEM images of the RS residues collected after enzymatic hydrolysis at 95-100°C (AOAC Method 991.43). A (1500X) and B (5000X): RS residue of GEMS-0067; C (1500X) and D (5000X): RS residue of B89*ae*. Arrows indicate fragmented, hollowed and half-shell-like granules and starch granule retained the shape.
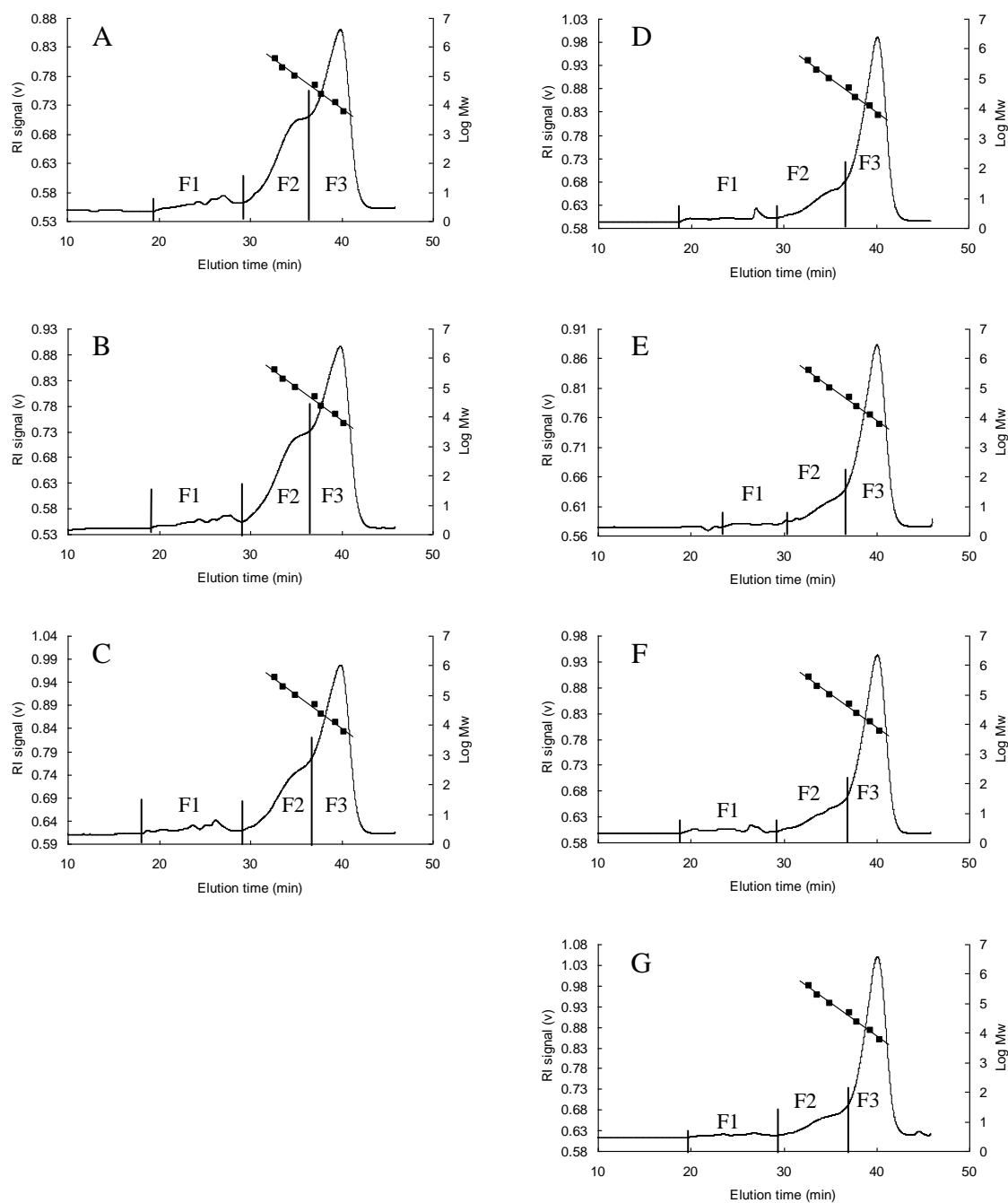
Fig. 3. High-performance size-exclusion chromatograms of the RS residues determined using analytical columns SB-806 and SB-804 (Showa Denko K.K., Tokyo, Japan). The RS residues were dispersed in DMSO (90%) at 100°C, precipitated using ethanol (20 X), collected, and then redissolved in hot water. Milli-Q water was used as eluent. A: GSOH 1, B: GSOH 2, C: GSOH 3, D: H99*ae*, E: OH43*ae*, F: B89*ae*, G: B84*ae*. ▬■▬: a pullulan standard curve with molecular weights of DP 36, 73, 146, 292, 617, 1148, and 2472. F1, F2, and F3 were large, medium, and small molecular-weight fractions of RS residues, respectively.
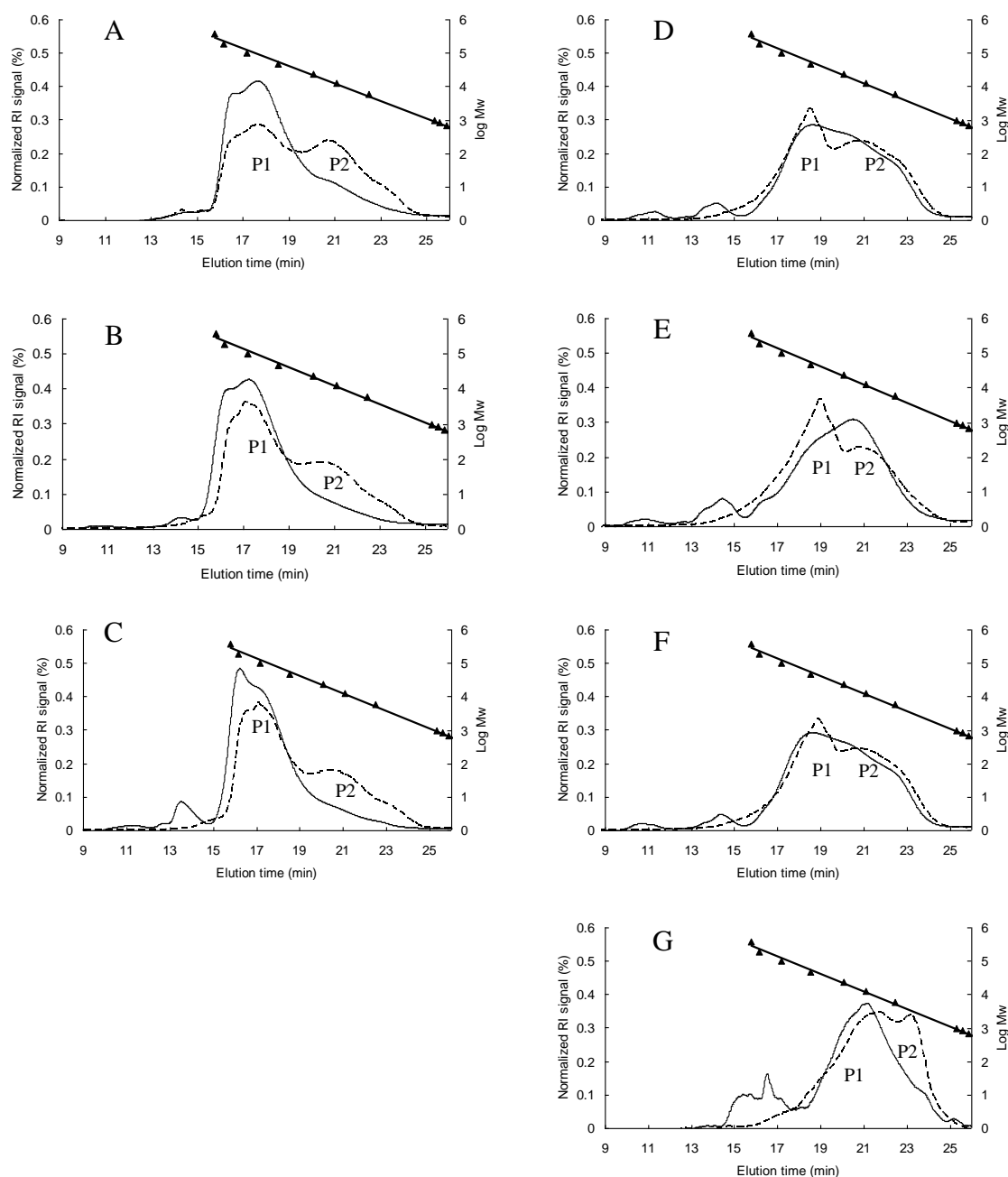
Fig. 4. High-performance size-exclusion chromatograms of the RS residues collected in the F2 fraction. The separation was conducted using a SB-803 analytical column (Showa Denko K.K., Tokyo, Japan). A: GSOH 1, B: GSOH 2, C: GSOH 3, D: H99*ae*, E: OH43*ae*, F: B89*ae*, G: B84*ae*. —— : Before debranching; - - - -: after debranching; —▲— : a standard curve of maltopentaose (DP 5), maltohexaose (DP 6), maltoheptaose (DP 7), and pullulan standards (DP 36, 73, 146, 292, 617, 1148, and 2472). P1 and P2: peaks of debranched F2 starch molecules.
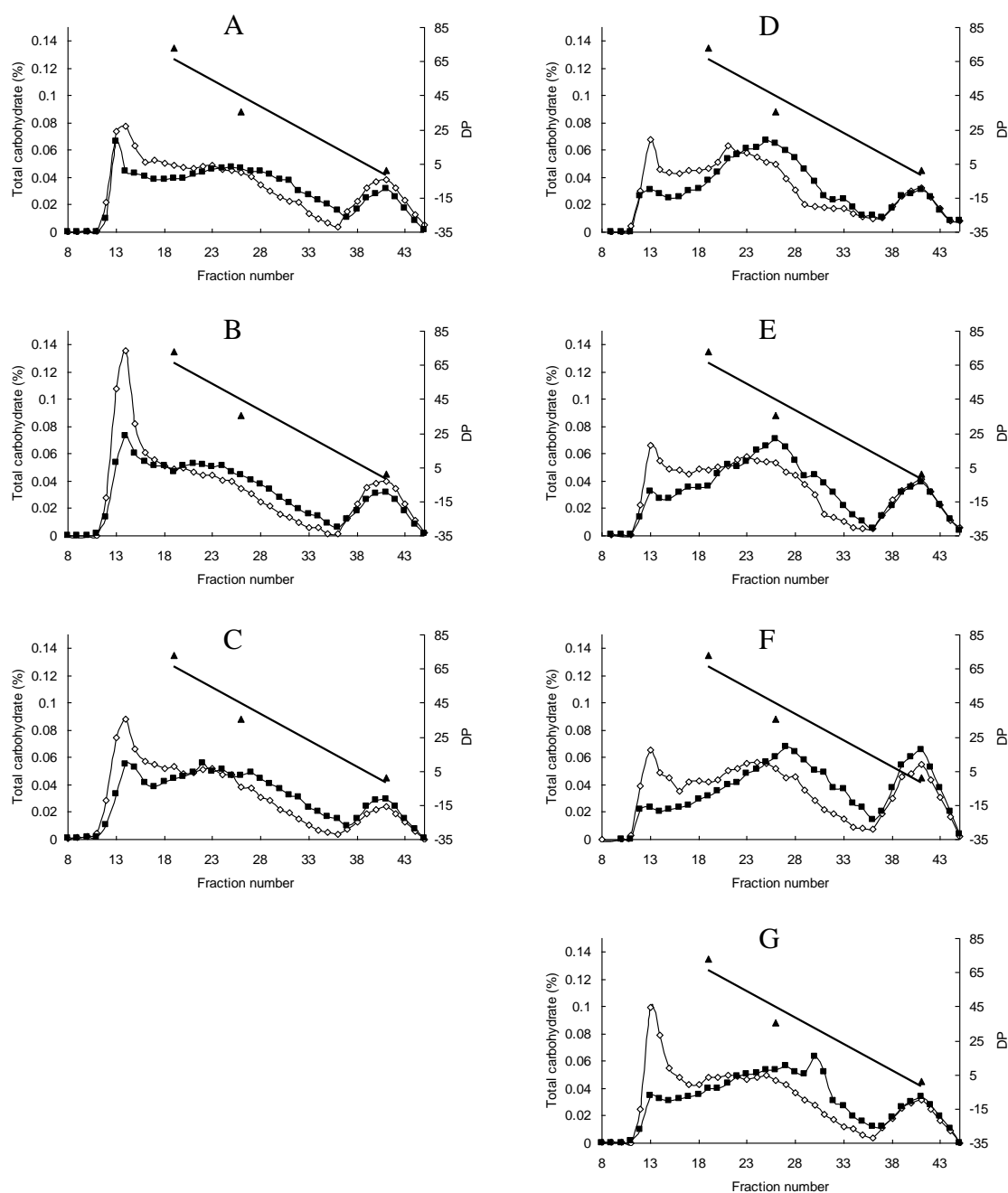
Fig. 5. Gel-permeation chromatograms of the RS residues collected in the F3 fraction determined using Bio-Gel P-30 gel (Bio-Rad Laboratories, Richmond, CA). A: GSOH 1, B: GSOH 2, C: GSOH 3, D: H99*ae*, E: OH43*ae*, F: B89*ae*, G: B84*ae*. ─◇─ : Before debranching; ─■─ : after debranching; ─▲─ : a standard curve of glucose and pullulan standards (DP 36 and 73). The glucose was used as an internal reference and eluted between 37 and 45 fractions.
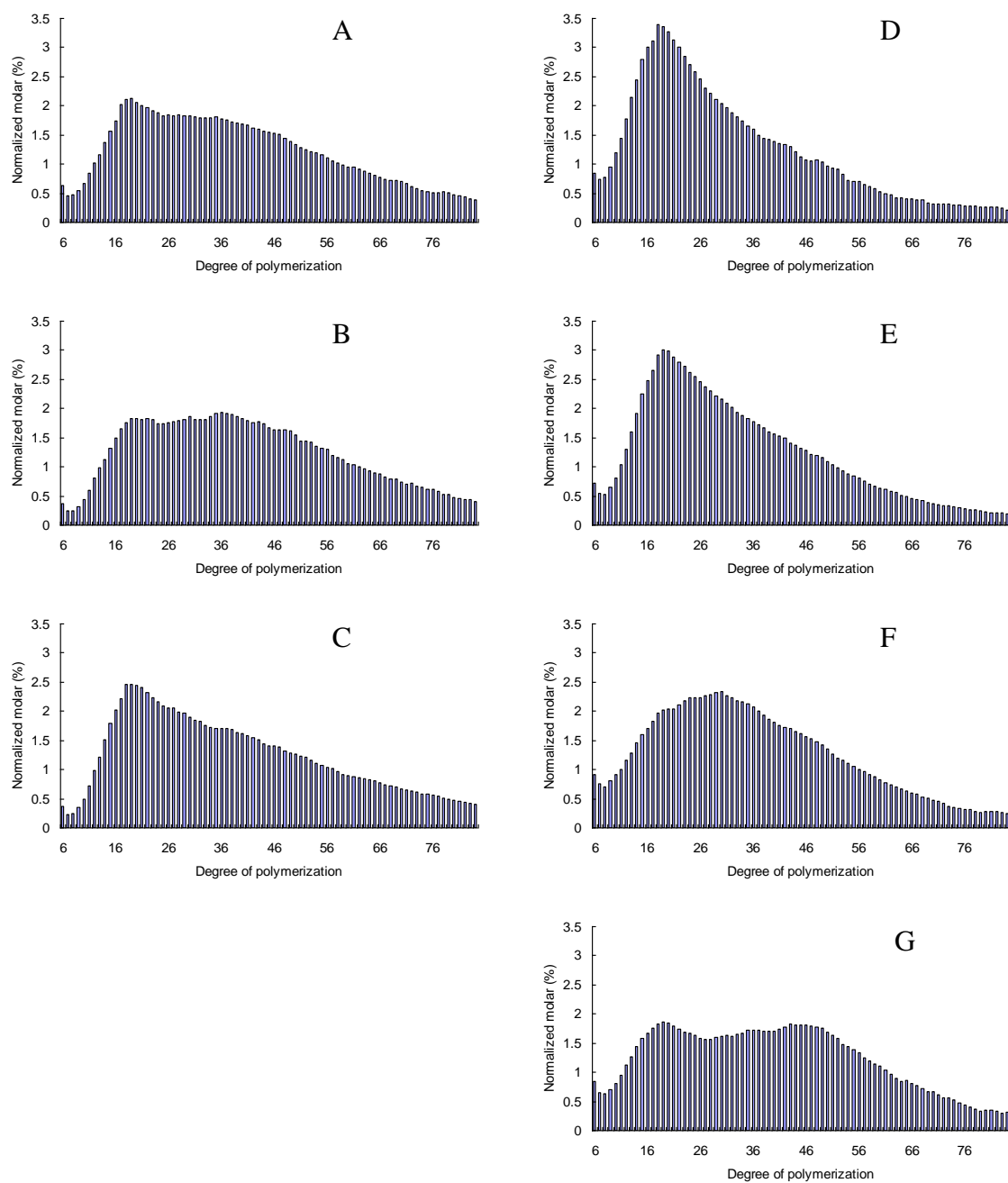
Fig. 6. Molar-based chain-length distributions of the debranched RS residues collected in the F3 fraction determined using FACE. A: GSOH 1, B: GSOH 2, C: GSOH 3, D: H99*ae*, E: OH43*ae*, F: B89*ae*, G: B84*ae*.

A

GSOH 1 (22.1%)

GSOH 2 (23.8%)

GSOH 3 (26.1%)

H99*ae* (28.8%)

OH43*ae* (27.5%)

B89*ae* (29.1%)

B84*ae* (33.0%)

Intensity

Two-theta (degree)
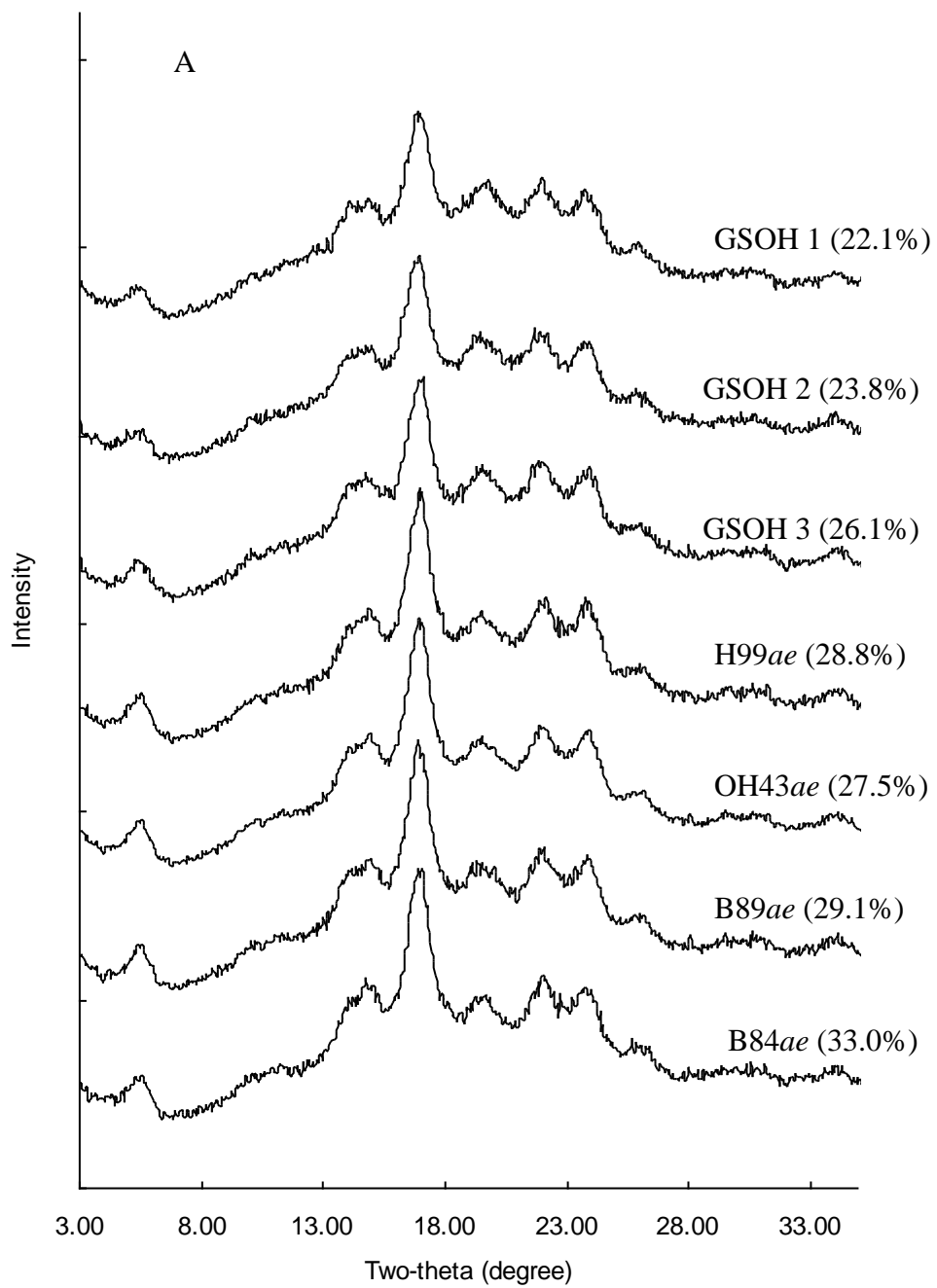
Fig. 7. X-ray diffraction patterns of (A) native starches and (B) RS residues. Crystallinity (%) is given in parentheses.

# CHAPTER 2. CHARACTERIZATION OF MAIZE AMYLOSE-EXTENDER (*ae*) MUTANT STARCHES: PART III. STRUCTURES AND PROPERTIES OF THE NAEGELI DEXTRINS

Hongxin Jiang [a], Sathaporn Srichuwong [a], Mark Campbell [b], Jay-lin Jane [a,*]

[a] Department of Food Science and Human Nutrition, Iowa State University, Ames, IA 50011, USA

[b] Division of Science, Truman State University, Kirksville, MO 63501, USA
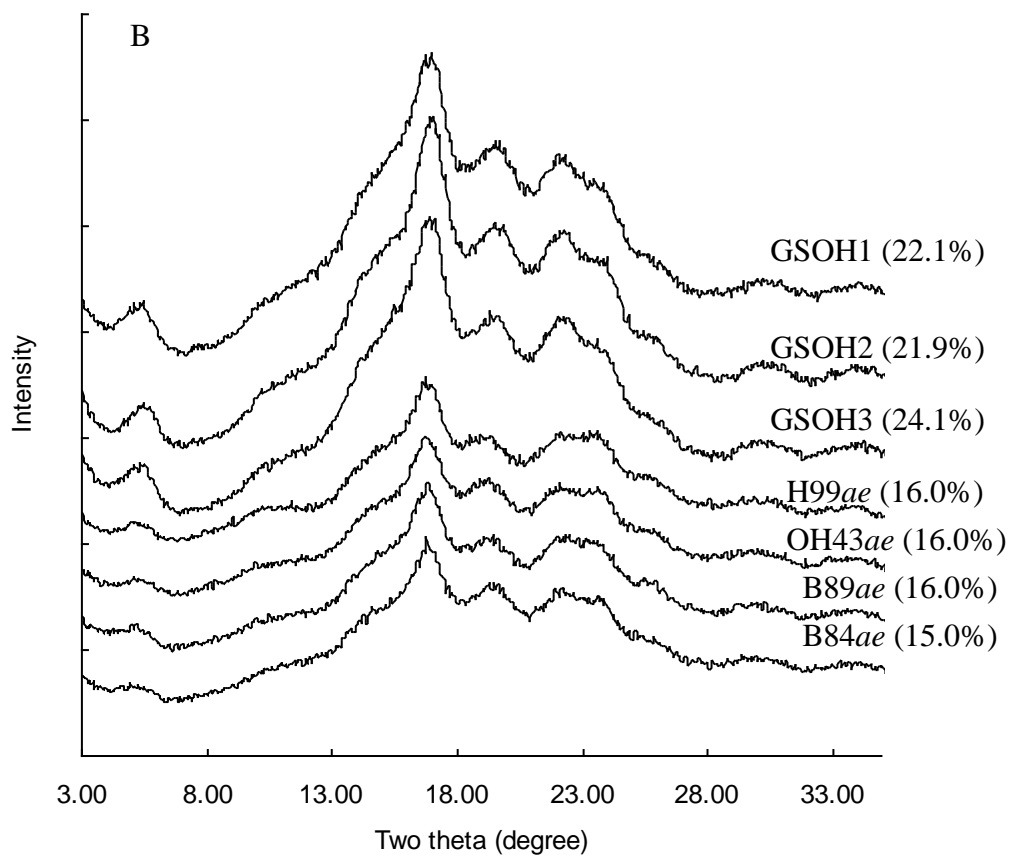
*Corresponding author:  Tel.: 01 515-294-9892; Fax: 01 515-294-8181; E-mail address: jjane@iastate.edu (J. Jane)

## Abstract

The objective of this study was to understand the crystalline structures of maize *ae*-mutant starches by analyzing the structures and properties of their Naegeli dextrins. After an exhaustive acid-hydrolysis of the starch granules with sulfuric acid (15.3%, v/v) at 38 $^{o}$C for up to 102 days, the maize *ae*-mutant starches produced 18.3-39.5% Naegeli dextrins. The Naegeli dextrins showed the B-type polymorph and displayed similar onset (45.1-51.4 $^{o}$C), peak (113.9-122.2 $^{o}$C), and conclusion (148.0-160.0 $^{o}$C) gelatinization temperatures and large enthalpy-changes (21.8-31.3 J/g) and percentage crystallinity (77.0-79.2%). The Naegeli dextrins showed unimodal molecular-size distributions with the peak molecular-size at degree of polymerization (DP) 16. The molecular-size distributions of the Naegeli dextrins did not significantly change after debranching with isoamylase, indicating predominantly linear molecules. The isoamylase-treated Naegeli dextrins had average chain-lengths of DP

23.8-27.5 and large proportions of long chains (DP $\geq$ 25, 36.7-52.7%), resulting from hydrolysis of amylose double helices.

**Keywords:** *ae*-mutant maize; High-amylose starch; Acid hydrolysis; Naegeli dextrin; Starch crystalline structure; Amylose double helices

## 1. Introduction

Acid hydrolysis of native starch granules has been commonly used to study the crystalline structures of starch granules (Robin et al., 1974; Robin et al., 1975; Biliaderis et al., 1981; Jane et al., 1997; Jacobs et al., 1998; Hoover, 2000; Wang & Wang, 2001; Gerard et al., 2002; Srichuwong et al., 2005; Li et al., 2007). Sulfuric acid and hydrochloric acid are used for the purpose, and the remaining starch residues after a prolonged hydrolysis at a moderate temperature are known as the Naegeli dextrin and Lintnerized starch, respectively (Hoover, 2000). Acid hydrolysis of starch granules shows two distinct rates during the course of the hydrolysis. The fast hydrolytic rate in the early stage is attributed to hydrolysis of amorphous starch in the starch granule, whereas the slower hydrolytic rate taking place later is slow erosion of the edge of crystalline starch in the starch granule. After the prolonged acid hydrolysis of starch granules, the remaining starch is considered as starch crystallites present in the starch granules, which resists acid hydrolysis (Kainuma & French, 1971; Robin et al., 1974; Robin et al., 1975; Biliaderis et al., 1981; Jane et al., 1997; Planchot et al., 1997; Jacobs et al., 1998; McPherson & Jane, 1999; Hoover, 2000; Perera et al., 2001; Wang & Wang, 2001; Srichuwong et al., 2005; Li et al., 2007).

A public high-amylose maize line registered as GEMS-0067 (PI 643420) was developed using germplasm obtained from USDA-ARS Germplasm Enhancement of Maize (GEM) project (Campbell et al., 2007). GEMS-0067 is an inbred maize line homozygous for the recessive amylose-extender (*ae*) and high-amylose modifier (HAM) genes (Campbell et al., 2007; Wu et al., 2009). Part I of this study reported that GEMS-0067 *ae*-line starches consisted of a significantly larger resistant-starch (RS) contents (39.4-43.2%) than maize *ae* single-mutant starches of H99*ae*, OH43*ae*, B89*ae*, and B84*ae* (11.5%-19.1%) (Li et al., 2008). Results of the part II study (Jiang et al., 2010a) demonstrated that long-chain double-helices of amylose/intermediate component (IC) retained semi-crystalline structures at 95-100 °C, which were resistant to enzymatic hydrolysis. Microscopic studies showed fusions between adjacent small granules in the amyloplast, likely through amylose interaction, to develop elongated starch granules (Jiang et al., 2010b). On the basis of these findings, Jiang et al. (2010a) proposed that the long-chain double-helical crystallites of amylose/IC molecules were present in the granules of native maize *ae*-mutant starches.

In the present study, we aimed to understand the starch crystalline structures present in the granules of the GEMS-0067 *ae*-line starches and the existing *ae*-line starches of H99*ae*, OH43*ae*, B89*ae*, and B84*ae*. To achieve this goal, we analyzed the contents and structures of the Naegeli dextrins obtained after prolonged acid hydrolysis of the native starch granules.

## 2. Materials and methods

### 2.1. Materials

Maize kernels of three GEMS-0067 *ae*-lines, GUAT209:S13×(OH43*ae*×H99*ae*) B-B-4-1-2-1-1 (GSOH 1), GUAT209:S13×(OH43*ae*×H99*ae*) B-B-4-4-2-1-1 (GSOH 2), and

GUAT209:S13×(OH43*ae*×H99*ae*) B-B-4-4-2-1-2 (GSOH 3), and four existing *ae*-lines of

H99*ae*, OH43*ae*, B89*ae*, and B84*ae*, were obtained from the USDA-ARS Germplasm

Enhancement of Maize (GEM) project at Truman State University (Kirksville, MO). These

GEMS-0067 *ae*-lines were F6 generation of GEMS-0067-derived maize *ae*-lines (Campbell

et al., 2007). All chemicals were reagent grade and obtained from Sigma-Aldrich Co. (St.

Louis, MO) or Fisher Scientific (Pittsburgh, PA). Crystalline *Pseudomonas* isoamylase (EC

3.2.1.68) obtained from Hayashibara Biochemical Laboratories, Inc. (Okayama, Japan) was

used for debranching the Naegeli dextrins.

## 2.2. Starch isolation

Endosperm starch was isolated from maize kernels using the method as described by

Li et al. (2008).

## 2.3. Acid hydrolysis of starch granules

Acid hydrolysis of starch granules was done following the method described by Jane

et al. (1997). Starch (5.0 g, dsb) was suspended in 100 mL of sulfuric acid (15.3%, v/v) and

incubated at 38 °C in a water bath. Starch suspensions were gently shaken daily by hand.

Starch suspensions (1.5 mL for each) were sampled on 2, 4, 6, 8, 10, 12, 21, 67, and 102 days

of acid hydrolysis, and centrifuged at 1000 *g* for 20 min. The supernatant was analyzed for

the total carbohydrate content to determine the degree of starch hydrolysis (Dubois et al.,

1956; Jane et al., 1997). The Naegeli dextrin remaining after 102 days of acid hydrolysis was

collected, washed by suspending it in an aqueous ethanol solution (50%, v/v, 40 mL) with

gentle shaking for 5 min, and centrifuged at 1000 *g* for 20 min. The supernatant was

discarded. The washing procedure was repeated until the supernatant reached pH ~6.0. The washed Naegeli dextrins were dehydrated by washing with 100% ethanol (40 mL) three times and dried at 37 °C for 24 h.

## 2.4. Molecular-size distributions of Naegeli dextrins before and after debranching

The prepared Naegeli dextrin (20.0 mg) was wetted with deionized distilled-water (0.2 mL), dispersed in dimethyl sulfoxide (DMSO) (1.8 mL) in a boiling-water bath for 1h, mechanically stirred at 25 °C for 16 h, precipitated with 20 volumes of ethanol, collected by centrifugation, and then dispersed in boiling water (9.0 mL) with mechanical stirring for 30 min. The dispersed Naegeli dextrin (4.5 mL) was mixed with an acetate buffer solution (0.5 mL, pH 3.5, 100 mM) and debranched using isoamylase (5 units) at 40 °C for 16 h following the method described by Li et al. (2008). The debranched sample was adjusted to pH 7 using a sodium hydroxide solution (0.5M), heated in a boiling-water bath for 15 min to inactivate the enzyme, and filtered through a membrane filter (1.2 μm pore size). The dispersed Naegeli dextrins and debranched Naegeli dextrins (80 μL for each, 2 mg/mL) were dried at 45 °C using a centrifugal vacuum evaporator for 3 h, labeled with 8-aminopyrene-1,3,6-trisulfonic acid (APTS, Cat. No. 09341, Sigma, St. Louis, MO), and analyzed using a fluorophore-assisted capillary-electrophoresis (FACE) (P/ACE MDQ, Beckman Coulter, Fullerton, CA) following the method of Jiang et al. (2010a).

## 2.5. X-ray diffractometry

The Naegeli dextrins obtained after acid hydrolysis of the starch granules for 102 days were equilibrated in a chamber with 100% relative humidity at 25 °C for 24 h. X-ray diffraction patterns and the percentage crystallinity of the Naegeli dextrins were determined using an X-ray diffractometer (D-500, Siemens, Madison, WI) with copper $K_\alpha$ radiation (Ao & Jane, 2007).

*2.6. Thermal properties of Naegeli dextrins*

Thermal properties of the Naegeli dextrins were analyzed using a differential scanning calorimeter (DSC) (DSC-7, Perkin-Elmer, Norwalk, CT) (Kasemsuwan et al., 1995). The Naegeli dextrin (~10.0 mg, dry basis) was mixed with ~30 µL of deionized distilled-water, sealed in a stainless-steel pan, and equilibrated at 25 °C overnight. The equilibrated sample was heated in the DSC from 10 to 180 °C at a rate of 10 °C/min. A sealed empty stainless-steel pan was used as the reference. Onset ($T_o$), peak ($T_p$), and conclusion ($T_c$) temperatures and enthalpy change ($\Delta H$) of starch gelatinization were obtained using Pyris software (Perkin-Elmer, Norwalk, CT).

## 3. Results and discussion

*3.1. Acid hydrolysis of starch granules*

Acid hydrolysis curves of *ae*-mutant- and normal-maize starches using sulfuric acid (15.3%, v/v) at 38 °C are shown in Fig. 1. The degrees of hydrolysis and hydrolysis rates of starches are summarized in Table 1. Biphasic patterns of hydrolysis were observed for all the starches, which were in agreement with previous reports (Jane et al., 1997; Jacobs et al., 1998;

Hoover, 2000; Srichuwong et al., 2005). As shown in Fig. 1 and Table 1, all the starches were rapidly hydrolyzed during the first 6 days of the acid hydrolysis with rates of 5.4-9.0% per day, which were attributed to hydrolysis of the amorphous starch in the granules. Slower hydrolysis rates (1.1-2.3% per day) observed from the $7^{th}$ to the $21^{st}$ day were likely erosion of the edge of crystalline starch in the granules (Robin et al., 1974; Robin et al., 1975; Biliaderis et al., 1981; Jacobs et al., 1998; Wang & Wang, 2001; Srichuwong et al., 2005; Li et al., 2007). The hydrolysis rates either reached plateaus or were very slow after 21 days. Factors that cause slow down and eventually stop the acid-hydrolysis of the crystalline starch in the granules have been proposed by Kainuma and French (1971); and they are 1) the dense packing of the starch molecules in the crystalline region reduces the penetration of hydronium ions; 2) the glucosidic bonds are buried in the interior of the double helix where the hydronium ions cannot readily reach; and 3) the glucose unit in the crystallite is in the $^{4}C_{1}$ chair conformation, which requires large activation energy to change to a half-chair conformation in order to be hydrolyzed (Kainuma & French, 1971).

GEMS-0067 *ae*-line starches were hydrolyzed by sulfuric acid at a slower rate than the existing *ae*-line starches and the normal maize starch (Fig. 1 and Table 1). The yields of the Naegeli dextrins were 37.4-39.5%, 18.3-26.7%, and 7.2% for the GEMS-0067 *ae*-line, the existing *ae*-line, and the normal maize starches, respectively (Table 1). The yields of the Naegeli dextrins were significantly correlated (r = 0.97, $p < 0.0001$) with the apparent-amylose contents of the starches reported by Jiang et al. (2010a). These results indicated that the increase in the Naegeli dextrin yield of GEMS-0067 *ae*-line starch resulted from the large quantity of long-chain double-helices of amylose/IC in the GEMS-0067 *ae*-line starch (Jiang et al., 2010a). This finding agreed with previous reports showing that starch granules with

greater amylose-contents were less susceptible to the acid hydrolysis (Jane et al., 1997; Shi et al., 1998). Depending on the source of the starch, native starch granules differ in their susceptibilities to the acid hydrolysis (Srichuwong et al., 2005). The A-type polymorph starch is hydrolyzed faster and to a greater extent than the B-type polymorph starch ( Kainuma & French, 1971; Robin et al., 1974; Robin et al., 1975; Jane et al., 1997; Srichuwong et al., 2005).

*3.2. Molecular-size distributions of Naegeli dextrins before and after debranching*

Molecular-size distributions of the Naegeli dextrins prepared after 102 days of acid hydrolysis are shown in Fig. 2. All the Naegeli dextrins showed unimodal molecular-size distributions with the peak molecular-size at degree of polymerization (DP) 16. The Naegeli dextrins were debranched with isoamylase, and the normalized molecular-size distributions of the debranched Naegeli dextrins in comparison with that of the counterparts without debranching are shown in Fig. 3. The normalized molecular-size distributions of the isoamylase-debranched Naegeli dextrins were similar to that of the Neageli dextrin counterparts without debranching except a slight increase in chains of DP 21-50 and a complementary decrease in chains of DP 11-20 (Fig. 3). The similarity of the branch-chain length distribution before and after debranching reaction indicated that the Naegeli dextrins consisted of primarily linear molecules. The slight increase in chains of DP 21-50 could be results of debranching of IC that was present in amylose/IC crystallites. This result agreed with previous report showing that the B-type polymorph starch had fewer branch-linkages located in the crystalline region of the starch granule, which were protected from acid hydrolysis (Jane et al., 1997).

The chain length distributions of the debranched Naegeli dextrins, which were all linear molecules and precisely reflected the lengths of the double helices of the Naegeli dextrins, were calculated and are summarized in Table 2. The debranched Naegeli dextrins consisted of chains of DP ≤ 12 (8.6-11.2%), DP 13-24 (38.7-54.1%), DP 25-36 (23.6-30.6%), and DP ≥ 37 (13.1-22.1%). The average chain lengths of the debranched Naegeli dextrins were between DP 23.8 and 27.5 (Table 2), which were substantially larger than that of debranched Naegeli dextrins and Lintnerized starches of the normal and *ae-waxy* starches (DP 13-16) (Jane et al., 1997; Perera et al., 2001; Srichuwong et al., 2005). The short double helices (DP < 25) (Fig. 3) of the Naegeli dextrins were mainly crystalline double-helical branch chains of amylopectin (Jane et al., 1997).

It is known that the Naegeli dextrins of retrograded amylose obtained after a prolonged acid hydrolysis has average DP 31, ranging from DP 25 to 50 (Jane & Robyt, 1984). The debranched Naegeli dextrins of the normal, waxy, and *ae* waxy maize starches have chain lengths mainly distributed between DP 6 and 25 (Jane et al., 1997), which are crystalline double-helical branch chains of the amylopectin (Jane et al., 1992; Kasemsuwan & Jane, 1994). Thus, the long chains of DP ≥ 25 in the debranched Naegeli dextrins of the maize *ae*-mutant starches (Fig. 3) could be attributed to the amylose double helices (Jiang et al., 2010a). The presence of amylose double helices in the Naegeli dextrins agreed with the high conclusion gelatinization-temperatures of the native maize *ae*-mutant starches (Li et al., 2008) and their RS residues obtained after digesting the maize *ae*-mutant starches with thermally stable α-amylase at 95-100 °C (Jiang et al., 2010a).

*3.3. X-ray diffraction patterns of Naegeli dextrins*

The X-ray diffraction patterns of the Naegeli dextrins obtained after a prolonged acid hydrolysis of the maize *ae*-mutant starch granules are shown in Fig. 4. All the Naegeli dextrins displayed the B-type polymorphic pattern and had percentages of crystallinity 77.0-79.2%, which were substantially greater than their native starch counterparts (22.8-33.0%) reported by Jiang et al. (2010a). The large percentages of crystallinity of the Naegeli dextrins (Fig. 4) suggested that the amorphous starch in the granules was mostly removed and the crystallites of double helices were retained after the prolonged acid hydrolysis. There were no peaks at 8°, 13°, and 20° (Zobel et al., 1967; Zobel, 1988) observed in the Naegeli dextrins (Fig. 4), indicating no crystalline amylose-lipid complex present in the Naegeli dextrins. This result was consistent with no crystalline amylose-lipid complex found in the native starch counterparts (Jiang et al., 2010a).

*3.4. Thermal properties of Naegeli dextrins*

DSC thermograms of the Naegeli dextrins are shown in Fig. 5. All the Naegeli dextrins displayed similar broad thermal-transitions with onset, peak, and conclusion gelatinization-temperatures of 45.1-51.4 $^{o}$C, 113.9-122.2 °C, and 148.0-160.0 °C, respectively (Table 3). The thermal-transition temperature ranges of the Naegeli dextrins were similar to those of the Lintnerized high-amylose maize starches as previously reported (Shi et al., 1998). The broad thermal-transition temperature ranges agreed with the broad chain-length distributions of the debranched Naegeli dextrins (Fig. 3).

The Naegeli dextrins of the GEMS-0067 *ae*-line starches displayed slightly higher gelatinization temperatures than that of the existing *ae*-line starches (Table 3). These results

were consistent with the longer double helices of the Naegeli dextrins of the GEMS-0067 *ae*-line starches than that of the existing *ae*-line starches (Table 2).

The very high temperatures for the peak (113.9-122.2 °C) and the conclusion gelatinization-temperatures (148.0-160.0 °C) of the Naegeli dextrins (Table 3) were attributed to their long double helices (Table 2 and Fig. 3). It has been reported that the onset, peak, and conclusion temperatures of the retrograded amylose were 131.9, 150.0, and 161.8 °C, respectively (Sievert & Pomeranz, 1989). Thus, the high conclusion gelatinization-temperatures of the Naegeli dextrins agreed with the presence of the amylose double helices.

The enthalpy changes of the Naegeli dextrins ranged from 21.8 to 31.3 J/g (Table 3), which were substantially larger than their native starch counterparts (11.7-17.4 J/g) (Li et al. 2008), indicating that the amorphous starch in the granules was mostly removed after the prolonged acid hydrolysis. Therefore, the Naegeli dextrins obtained after 102 days of acid hydrolysis of the starch granules were highly ordered crystallites of double helices.

## 4. Conclusions

After a prolonged acid hydrolysis, GEMS-0067 *ae*-line starches produced substantially larger yields of Naegeli dextrins than the existing *ae*-line starches, which were attributed to the greater amylose contents in the GEMS-0067 *ae*-line starches. All the Naegeli dextrins displayed the B-type polymorph and had highly crystalline structures of double helices. All the Naegeli dextrins consisted of essentially linear molecules and showed unimodal molecular-size distributions with the peak molecular-size at DP 16. The average chain-lengths of the double helices in the Naegeli dextrins were between DP 23.8 and 27.5. All the Naegeli dextrins displayed similar gelatinization-temperatures of 45.1-51.4 °C, 113.9-

122.2 $^{\circ}$C, and 148.0-160.0 $^{\circ}$C for $T_o$, $T_p$, and $T_c$, respectively. Results of this study supported the presence of amylose double-helical crystallites in the native maize *ae*-mutant starches, which contributed to the resistance of enzymatic hydrolysis at 95-100 °C.

**Acknowledgements**

**References**

Ao, Z., & Jane, J. (2007). Characterization and modeling of the A- and B-granule starches of wheat, triticale, and barley. *Carbohydrate Polymers, 67*, 46-55.

Biliaderis, C. G., Grant, D. R., & Vose, J. R. (1981). Structural characterization of legume starches. II. Studies on acid-treated starches. *Cereal Chemistry, 58*, 502-507.

Campbell, M. R., Jane, J., Pollak, L., Blanco, M., & O'Brien, A. (2007). Registration of maize germplasm line GEMS-0067. *Journal of Plant Registrations, 1*, 60-61.

Dubois, M., Gilles, K. A., Hamilton, J. K., Rebers, P. A., & Smith, F. (1956). Colorimetric method for determination of sugars and related substances. *Analytical Chemistry, 28*, 350-356.

Gerard, C., Colonna, P., Buleon, A., & Planchot, V. (2002). Order in maize mutant starches revealed by mild acid hydrolysis. *Carbohydrate Polymers, 48*, 131-141.

Hoover, R. (2000). Acid-treated starches. *Food Reviews International, 16*, 369-392.

Jacobs, H., Eerlingen, R. C., Rouseu, N., Colonna, P., & Delcour, J. A. (1998). Acid

hydrolysis of native and annealed wheat, potato and pea starches - DSC melting features and chain length distributions of lintnerized starches. *Carbohydrate Research, 308*, 359-371.

Jane, J., Wong, K.-S., & McPherson, A. E. (1997). Branch-structure difference in starches of A- and B-type x-ray patterns revealed by their Naegeli dextrins. *Carbohydrate Research, 300*, 219-227.

Jane, J., & Robyt, J. F. (1984). Structure studies of amylose-V complexes and retrograded amylose by action of alpha amylases, and a new method for preparing amylodextrins. *Carbohydrate Research, 132*, 105-118.

Jane, J., Xu, A., Radosavljevic, M., & Seib, P. A. (1992). Location of amylose in normal starch granules. I. Susceptibility of amylose and amylopectin to cross-linking reagents. *Cereal Chemistry, 69*, 405-409.

Jiang, H., Campbell, M., Blanco, M., & Jane, J. (2010a). Characterization of maize amylose-extender (*ae*) mutant starches. Part II: Structures and properties of starch residues remaining after enzymatic hydrolysis at boiling-water temperature. *Carbohydrate Polymers*, *80*, 1-12.

Jiang, H., Horner, H. T., Pepper, T. M., Blanco, M., Campbell, M., & Jane, J. (2010b). Formation of elongated starch granules in high-amylose maize. *Carbohydrate Polymers*, *80*, 534-539.

Kainuma, K., & French, D. (1971). Naegeli amylodextrin and its relation to starch granule structure. I. Preparation and properties of amylodextrins from various starch types. *Biopolymers, 10*, 1673-1680.

Kasemsuwan, T., & Jane, J. (1994). Location of amylose in normal starch granules. II.

Locations of phosphodiester crosslinking revealed by phosphorus-31 nuclear magnetic resonance. *Cereal Chemistry, 71*, 282-287.

Kasemsuwan, T., Jane, J., Schnable, P., Stinard, P., & Robertson, D. (1995). Characterization of the dominant mutant amylose-extender (Ae1-5180) maize starch. *Cereal Chemistry, 72*, 457-464.

Li, L., Jiang, H., Campbell, M., Blanco, M., & Jane, J. (2008). Characterization of maize amylose-extender (*ae*) mutant starches. Part I: Relationship between resistant starch contents and molecular structures. *Carbohydrate Polymers, 74*, 396-404.

Li, W., Corke, H., & Beta, T. (2007). Kinetics of hydrolysis and changes in amylose content during preparation of microcrystalline starch from high-amylose maize starches. *Carbohydrate Polymers, 69*, 398-405.

McPherson, A. E., & Jane, J. (1999). Comparison of waxy potato with other root and tuber starches. *Carbohydrate Polymers, 40*, 57-70.

Perera, C., Lu, Z., Sell, J., & Jane, J. (2001). Comparison of physicochemical properties and structures of *sugary-2* cornstarch with normal and waxy cultivars. *Cereal Chemistry, 78*, 249-256.

Planchot, V., Colonna, P., & Buleon, A. (1997). Enzymatic hydrolysis of alpha-glucan crystallites. *Carbohydrate Research, 298*, 319-326.

Robin, J. P., Mercier, C., Charbonniere, R., & Guilbot, A. (1974). Lintnerized starches. Gel filtration and enzymic studies of insoluble residues from prolonged acid treatment of potato starch. *Cereal Chemistry, 51*, 389-406.

Robin, J. P., Mercier, C., Duprat, F., Charbonniere, R., & Guilbot, A. (1975). Lintnerized

starches. Chromatographic and enzymic studies of insoluble residues from hydrochloric acid hydrolysis of cereal starches, particularly waxy maize starch. *Starch/Staerke, 27*, 36-45.

Shi, Y.-C., Capitani, T., Trzasko, P., & Jeffcoat, R. (1998). Molecular structure of a low-amylopectin starch and other high-amylose maize starches. *Journal of Cereal Science, 27*, 289-299.

Sievert, D., & Pomeranz, Y. (1989). Enzyme-resistant starch. I. Characterization and evaluation by enzymic, thermoanalytical, and microscopic methods. *Cereal Chemistry, 66*, 342-347.

Srichuwong, S., Isono, N., Mishima, T., & Hisamatsu, M. (2005). Structure of Lintnerized starch is related to X-ray diffraction pattern and susceptibility to acid and enzyme hydrolysis of starch granules. *International Journal of Biological Macromolecules, 37*, 115-121.

Wang, L., & Wang, Y.-J. (2001). Structures and physicochemical properties of acid-thinned corn, potato and rice starches. *Starch/Staerke, 53*, 570-576.

Wu, Y., Campbell, M., Yen, Y., Wicks, Z., III, & Ibrahim, A. M. H. (2009). Genetic analysis of high amylose content in maize (Zea mays L.) using a triploid endosperm model. *Euphytica, 166*, 155-164.

Zobel, H. F. (1988). Starch crystal transformations and their industrial importance. *Starch/Staerke, 40*, 1-7.

Zobel, H. F., French, A. D., & Hinkle, M. E. (1967). X-ray diffraction of oriented amylose fibers. II. Structure of V-amyloses. *Biopolymers, 5*, 837-845.

Table 1
Acid-hydrolysis of maize starches

| Sample | Degree of hydrolysis (%) | | | Hydrolysis rate (% per day) | | Naegeli dextrin[a] |
|---|---|---|---|---|---|---|
| | 6 days | 21 days | 102 days | 0-6 days | 7-21 days | yield (%) |
| GSOH 1 | $32.3 \pm 0.2$ | $52.4 \pm 0.1$ | $62.3 \pm 0.6$ | 5.4 | 1.3 | $37.7 \pm 0.6$ |
| GSOH 2 | $33.0 \pm 1.2$ | $49.7 \pm 0.4$ | $60.5 \pm 0.9$ | 5.5 | 1.1 | $39.5 \pm 0.9$ |
| GSOH 3 | $34.2 \pm 0.2$ | $51.1 \pm 0.8$ | $62.6 \pm 0.5$ | 5.7 | 1.1 | $37.4 \pm 0.5$ |
| H99*ae* | $39.3 \pm 2.4$ | $64.0 \pm 1.3$ | $73.3 \pm 0.1$ | 6.6 | 1.6 | $26.7 \pm 0.1$ |
| OH43*ae* | $44.9 \pm 0.5$ | $67.4 \pm 0.2$ | $81.7 \pm 2.5$ | 7.5 | 1.5 | $18.3 \pm 2.5$ |
| B89*ae* | $41.7 \pm 1.3$ | $65.6 \pm 0.5$ | $76.1 \pm 0.8$ | 7.0 | 1.6 | $23.9 \pm 0.8$ |
| B84*ae* | $42.0 \pm 0.1$ | $66.7 \pm 0.4$ | $75.1 \pm 1.4$ | 7.0 | 1.6 | $24.9 \pm 1.4$ |
| Normal maize | $54.1 \pm 0.7$ | $88.4 \pm 0.0$ | $92.8 \pm 1.5$ | 9.0 | 2.3 | $7.2 \pm 1.5$ |

[a] Naegeli dextrin was the residue remaining after sulfuric acid (15.3%, v/v) hydrolysis of starch granules at 38 °C for 102 days.

Table 2
Molecular-size distributions of debranched Naegeli dextrins[a, b]

| Sample | DP≤12[c] | DP13-24 | DP25-36 | DP≥37 | Average DP |
|--------|--------|--------|--------|--------|--------|
| GSOH 1 | 11.2 ± 0.2 | 42.9 ± 0.1 | 28.0 ± 0.7 | 17.9 ± 0.6 | 25.6 ± 0.3 |
| GSOH 2 | 8.6 ± 0.2 | 38.7 ± 0.7 | 30.6 ± 0.7 | 22.1 ± 1.5 | 27.5 ± 0.7 |
| GSOH 3 | 9.3 ± 0.1 | 40.0 ± 0.1 | 28.9 ± 0.2 | 21.8 ± 0.4 | 27.3 ± 0.2 |
| H99*ae* | 9.5 ± 0.1 | 52.9 ± 0.8 | 24.4 ± 0.1 | 13.2 ± 0.8 | 23.8 ± 0.2 |
| OH43*ae* | 8.7 ± 0.1 | 49.3 ± 0.1 | 26.9 ± 0.2 | 15.1 ± 0.2 | 24.9 ± 0.1 |
| B89*ae* | 9.2 ± 0.1 | 54.1 ± 0.9 | 23.6 ± 0.0 | 13.1 ± 1.0 | 23.9 ± 0.3 |
| B84*ae* | 9.5 ± 0.3 | 51.8 ± 1.1 | 25.1 ± 0.0 | 13.6 ± 0.7 | 24.1 ± 0.2 |

[a] Naegeli dextrin was the residue remaining after sulfuric acid (15.3%, v/v) hydrolysis of starch granules at 38 °C for 102 days.
[b] The molecular-size distributions of debranched Naegeli dextrins were analyzed using a fluorophore-assisted capillary-electrophoresis.
[c] DP = degree of polymerization.

Table 3
Thermal properties of Naegeli dextrins[a, b]

| Sample | $T_o$ (°C) | $T_p$ (°C) | $T_c$ (°C) | $\Delta H$ (J/g) |
|---|---|---|---|---|
| GOSH 1 | 51.2 ± 0.8 | 122.2 ± 0.0 | 158.3 ± 0.3 | 27.1 ± 1.0 |
| GOSH 2 | 51.3 ± 0.1 | 121.9 ± 0.1 | 158.3 ± 0.7 | 29.1 ± 0.7 |
| GOSH 3 | 51.4 ± 0.2 | 122.0 ± 0.1 | 160.0 ± 0.0 | 31.3 ± 1.3 |
| H99*ae* | 45.1 ± 0.0 | 119.0 ± 0.5 | 156.5 ± 1.5 | 28.5 ± 1.5 |
| OH43*ae* | 50.5 ± 0.5 | 113.9 ± 0.2 | 148.3± 1.8 | 21.8 ± 0.6 |
| B89*ae* | 51.0 ± 0.0 | 115.5 ± 0.9 | 148.0 ± 2.0 | 22.0 ± 0.6 |
| B84*ae* | 50.5 ± 0.5 | 115.8 ± 0.9 | 154.1 ± 0.1 | 22.7 ± 1.6 |

[a] Naegeli dextrin was the residue remaining after sulfuric acid (15.3%, v/v) hydrolysis of starch granules at 38 °C  for 102 days.

[b] Samples (~10.0 mg, dry basis) and deionized distilled-water (~30.0 μL) were used for the analysis; $T_o$, $T_p$, $T_c$ and $\Delta H$ are onset, peak, and conclusion temperatures, and enthalpy change, respectively.
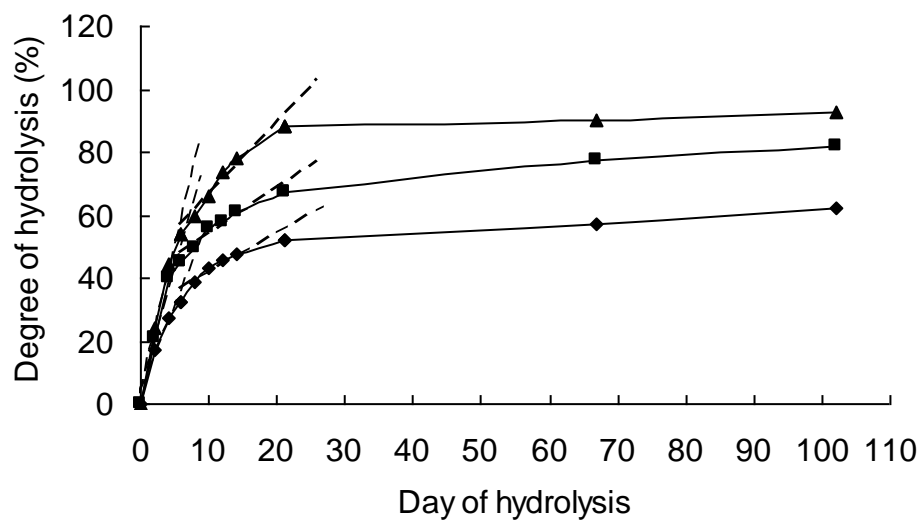
Fig. 1. Acid hydrolysis of starch granules of representative varieties with sulfuric acid (15.3%, v/v) at 38 °C. ◆, GSOH 1; ■, OH43*ae*; ▲, Normal maize. Dashed lines are trend lines for the fast and slow hydrolyses of the starch granules. The degree of hydrolysis was determined by measuring the soluble sugars in the supernatant.
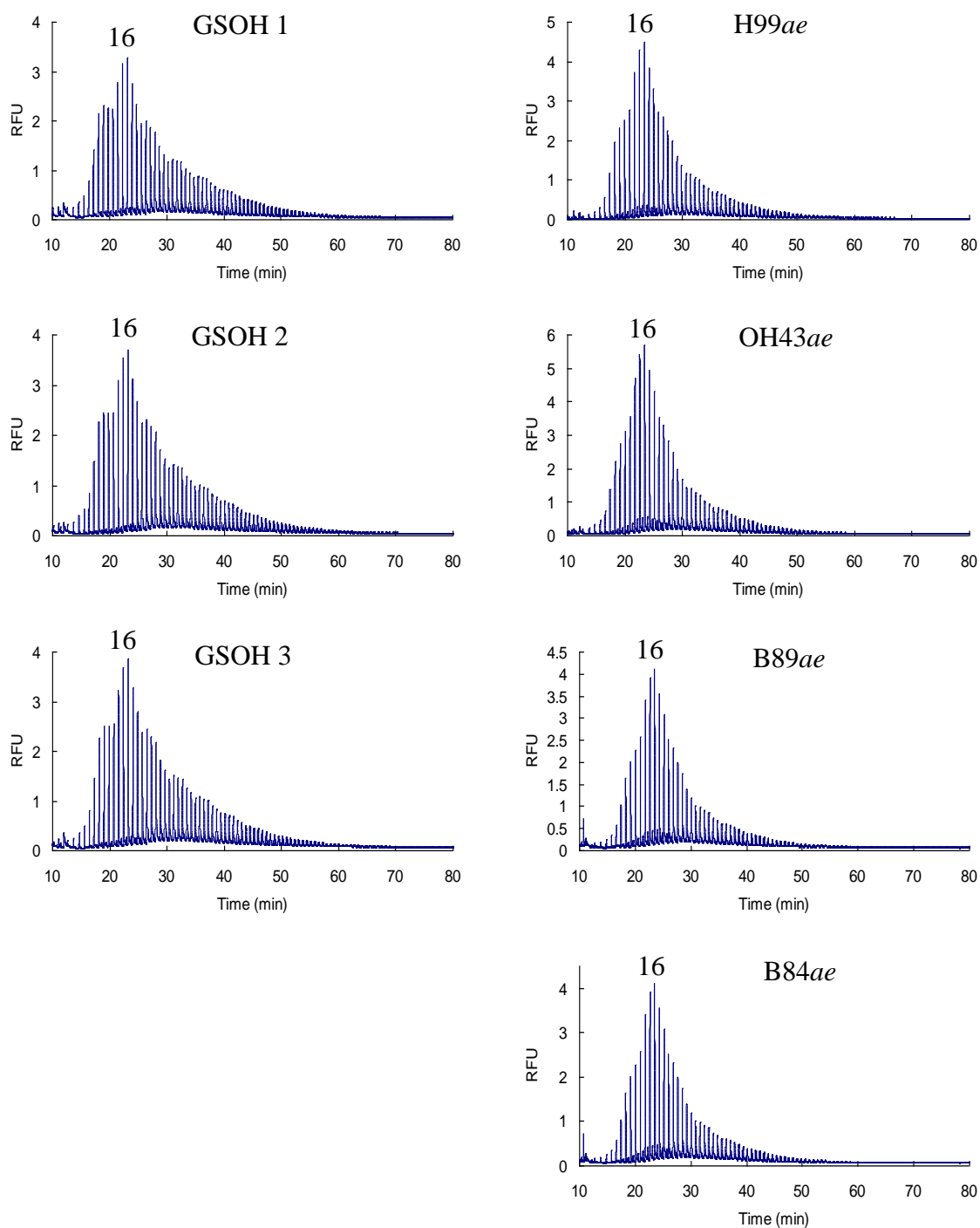
Fig. 2. Molecular-size distributions of Naegeli dextrins determined using a fluorophore-assisted capillary-electrophoresis. The Naegeli dextrins were prepared from sulfuric acid (15.3%, v/v) hydrolysis of maize *ae*-mutant starches at 38 °C for 102 days. RFU: relative fluorescence units. The peak molecular-size of the Naegeli dextrins was degree of polymerization (DP) 16.
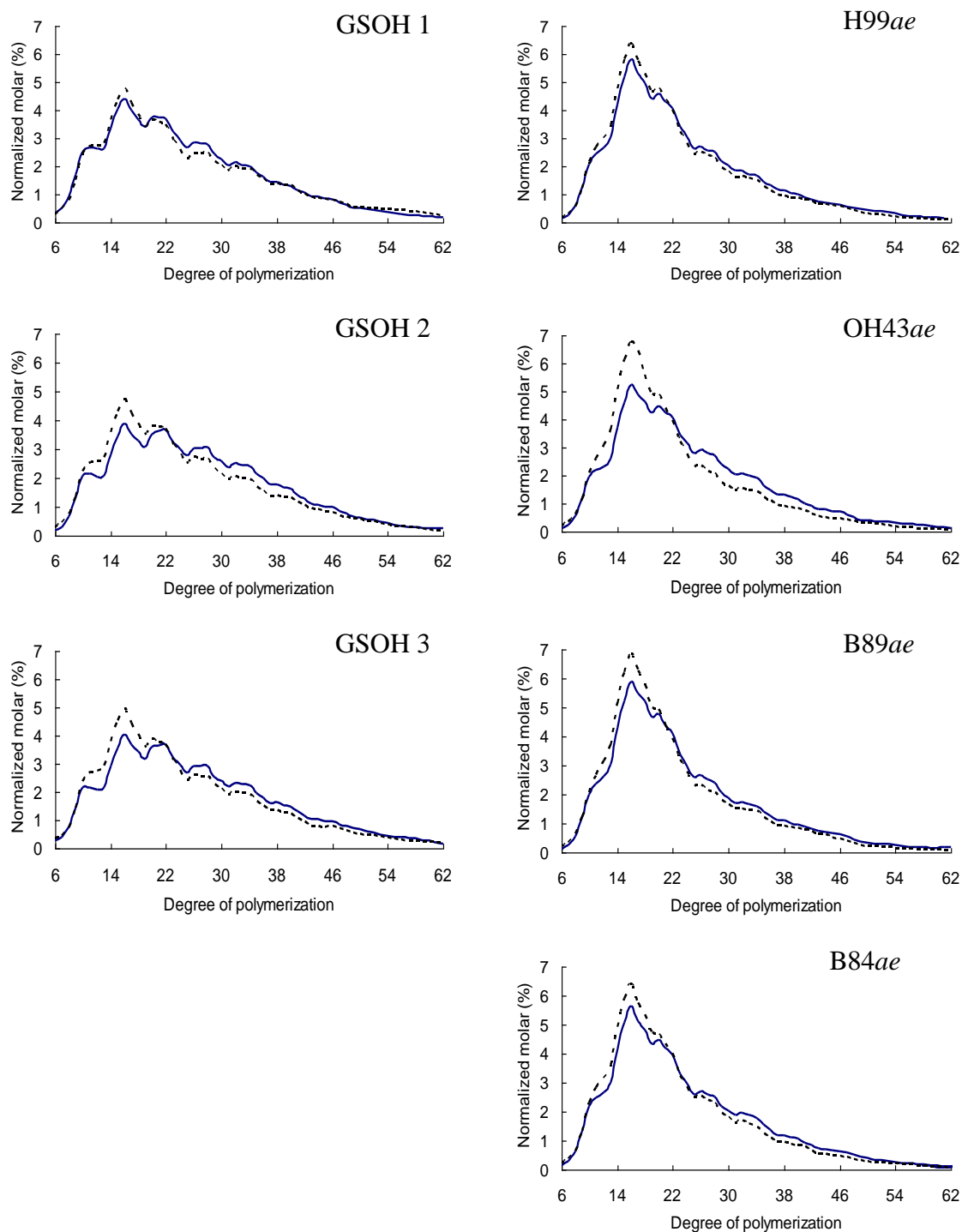
Fig. 3. Normalized molecular-size distributions of isoamylase-debranched Naegeli dextrins
( —— ) and the Naegeli dextrins without debranching (- - - -) determined using a
fluorophore-assisted capillary-electrophoresis. The Naegeli dextrins were prepared from
sulfuric acid (15.3%, v/v) hydrolysis of maize *ae*-mutant starches at 38 °C for 102 days.
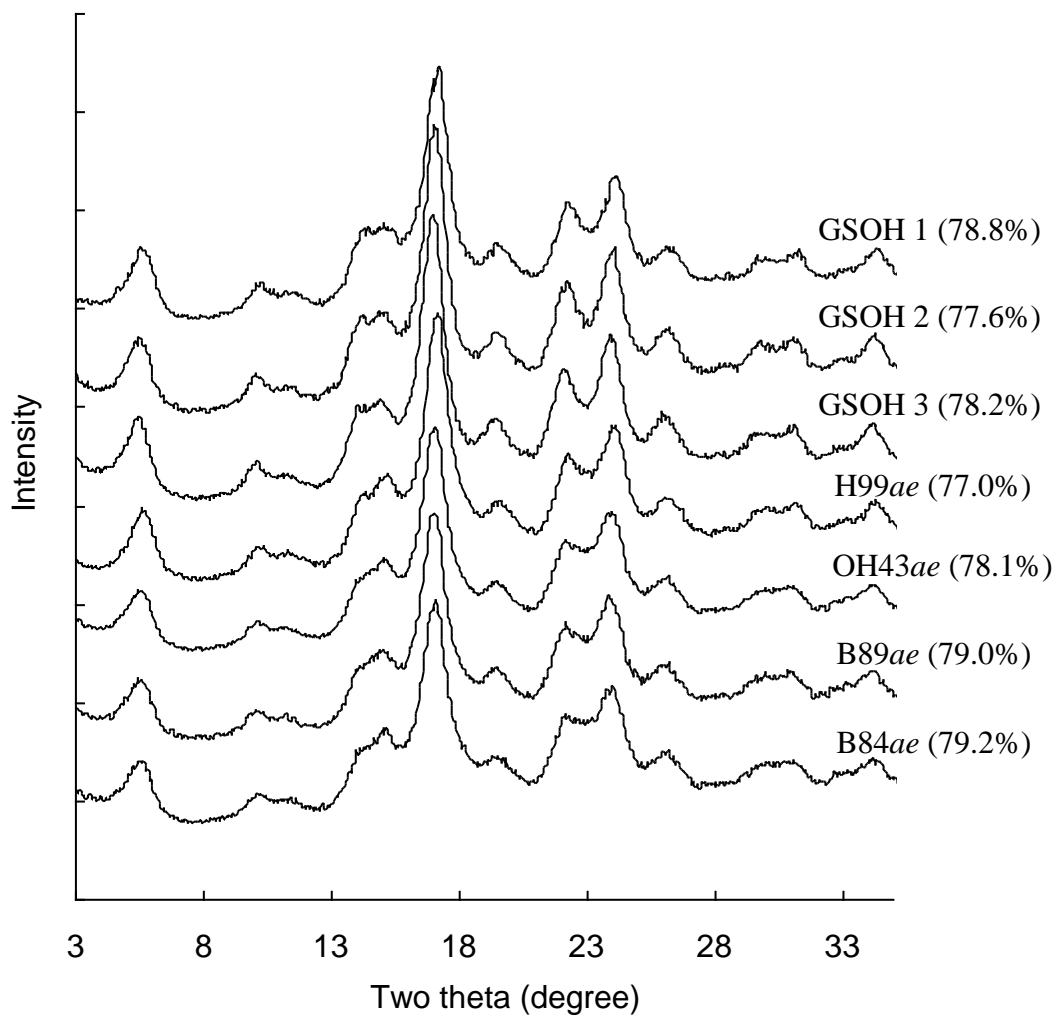
Fig. 4. X-ray diffraction patterns of Naegeli dextrins prepared from sulfuric acid (15.3%, v/v) hydrolysis of maize *ae*-mutant starches at 38 °C for 102 days. The percentage crystallinity is given in parentheses.
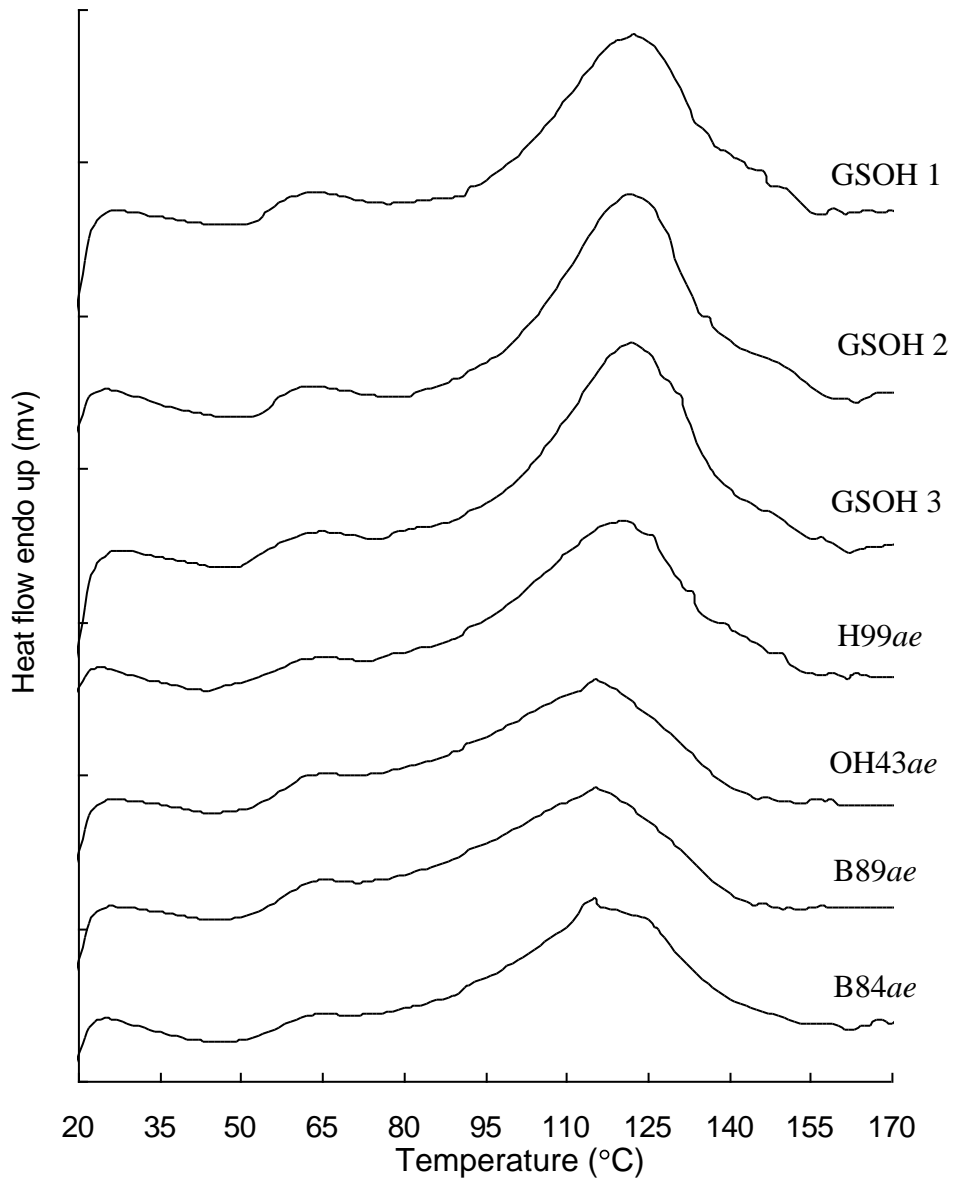
Fig. 5. DSC thermograms of Naegeli dextrins prepared from sulfuric acid (15.3%, v/v) hydrolysis of maize *ae*-mutant starches at 38 °C for 102 days.

# CHAPTER 3. RESISTANT-STARCH FORMATION IN HIGH-AMYLOSE MAIZE STARCH DURING KERNEL DEVELOPMENT

A paper to be submitted to the *Journal of Agricultural and Food Chemistry*

Hongxin Jiang,[†] Junyi Lio,[†] Mike Blanco,[‡] Mark Campbell,[§] Jay-lin Jane *[,†]

[†] Department of Food Science and Human Nutrition, Iowa State University, Ames, IA 50011, USA

[‡] USDA-ARS/Plant Introduction Station Research Unit, Ames, IA 50011, USA

[§] Division of Science, Truman State University, Kirksville, MO 63501, USA

*Corresponding author: Tel: 01 515-294-9892; Fax: 01 515-294-8181; E-mail address: jjane@iastate.edu (J. Jane)

**Abstract**

The objective of this study was to understand the resistant-starch (RS) formation during the kernel development of high-amylose maize, GEMS-0067 line. The RS content of the starch, determined using AOAC Method 991.43 for total dietary fiber, increased with the kernel maturation and the increase in amylose/intermediate component (IC) content of the starch. Gelatinization of the native starches showed a major thermal-transition with peak temperature at 76.6-81.0°C. An additional peak (~97.1°C) first appeared on 20 days after pollination and then developed to a significant peak on later dates. After removal of lipids from the starch, this peak disappeared but the conclusion gelatinization-temperature remained the same. The proportion of the enthalpy change of the thermal transition above 95°C, calculated from the thermogram of the defatted starch, increased with kernel maturation and significantly correlated with the RS content of the starch (r=0.98). These

results showed that the increase in the long-chain double-helical crystallites of amylose/IC in the starch resulted in the increase in the RS content of the starch during the kernel development.

**Keywords**: Resistant starch; High-amylose maize starch; *ae* mutant; Long-chain double helices; Amylose; Amylose-lipid complex; Kernel development

## INTRODUCTION

Resistant starch (RS) is a portion of starch that cannot be hydrolyzed by enzymes in human digestive tract and is fermented by bacteria in the large intestine. RS present in high-amylose maize starch has been reported to have many health benefits, including prevention of colon cancer, type II diabetes, obesity, and cardiovascular disease (*1-12*).

A new public high-amylose maize line, GEMS-0067 (PI 643420), was developed by Dr. Mark Campbell at Truman State University in Kirksville, MO, working cooperatively with the USDA-ARS Germplasm Enhancement of Maize (GEM) Project in Ames, IA. The GEMS-0067 maize line is a homozygous mutant of the amylose-extender (*ae*) gene and contains high-amylose modifier (HAM) gene(s) (*13*). GEMS-0067 starches consist of 83.1-85.6% apparent-amylose, greater than the maize *ae* single-mutant starches of H99*ae*, OH43*ae*, B89*ae*, and B84*ae* (61.7-67.7%) (*14*) and normal maize starch (~30%) (*15*). The RS contents of the GEMS-0067 starches, determined using thermally stable $\alpha$-amylase at 95-100°C (AOAC Method 991.43) (*16*), are 39.4-43.2%, which are higher than that of the maize *ae* single-mutant starches (11.5-19.1%) (*14*) and normal maize starch (~1.5%) (*17*). The RS content increases with the increase in the apparent-amylose content (*14*).

The GEMS-0067 starches consist of 22.6-32.0% elongated starch granules. These proportions of the elongated starch granules of the GEMS-0067 starches are much larger than the maize *ae* single-mutant starches (5.2-7.7%) (*18*) and normal maize starch (0%) (*19*). These elongated starch granules are formed by fusion of small granules through amylose interaction in the amyloplast at the early stage of granule development (*20*).

The RS in the maize *ae*-mutant starch is attributed to long-chain double-helical crystallites of amylose/intermediate component (IC) present in the starch granules. These amylose/IC crystallites, having high gelatinization temperature (>95°C), maintain semi-crystalline structures at 95-100°C and, thus, are resistant to enzyme hydrolysis by thermally stable α-amylase at 95-100°C (*14, 18, 21*). The objective of the current study was to understand RS formation during kernel development of the high-amylose maize GEMS-0067 line.

## MATERIALS AND METHODS

**Materials.** GEMS-0067 maize plants were grown in the field of the USDA-ARS North Central Regional Plant Introduction Station (NCRPIS) in Ames, IA in 2007 and 2009 crop years. Plants were self-pollinated by hand, and ears were harvested on 15, 20, 30, 40, and 54 (mature) days after pollination (DAP). Maize kernels were removed from ears and stored at -20 °C until analysis. All chemicals were reagent grade and were purchased from Sigma-Aldrich Chemical Co. (St. Louis, MO) or Fisher Scientific (Pittsburgh, PA).

**Starch isolation.** Starch was isolated from maize endosperms using the method reported by Li et al. (*14*).

**RS content of starch**. The RS content of native starch was determined using AOAC
Method 991.43 for total dietary fiber (*16*) as described by Li et al. (*14*).

**Amylose/IC content of starch.** Amylose/IC content of the starch was determined using
Sepharose CL-2B gel-permeation chromatography (GPC) (*22*) followed by total
carbohydrate (Phenol-sulfuric acid) (*23*) and blue value analyses (*24*).

**Lipid content of starch.** The lipid content of the starch was determined using 85%
methanol (v/v) extraction in a Soxhlet extractor for 24h (*25*). The starch samples after
removal of lipids were dried at 37°C overnight.

**Scanning electron microscopy (SEM).** GEMS-0067 starches obtained at different
kernel-developmental stages were coated with gold-palladium (60:40). SEM images of starch
granules were produced using a scanning electron microscope (JEOL 5800, www.jeol.com)
at 10 kV in the Microscopy and NanoImaging Facility at Iowa State University, Ames, IA
(*26*).

**X-ray diffractometry**. Native GEMS-0067 starches were equilibrated in a chamber with
100% relative humidity at 25 °C for 24 h. X-ray diffraction patterns of the starches were
determined using an X-ray diffractometer (D-500, Siemens, Madison, WI) with copper $K_\alpha$
radiation. The percentage crystallinity of starch was determined using the method described
previously (*26*).

**Thermal properties of starch.** Thermal properties of GEMS-0067 starches isolated from
kernels harvested at different developmental stages were analyzed using a differential
scanning calorimeter (DSC) (DSC-7, Perkin-Elmer, Norwalk, CT) as reported previously (*14,
27*). Starch (~6 mg, dry starch basis) was precisely weighed and mixed with 3 times (by
weight) of deionized distilled-water (~18 μL). The mixture was sealed in a stainless-steel pan

and equilibrated at 25 °C for 1h. The starch sample was then heated from 10 to 180 °C at a rate of 10°C/min. A sealed empty stainless-steel pan was used as the reference. Onset ($T_o$), peak ($T_p$), and conclusion ($T_c$) temperatures and enthalpy changes ($\Delta H$) of starch gelatinization were determined using Pyris software (Perkin-Elmer, Norwalk, CT).

## RESULTS AND DISCUSSION

**RS, amylopectin, amylose/IC, and lipid contents of starch.** The RS contents of the GEMS-0067 starches isolated from kernels harvested at different developmental stages in 2007 and 2009 growing seasons are shown in **Table 1**. The RS contents of the GEMS-0067 starches grown in both 2007 and 2009 crop years increased with kernel maturation and reached a plateau after 40 DAP.

Sepharose CL-2B gel-permeation chromatograms of the GEMS-0067 starches obtained at different developmental stages are shown in **Figure 1**. The amylopectin molecules were eluted between fractions 11 and 18, and the amylose/IC molecules were eluted between fractions 19 and 45 (**Figure 1**). It is known that normal maize starch consists of amylopectin and amylose molecules, whereas maize *ae*-mutant starch also contains IC molecules that have longer branch chains and smaller molecular weights than amylopectin. The molecular weight of the IC is similar to that of amylose molecules and, thus, the IC coeluted with amylose in the GPC profile (*14, 28-30*).

The amylose/IC contents of the GEMS-0067 starches obtained at different kernel-developmental stages are summarized in **Table 1**. The amylose/IC contents of the GEMS-0067 starches grown in both 2007 and 2009 crop years increased with kernel maturation and reached the plateau on around 40 DAP. This trend agreed with the result previously reported

for high-amylose maize (*31*) and was similar to the increase in amylose content of normal maize starch during the kernel development (*32*).

The RS content of the starch at different kernel-developmental stages increased with the increase in amylose/IC content, having correlation coefficients of 0.99 ($p < 0.001$) for both 2007 and 2009 crop years (**Table 1**). These results indicated that amylose/IC molecules were principal components for RS formation during the kernel development. It has been shown that amylose/IC molecules in high-amylose maize starch form long-chain double-helical crystallites (*18*), which were resistant to enzymatic hydrolysis at 95-100°C.

The lipid contents of the starches isolated at different kernel-developmental stages are summarized in **Table 1**. In general, the lipid contents of the starches grown in both 2007 and 2009 crop years increased with kernel maturation. It is known that lipids present in starch granules reduce the enzymatic hydrolysis of the granules at 95-100 °C (*18*).

**Morphology of starch granules.** SEM images of the GEMS-0067 starches are shown in **Figure 2**. All the GEMS-0067 starches obtained at different kernel-developmental stages consisted of mainly two types of starch granules, spherical and elongated, as previously reported (*18, 20, 31, 33*). Starch harvested on 15 DAP (**Figure 2A**) had smaller granule sizes and consisted of more spherical granules and fewer elongated granules than the starches harvested on later dates (**Figure 2B-E**). These morphological images showed that starch granules of 15 DAP were immature and were expected to further grow by apposition to increase the granule size. These small granules would eventually become the inner part of mature and large granules. The amylopectin content (calculated by subtracting the amylose/IC content from 100%) of the starch harvested on 15 DAP (44.8%) was much larger than those of the starches harvested on later dates (21.6-11.4%) (Calculated from **Table 1**).

These results indicated that amylopectin molecules were more concentrated at the core and inner part of the mature starch granule. The results agreed with previous reports of starch granule structures, showing that amylose molecules were more concentrated at the periphery of starch granules (*34-36*). Most starch granules harvested on 15 DAP (**Figure 2A'**) and a few granules in the starches harvested on later dates appeared to have a rough surface structure (**Figures 2B-E**). This feature was different from the smooth surface of the normal maize starch granules during kernel development (*14*). The rough surface of the GEMS-0067 starch granules could be attributed to amylose/IC crystallites of the starch, which lacked branch-chains to fill up the spherical surface (*26*).

Starch harvested on 15 DAP consisted of less amylose/IC content and a smaller proportion of elongated starch granules than the starches harvested on 20 DAP and later dates (**Table 1** and **Figures 2**). These results were consistent with previous reports showing that the proportion of the elongated starch granules increased with kernel maturation (*31*) and with the increase in the amylose content (*18, 20, 31*). It also has been reported that elongated starch granules consist of more RS (*18*).

**Crystallinity of starch granules.** X-ray diffraction patterns of the GEMS-0067 starches harvested at different developmental stages are shown in **Figure 3**. All the starches displayed the B-type polymorph. There was no V-type X-ray diffraction pattern of $2\theta$ peaks at 8°, 13°, and 20° (*37-39*) observed for any of the starches, indicating that no crystalline amylose-lipid complex was present in the starch granule.

The percentage of crystallinity of the starch (**Figure 3**) decreased with the kernel maturation and the increase in the amylose/IC content ($r = -0.90$, $p < 0.05$). The starch of 15 DAP had the greatest percentage crystallinity, resulting from its largest amylopectin content.

Amylopectin molecules in normal starch granules are predominantly crystalline because their clustered branch chains and abundant free ends, which are prompt to crystallize. Amylose molecules in normal starch granules are amorphous because of the low concentration and being interspersed among amylopectin (*40, 41*). The amylose/IC molecules were dominant components in the maize *ae*-mutant starch granules and were known to interact with one another to form double helices and contribute to the total starch crystallinity (*18*).

**Thermal properties of the starch.** DSC thermograms of the GEMS-0067 starches are shown in **Figure 4**, and the thermal properties are summarized in **Table 2**. The onset gelatinization-temperatures ($T_o$) were 68.8-69.9°C for the starches harvested on 15, 20, and 30 DAP and then gradually decreased to 64.9°C on 54 DAP (**Table 2**). These results showed a similar trend to that of the $T_o$ of normal maize starch (B73) during the kernel development. The normal maize starch reaches the maximum $T_o$ (69.0°C) on 14 DAP and then decreased to 62.8°C at kernel maturation (*32*).

All the native starches showed a gelatinization thermal-transition peak with the peak temperature ($T_{p1}$) increasing from 76.6 to 81.0°C (**Table 2** and **Figure 4**). The intensity of the peak decreased with kernel maturation and with the increase in amylose/IC content (**Table 1** and **Figure 4**), indicating that this peak was likely due to the dissociation of short-chain double-helical crystallites of the amylopectin molecules (*14, 18, 27*). An additional peak ($T_{p2}$, ~97.1°C) first appeared as a shoulder on 20 DAP, became a minor peak on 30 DAP, and then developed to a significant peak on 40 and 54 DAP (**Figure 4**). The size of this peak coincided with the lipid content of the starch (**Table 1**), and the peak shown in **Figure 4** disappeared after removal of lipids from the starch (**Figure 5**). These results suggested that

the additional peak at ~97.1°C (**Figure 4**) corresponded to the melting of amylose-lipid complex (*42, 43*). It is known that the content of amylose-lipid complex in wheat, barely, and rye starch increases with kernel maturation (*44*). The presence of lipids in starch granules has been reported to reduce the enzyme digestibility of the granules at 95-100°C (*18*).

The conclusion gelatinization-temperatures of the native starches increased from 105.0°C on 15 DAP to 117.8-122.2°C on later dates (**Table 2**). After removal of the lipids from the starches, the conclusion gelatinization-temperatures remained about the same. The proportion of the enthalpy change of the thermal transition above 95°C (**Figure 5**) increased with kernel maturation and significantly correlated with the RS content of the starch with a correlation coefficient of 0.98 ($p < 0.05$). These results confirmed that long-chain double-helical crystallites of amylose/IC present in the starch granule increased with kernel maturation of the GEMS-0067. The long-chain double helical crystallites maintained semi-crystalline structures at 95-100 °C and, thus, were resistant to enzymatic hydrolysis (*14, 18*).

**CONCLUSION**

The RS content of GEMS-0067 starch increased with kernel maturation and with the increase in the amylose/IC content of the starch. Starch granules isolated from kernels harvested on 15 DAP had smaller granule sizes and consisted of more spherical granules and fewer elongated granules than those harvested on later dates. The amylopectin molecules were more concentrated in the starch granules harvested on 15 DAP and at the core and inner part of the mature granules. The increase in the amylose/IC content of the starch during kernel development led to the formation of long-chain double-helical crystallites that had

gelatinization temperature above 95°C and resulted in the increase in the RS content of the starch. The increase in the lipid content of the starch could also reduce enzyme digestibility of the starch.

**ACKNOWLEDGEMENTS**

**LITERATURE CITED**

(1) Englyst, H. N.; Macfarlane, G. T. Breakdown of resistant and readily digestible starch by human gut bacteria. *J. Sci. Food. Agric.* **1986,** 37 (7), 699-706.

(2) Englyst, H. N.; Cummings, J. H. Digestion of the polysaccharides of some cereal food in the human small intestine. *Am. J. Clin. Nutr.* **1985,** 42 (5), 778-87.

(3) Robertson, M. D.; Bickerton, A. S.; Dennis, A. L.; Vidal, H.; Frayn, K. N. Insulin-sensitizing effects of dietary resistant starch and effects on skeletal muscle and adipose tissue metabolism. *Am. J. Clin. Nutr.* **2005,** 82 (3), 559-567.

(4) Robertson, M. D.; Currie, J. M.; Morgan, L. M.; Jewell, D. P.; Frayn, K. N. Prior short-term consumption of resistant starch enhances postprandial insulin sensitivity in healthy subjects. *Diabetologia* **2003,** 46 (5), 659-665.

(5) Behall, K. M.; Scholfield, D. J.; Hallfrisch, J. G.; Liljeberg-Elmstaahl, H. G. M. Consumption of both resistant starch and beta -glucan improves postprandial plasma glucose and insulin in women. *Diabetes Care* **2006,** 29 (5), 976-981.

(6) Behall, K. M.; Scholfield, D. J.; Hallfrisch, J. G. Barley [beta]-glucan reduces plasma glucose and insulin responses compared with resistant starch in men. *Nutr. Res.* **2006,** 26 (12), 644-650.

(7) Zhang, W.; Wang, H.; Zhang, Y.; Yang, Y. Effects of resistant starch on insulin resistance of type 2 mellitus patients. *Chinese J. Prev. Med.* **2007,** 41 (2), 101-104.

(8) Higgins, J. A.; Higbee, D. R.; Donahoo, W. T.; Brown, I. L.; Bell, M. L.; Bessesen, D. H. Resistant starch consumption promotes lipid oxidation. *Nutr. Metab.* **2004,** 1, 8.

(9) Pawlak, D. B.; Kushner, J. A.; Ludwig, D. S. Effects of dietary glycaemic index on adiposity, glucose homoeostasis, and plasma lipids in animals. *Lancet* **2004,** 364 (9436), 778-785.

(10) Dronamraju, S. S.; Coxhead, J. M.; Kelly, S. B.; Burn, J.; Mathers, J. C. Cell kinetics and gene expression changes in colorectal cancer patients given resistant starch: a randomised controlled trial. *Gut* **2009,** 58 (3), 413-420.

(11) Van Munster, I. P.; Tangerman, A.; Nagengast, F. M. Effect of resistant starch on colonic fermentation, bile acid metabolism, and mucosal proliferation. *Dig. Dis. Sci.* **1994,** 39 (4), 834-42.

(12) Sajilata, M. G.; Singhal, R. S.; Kulkarni, P. R. Resistant starch - A review. *Compr. Rev. Food Sci. F.* **2006,** 5 (1), 1-17.

(13) Campbell, M. R.; Jane, J.; Pollak, L.; Blanco, M.; O'Brien, A. Registration of maize germplasm line GEMS-0067. *J. Plant Registra.* **2007,** 1, 60-61.

(14) Li, L.; Jiang, H.; Campbell, M.; Blanco, M.; Jane, J. Characterization of maize amylose-extender (*ae*) mutant starches: Part I. Relationship between resistant starch contents and molecular structures. *Carbohydr. Polym.* **2008,** 74 (3), 396-404.

(15) Hasjim, J.; Srichuwong, S.; Scott, M. P.; Jane, J. Kernel composition, starch structure, and enzyme digestibility of opaque-2 maize and quality protein maize. *J. Agric. Food Chem.* **2009,** 57 (5), 2049-2055.

(16) AOAC Association of Official Analytical Chemists (AOAC) Official Method 991.43. Total, soluble, and insoluble dietary fiber in foods. In *Official methods of analysis of the AOAC international*, 17th ed. Rev.2 ed.; Horwithz, W., Ed. AOAC International: Gaithersburg, Maryland, 2003.

(17) Hasjim, J.; Jane, J. Production of resistant starch by extrusion cooking of acid-modified normal-maize starch. *J. Food Sci.* **2009,** 74 (7), C556-C562.

(18) Jiang, H.; Campbell, M.; Blanco, M.; Jane, J. Characterization of maize amylose-extender (*ae*) mutant starches. Part II: Structures and properties of starch residues remaining after enzymatic hydrolysis at boiling-water temperature. *Carbohydr. Polym.* **2010,** 80 (1), 1-12.

(19) Perera, C.; Lu, Z.; Sell, J.; Jane, J. Comparison of physicochemical properties and structures of sugary-2 cornstarch with normal and waxy cultivars. *Cereal Chem.* **2001,** 78 (3), 249-256.

(20) Jiang, H.; Horner, H. T.; Pepper, T. M.; Blanco, M.; Campbell, M.; Jane, J. Formation of elongated starch granules in high-amylose maize. *Carbohydr. Polym.* **2010,** 80 (2), 534-539.

(21) Jiang, H.; Srichuwong, S.; Campbell, M.; Jane, J. Characterization of maize amylose-extender (*ae*) mutant starches. Part III: Structures and properties of the Naegeli dextrins. *Carbohydr. Polym.* **2010**, Submitted.

(22) Jane, J.; Chen, J. F. Effect of amylose molecular size and amylopectin branch chain length on paste properties of starch. *Cereal Chem.* **1992,** 69 (1), 60-5.

(23) Dubois, M.; Gilles, K. A.; Hamilton, J. K.; Rebers, P. A.; Smith, F. Colorimetric method for determination of sugars and related substances. *Anal. Chem.* **1956,** 28, 350-6.

(24) Juliano, B. O. Asimplified assay for milled-rice amylose. *Cereal Sci. Today* **1971,** 16, 334-340.

(25) Schoch, T. J. Noncarbohydrate substances in the cereal starches. *J. Am. Chem. Soc.* **1942,** 64, 2954-6.

(26) Ao, Z.; Jane, J. Characterization and modeling of the A- and B-granule starches of wheat, triticale, and barley. *Carbohydr. Polym.* **2007,** 67 (1), 46-55.

(27) Kasemsuwan, T.; Jane, J.; Schnable, P.; Stinard, P.; Robertson, D. Characterization of the dominant mutant amylose-extender (Ae1-5180) maize starch. *Cereal Chem.* **1995,** 72 (5), 457-64.

(28) Klucinec, J. D.; Thompson, D. B. Fractionation of high-amylose maize starches by differential alcohol precipitation and chromatography of the fractions. *Cereal Chem.* **1998,** 75 (6), 887-896.

(29) Baba, T.; Arai, Y. Structural features of amylomaize starch .3. Structural characterization of amylopectin and intermediate material in amylomaize starch granules. *Agr. Biol. Chem. Tokyo* **1984,** 48 (7), 1763-1775.

(30) Wang, Y. J.; White, P.; Pollak, L.; Jane, J. Amylopectin and intermediate materials in starches from mutant genotypes of the Oh43 inbred line. *Cereal Chem.* **1993,** 70 (5), 521-5.

(31) Mercier, C.; Charbonniere, R.; Gallant, D.; Guilbot, A. Development of some characteristics of starches extracted from normal corn and amylomaize grains during their formation. *Staerke* **1970,** 22 (1), 9-16.

(32) Li, L.; Blanco, M.; Jane, J. Physicochemical properties of endosperm and pericarp starches during maize development. *Carbohydr. Polym.* **2007,** 67 (4), 630-639.

(33) Wolf, M. J.; Seckinger, H. L.; Dimler, R. J. Microscopic characteristics of high-amylose corn starches. *Staerke* **1964,** 16 (12), 377-82.

(34) Jane, J.; Shen, J. J. Internal structure of the potato starch granule revealed by chemical gelatinization. *Carbohydr. Res.* **1993,** 247, 279-90.

(35) Pan, D. D.; Jane, J. Internal structure of normal maize starch granules revealed by chemical surface gelatinization. *Biomacromolecules* **2000,** 1 (1), 126-132.

(36) Jane, J.; Ao, Z.; Duvick, S. A.; Wiklund, M.; Yoo, S.-H.; Wong, K.-S.; Gardner, C. Structures of amylopectin and starch granules: How are they synthesized? *J. Appl. Glycosci.* **2003,** 50 (2), 167-172.

(37) Zobel, H. F.; French, A. D.; Hinkle, M. E. X-ray diffraction of oriented amylose fibers. II. Structure of V-amyloses. *Biopolymers* **1967,** 5 (9), 837-45.

(38) Zobel, H. F. Starch crystal transformations and their industrial importance. *Starch/Staerke* **1988,** 40 (1), 1-7.

(39) Czuchajowska, Z.; Sievert, D.; Pomeranz, Y. Enzyme-resistant starch. IV. Effects of complexing lipids. *Cereal Chem.* **1991,** 68 (5), 537-42.

(40) Jane, J.; Xu, A.; Radosavljevic, M.; Seib, P. A. Location of amylose in normal starch granules. I. Susceptibility of amylose and amylopectin to cross-linking reagents. *Cereal Chem.* **1992,** 69 (4), 405-9.

(41) French, D. Organization of starch granules. In *Starch: Chemistry and Technology,* 2 ed.; Whistler, R. L.; BeMiller, J. N.; Paschall, E. F., Eds. Academic Press: New York, 1984; pp 183-247.

(42) Tufvesson, F.; Wahlgren, M.; Eliasson, A.-C. Formation of amylose-lipid complexes and effects of temperature treatment. Part 1. Monoglycerides. *Starch/Staerke* **2003,** 55 (2), 61-71.

(43) Tufvesson, F.; Wahlgren, M.; Eliasson, A.-C. Formation of amylose-lipid complexes and effects of temperature treatment. Part 2. Fatty acids. *Starch/Staerke* **2003,** 55 (3-4), 138-149.

(44) Karlsson, R.; Olered, R.; Eliasson, A. C. Changes in starch granule size distribution and starch gelatinization properties during development and maturation of wheat, barley and rye. *Starch/Staerke* **1983,** 35 (10), 335-40.

**Table 1.** RS, Amylose/Intermediate Component (IC), and Lipid Contents of GEMS-0067 Starches Harvested at Different Kernel-Developmental Stages

| Sample | RS[a] (%) | | Amylose/IC[b] (%) | | Lipid (%) | |
|---|---|---|---|---|---|---|
| | 2007 crop year | 2009 crop year | 2007 crop year | 2009 crop year | 2007 crop year | 2009 crop year |
| 15 DAP[c] | $9.0 \pm 1.2$ | $10.1 \pm 0.1$ | $55.2 \pm 0.5$ | $54.5 \pm 0.3$ | Not determined | Not determined |
| 20 DAP | $26.4 \pm 0.1$ | $25.3 \pm 0.7$ | $78.4 \pm 0.2$ | $76.9 \pm 0.6$ | $0.43 \pm 0.03$ | $0.25^{d}$ |
| 30 DAP | $29.6 \pm 0.8$ | $28.4 \pm 0.3$ | $81.9 \pm 0.3$ | $84.3 \pm 0.8$ | $0.42 \pm 0.02$ | 0.39 |
| 40 DAP | $32.0 \pm 0.1$ | $32.9 \pm 0.4$ | $88.6 \pm 1.3$ | $89.5 \pm 0.1$ | $0.62 \pm 0.03$ | 0.45 |
| 54 DAP | $32.1 \pm 0.3$ | $33.8 \pm 0.2$ | $87.6 \pm 0.4$ | $88.8 \pm 0.4$ | $0.64 \pm 0.01$ | 0.50 |
| Coefficient between RS and amylose/IC content | | | $0.99^{e}$ | $0.99^{e}$ | | |

[a] Resistant starch (RS) content was determined using AOAC method 991.43 for total dietary fiber.

[b] Amylose/IC contents were determined using Sepharose CL-2B gel-permeation chromatography followed by the total carbohydrate (phenol-sulfuric acid) determination.

[c] DAP: days after pollination.

[d] Values were analyzed one time because of limit material available.

[e] $p < 0.001$.

**Table 2.** Thermal Properties of native GEMS-0067 Starches Harvested at Different Kernel-Developmental Stages[a]

| Sample | Thermal properties | | | | |
|---|---|---|---|---|---|
| | $T_o$ (°C) | $T_{p1}$ (°C) | $T_{p2}$ (°C) | $T_c$ (°C) | $\Delta H$ (J/g) |
| 15 DAP[b] | 69.5 ± 0.1 | 76.6 ± 0.6 | Nd[c] | 105.0 ± 0.7 | 16.9 ± 0.2 |
| 20 DAP | 68.8 ± 1.0 | 78.5 ± 0.2 | 96.7 ± 0.2 | 119.3 ± 2.5 | 12.3 ± 0.6 |
| 30 DAP | 69.9 ± 0.5 | 79.5 ± 0.2 | 98.3 ± 0.6 | 122.2 ± 0.2 | 14.2 ± 0.8 |
| 40 DAP | 66.1 ± 0.7 | 80.2 ± 0.7 | 97.1 ± 0.4 | 122.0 ± 0.5 | 11.3 ± 0.5 |
| 54 DAP | 64.9 ± 0.3 | 81.0 ± 0.6 | 96.2 ± 0.9 | 117.8 ± 1.9 | 11.8 ± 1.3 |

[a] Samples (~6.0 mg, db) and deionized distilled-water (~18.0 μL) were used for the analysis;

$T_o$, $T_{p1}$, $T_{p2}$, $T_c$, and $\Delta H$ are onset, peak 1, peak 2, and conclusion temperatures, and enthalpy change, respectively.

[b] DAP: days after pollination.
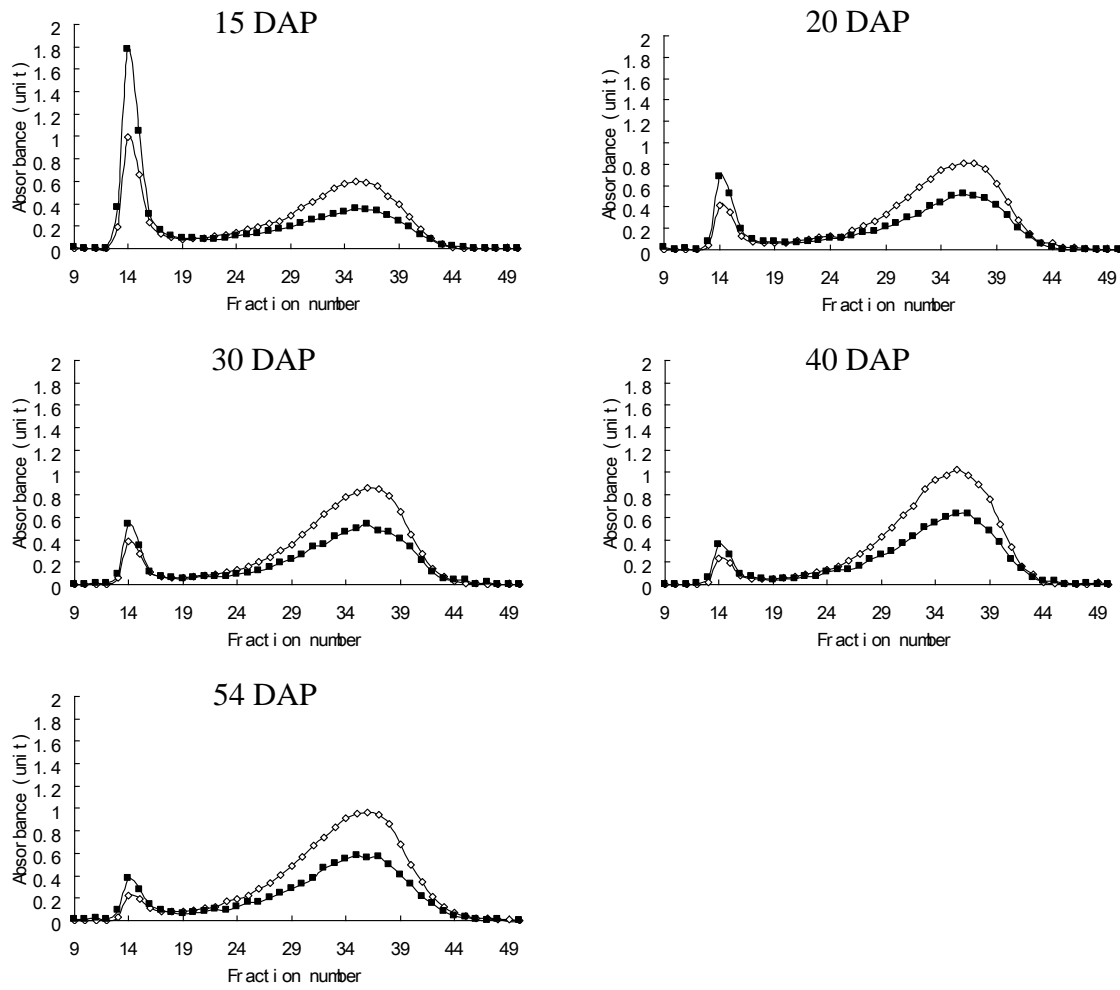
[c] Nd = not detectable.

**Figure 1.** Sepharose CL-2B gel-permeation chromatographic profiles of GEMS-0067 starches harvested at different kernel-developmental stages. —◇— blue value; —■— total carbohydrate. DAP: days after pollination.
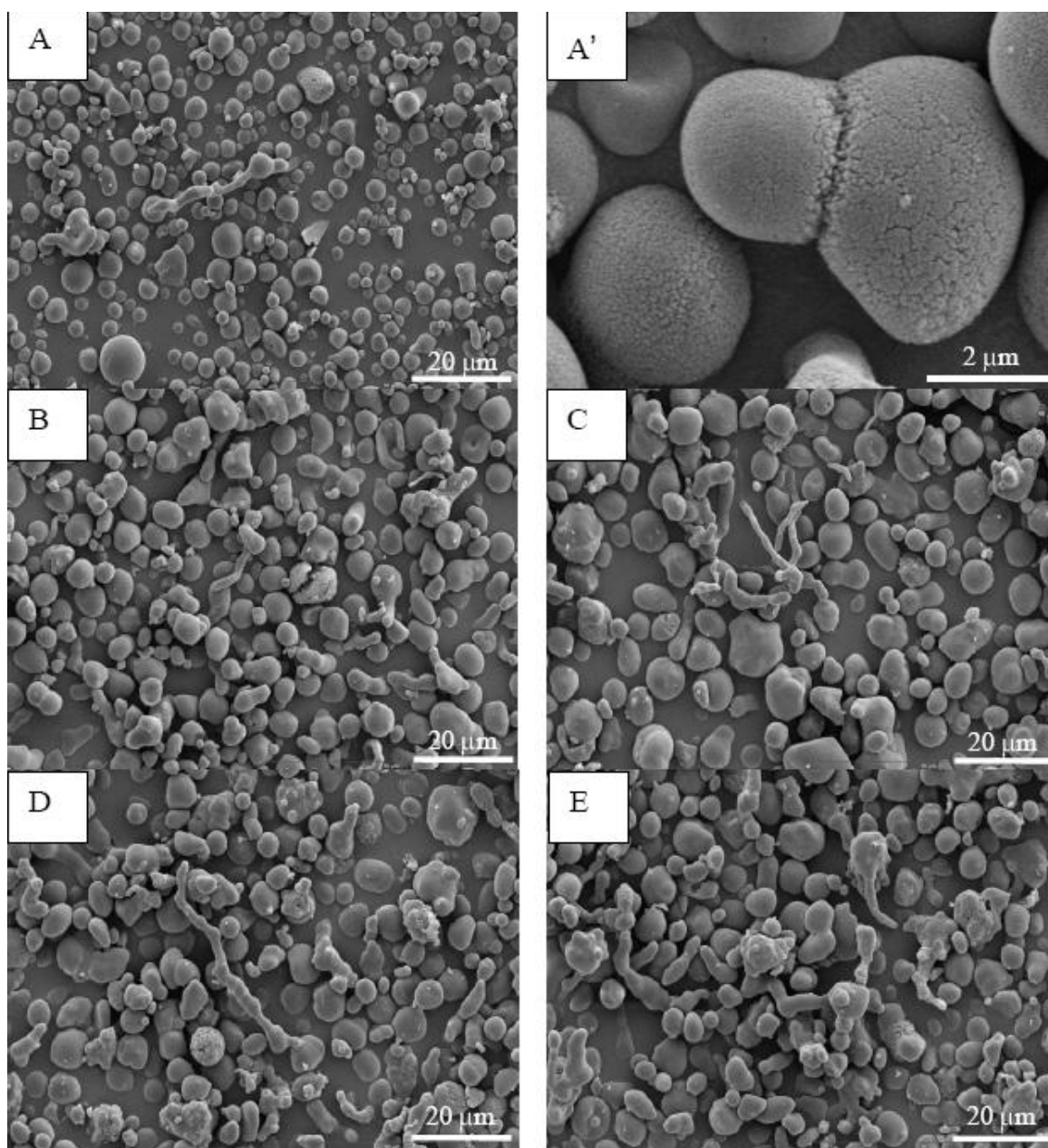
**Figure 2.** Scanning electron micrographs of GEMS-0067 starches harvested at different kernel-developmental stages. A and A': 15 days after pollination (DAP); B: 20 DAP; C: 30 DAP; D: 40 DAP; and E: 54 DAP.

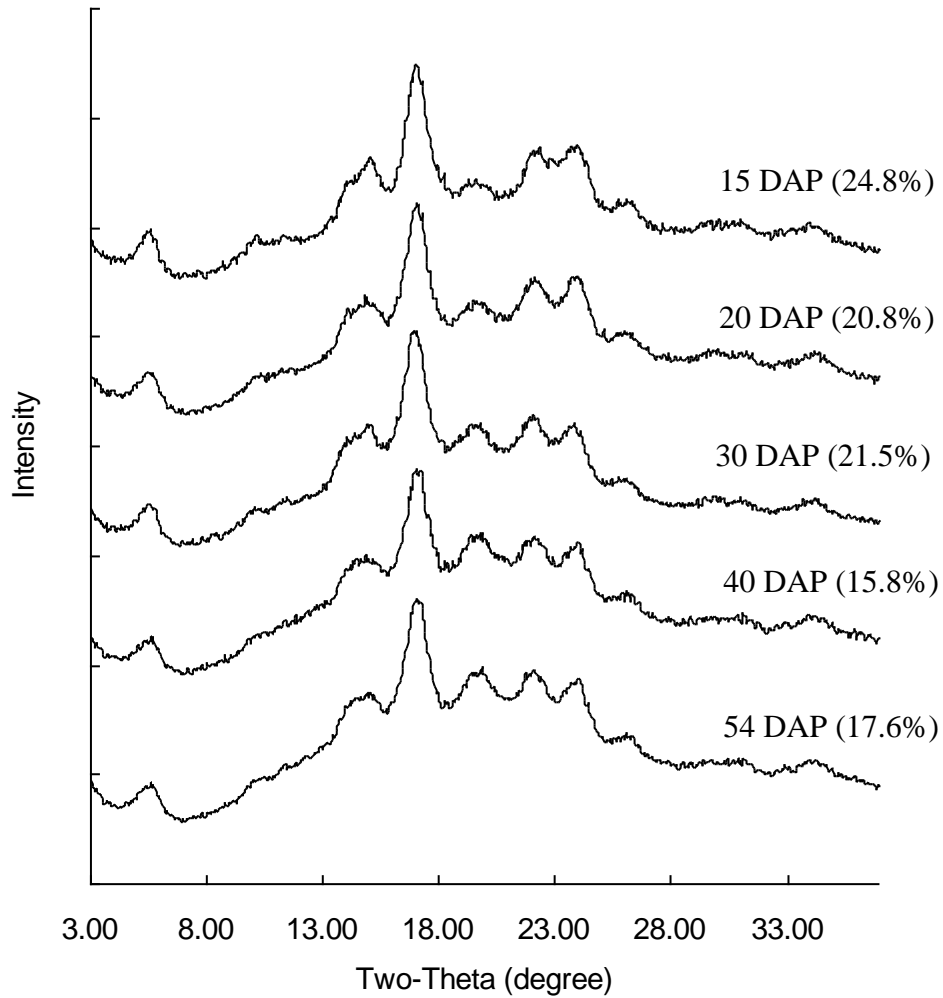**Figure 3.** X-ray diffraction patterns of GEMS-0067 starches harvested at different kernel-developmental stages. Percentage crystallinity (%) is given in parentheses. DAP: days after pollination.

**Figure 4**. DSC thermograms of GEMS-0067 starches harvested at different developmental stages. DAP: days after pollination. The peak area above dashed line indicates melting of amylose-lipid complex.
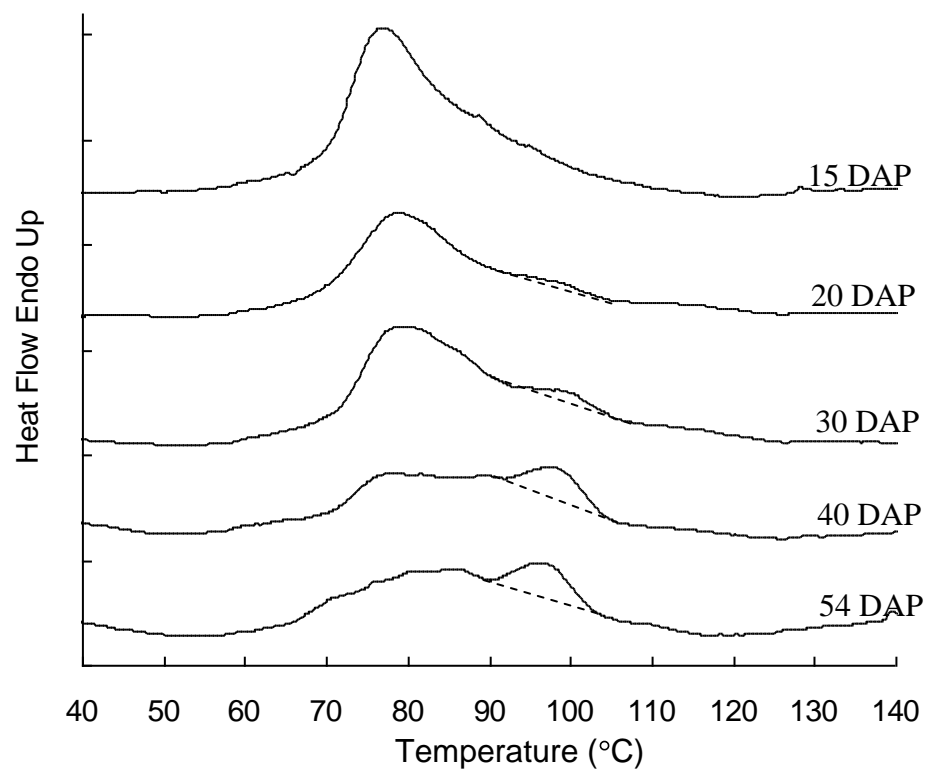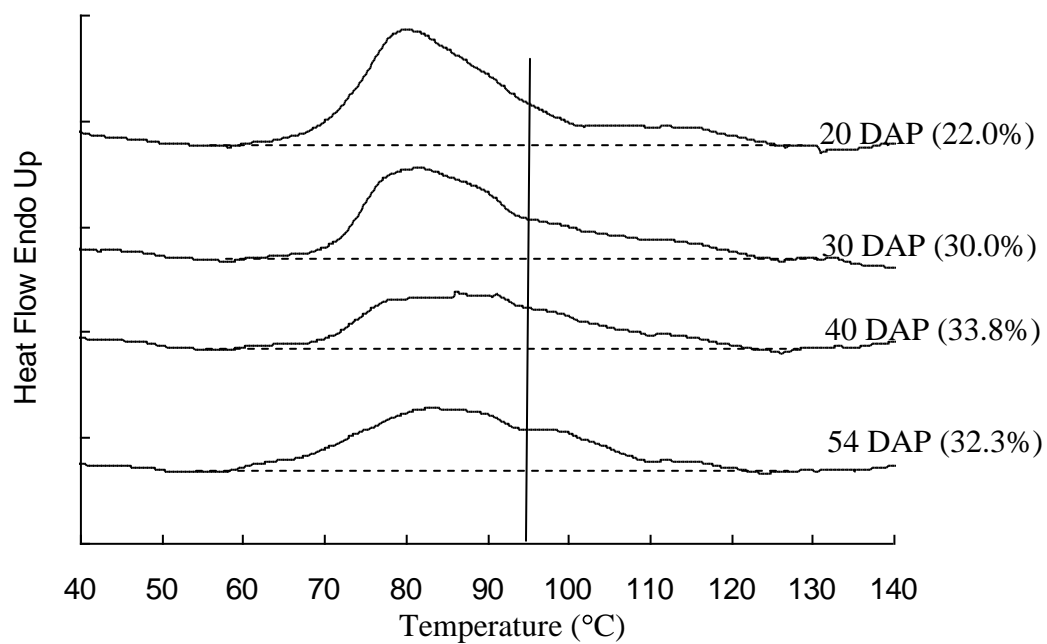
**Figure 5.** DSC thermograms of methanol-defatted GEMS-0067 starches harvested at different developmental stages. DAP: days after pollination. The proportion of the enthalpy change of the thermal-transition above 95°C is given in parentheses.

# CHAPTER 4. FORMATION OF ELONGATED STARCH GRANULES IN HIGH-AMYLOSE MAIZE

Hongxin Jiang [a], Harry T. Horner [b], Tracey M. Pepper [b], Michael Blanco [c], Mark

Campbell [d], Jay-lin Jane [a,*]

[a] Department of Food Science and Human Nutrition, Iowa State University, Ames, Iowa

50011, USA.

[b] Department of Genetics, Development and Cell Biology & Microscopy and NanoImaging

Facility, Iowa State University, Ames, IA 50011, USA.

[c] USDA-ARS/Plant Introduction Research Unit, Ames, IA 50011, USA.

[d] Truman State University, Kirksville, MO 63501, USA.

* Corresponding author. Tel: +1 515 294 9892. Fax: +1 515 294 8181. E-mail address:

jjane@iastate.edu (J. Jane).

## Abstract

GEMS-0067 maize starch contains up to 32% elongated starch granules, much higher

than amylose-extender (*ae*) single-mutant maize starch (~7%) and normal (non-mutant)

maize starch (0%). These elongated granules are highly resistant to enzymatic hydrolysis at

95-100°C, which function as resistant starch. The structure and formation of these elongated

starch granules, however, were not known. In this study, light, confocal laser-scanning,

scanning electron, and transmission electron microscopy were used to reveal the structure

and formation of these elongated starch granules. The transmission electron micrographs

showed fusion through amylose interaction between adjacent small granules in the

amyloplast at the early stage of granule development. A mechanistic model for the formation of elongated starch granules is proposed.

**Keywords:** High-amylose maize starch; Amylose-extender mutant; Resistant starch; Starch structure; Long-chain double-helical crystallite; Elongated starch granule; Starch granule formation

## 1. Introduction

Starch exists widely in seeds, roots, tubers, and fruits as an energy reserve of plants (Robyt, 1998). Because starch is a renewable, economical, and environmentally friendly biopolymer, it is widely used in food and non-food applications, such as a thickener, binder, film, and foam (Richardson et al., 2000). There has been an increased interest in producing resistant starch (RS) from high-amylose maize starch. RS is a portion of starch that cannot be hydrolyzed by human digestive enzymes and functions as a prebiotic for bacterial fermentation in the large intestine (Englyst & Cummings, 1985; Englyst & Macfarlane, 1986). RS from high-amylose maize starch has been reported to provide many health benefits. When RS is used to replace rapidly digestible starch in food, it lowers the glycemic and insulin responses and reduces the risk for developing type II diabetes, obesity, and cardiovascular disease (Behall et al., 2006a; Behall et al., 2006b; Robertson et al., 2005; Robertson et al., 2003; Zhang et al., 2007). RS lowers calories of foods (Behall & Howe, 1996) and enhances lipid oxidation (Higgins et al., 2004), which reduce body fat and impact body composition (Pawlak et al., 2004). Fermentation of RS in the colon promotes a healthy

colon and reduces the risk of colon cancer (Dronamraju et al., 2009; Van Munster et al., 1994).

Normal maize starch contains less than 1% RS (AOAC, 2003), whereas starch of maize *ae* single-mutant has ~15% RS (Li et al., 2008). A recently developed GEMS-0067 high-amylose maize starch, through the USDA-ARS Germplasm Enhancement of Maize (GEM) Project, contains up to 43.2% RS (Li et al., 2008). The GEMS-0067 is an inbred line of maize homozygous mutant of *ae* gene and a high-amylose modifier (HAM) gene (Campbell et al., 2007).

Normal maize starch is composed of ~30% primarily linear amylose and ~70% highly-branched amylopectin, which are organized in granules with a semi-crystalline structure of double helices. Amylose is a polysaccharide of essentially (1→4)-linked α-D-glucopyranose, and exists in an amorphous state within the normal maize starch granule. Amylopectin molecules consist of (α1→6) linked branch-chains of (1→4) α-D-glucopyranose, which contribute to the crystallinity of starch (French, 1984; Jane et al., 1992; Kasemsuwan & Jane, 1994). The GEMS-0067 starch consists of ~85% amylose, much greater than normal maize starch (~30%) and starches of maize *ae* single-mutant (50-70%) (Li et al., 2007; Li et al., 2008).

Normal maize starch has starch granules with spherical and angular shapes, whereas high-amylose maize (*ae* single-mutant) starch consists of ~7% elongated granules (Jiang et al., 2009; Perera et al., 2001). The GEMS-0067 starch consists of up to 32% elongated starch granules (Jiang et al., 2009). The elongated starch granules and the outer layer of the spherical starch granules are highly resistant to enzymatic hydrolysis and remain in the RS residue that consists of partially hydrolyzed amylose with molecular weights of DP 411-675

(Jiang et al., 2009). It is of great interest to understand how the elongated starch granules are formed during kernel development and the RS formation in the high-amylose maize starch. In this study, we used different microscopic approaches to reveal the internal structures and the formation of elongated starch granules during kernel development. Combining these results with the chemical structures of the starch crystallites reported previously (Jiang et al., 2009), we propose a mechanism of the development of elongated granules.

## 2. Materials and Methods

### 2.1. Materials

GEMS-0067 (High-amylose maize) and B73 (normal maize) maize lines were planted in the field at the USDA-ARS North Central Regional Plant Introduction Station (NCRPIS) in Ames, IA in 2007. Plants were self-pollinated by hand pollination, and ears of GEMS-0067 and B73 were harvested on 20 days after pollination (DAP) and after the physiological maturation of the maize kernels (54 DAP).

### 2.2. Starch isolation

Starch was isolated from mature maize endosperm using the method described by Li et al. (2008).

### 2.3. Scanning electron microscopy

Images of the starch granules were collected using a scanning electron microscope (JEOL 5800, www.jeol.com) in the Microscopy and NanoImaging Facility, Iowa State

University, Ames IA 50011. The starch samples were coated with palladium-gold (60:40) and viewed at 10 kV.

## 2.4. Light microscopy

Native starch granules were viewed and imaged using polarizing and phase-contrast optics using a compound light microscope (Zeiss Axioplan 2, www.zeiss.com) equipped with a digital AxioCam MRC color camera and Axiovison rel 4.5 software.

## 2.5. Confocal laser-scanning microscopy (CLSM)

The CLSM was conducted following the method described by Glaring et al. (2006). Starch (~12% MC, 4.0 mg) was dried at 45°C using a centrifugal vacuum evaporator for 2 h. Four µL of 8-aminopyrene-1,3,6-trisulfonic acid (APTS, Cat. No. 09341, www.sigmaaldrich.com) solution (0.02M APTS in 15% acetic acid) and 4 µL of sodium cyanoborohydride (1M in tetrahydrofuran, Cat. No. 296813, www.sigmaaldrich.com) were added to the dried starch sample. The mixture was incubated at 30°C for 16 h. The APTS-stained starch granules were viewed using a confocal laser-scanning microscope (TCS SP5 X, www.leica.com) at the Confocal Microscopy and Image Analysis Facility, Iowa State University, Ames IA 50011. A laser beam with 488 nm wavelength was used for excitation. The emission peak was detected between 500 and 535 nm.

## 2.6. Transmission electron microscopy (TEM)

The endosperm tissues of GEMS-0067 and B73 kernels harvested on 20 DAP were prepared for TEM following the method of Horner et al. (2007). Observations of the fixed

tissues were made using a transmission electron microscope (JEOL 2100, www.jeol.com), and images were captured using a high-resolution digital camera (U-1000, www.gatan.com).

## 3. Results and discussion

### 3.1. Morphology of GEMS-0067 starch granules

GEMS-0067 starch consisted of mainly spherical and elongated starch granules (Fig. 1) as reported by Jiang et al. (Jiang et al., 2009). The elongated starch granules displayed shapes including rods, filaments, and triangles (Fig. 1). It has been shown that maize *ae*-mutant starches contain elongated granules (Boyer et al., 1976; Mercier et al., 1970; Shi & Jeffcoat, 2001; Sidebottom et al., 1998; Wolf et al., 1964) and normal maize starch contains starch granules mainly with spherical and angular shapes (Perera et al., 2001; Wongsagonsup et al., 2008). The proportion of the elongated starch granules in the maize *ae*-mutant starches increases with the increase in amylose content (Jiang et al., 2009).

### 3.2. Birefringence of GEMS-0067 starch granules

The starch granules were viewed both with polarizing (Fig. 2A) and phase-contrast light microscopy (Fig. 2B). Between crossed polarizers, GEMS-0067 starch granules displayed different patterns of birefringence (Fig. 2A). Most spherical starch granules exhibited bright Maltese-crosses (Fig. 2A-a), which were similar to those observed in normal maize starch granules (Wongsagonsup et al., 2008). This birefringence pattern indicated that the starch molecules were aligned in a radial order centered at the hilum (growth center) and were perpendicular to the granule surface. The birefringence patterns of elongated starch granules varied and could be classified into three types: type 1 birefringence pattern

displayed overlapping of several Maltese-crosses (Fig. 2A-b, c, d); type 2 birefringence pattern consisted of combinations of one or more Maltese-crosses and weak to no birefringence on other parts of the granule (Fig. 2A-e, f); and type 3 exhibited no birefringence or only weak birefringence along the edge of the elongated granule (Fig. 2A-g, h). The birefringence patterns of the GEMS-0067 starch granules agreed with that of high-amylose starch reported by Wolf et al. (1964).

Birefringence patterns are results of orderly aligned polymers or crystallites. Thus, the birefringence patterns of starch granules provide information about the orientations and alignments of starch molecules in different regions of the granule (French, 1984). The different birefringence patterns of the GEMS-0067 starch granules indicated that the arrangement of starch molecules varied between granules and within a granule. The overlapping of several Maltese crosses (Fig. 2A-b, c, d) in one granule could result from the fusion of starch granules within an amyloplast during the kernel development.

*3.3. Internal structure of elongated starch granules*

The reductive amination of reducing sugar with a fluorophore, 8-aminopyrene-1,3,6-trisulfonic acid (APTS), has been well studied (Morell et al., 1998; O'Shea et al., 1998). Because amylose and amylopectin molecules possess reducing ends that could be attached by APTS, CLSM images of APTS-stained starch granules provided information about the internal structure of the starch granules (Glaring et al., 2006). The CLSM images show most spherical granules displaying bright color around one hilum (Fig. 3a), indicating that each of the resulting spherical granules was developed from one single granule. The APTS-staining pattern of the elongated granules revealed multiple regions with different intensities of

fluorescence (Figs. 3b-g), similar to that observed by Glaring et al. (Glaring et al., 2006), and indicating that the elongated granules could be formed from the fusion of several small granules.

*3.4. Formation of elongated starch granules*

To understand starch granule formation during kernel development, endosperm tissues of maize kernels at an early stage were harvested on 20 days after pollination (DAP) and used for TEM studies. TEM images of subaleurone layers from B73 (normal maize) and GEMS-0067 endosperms are shown in Fig. 4 & 5, respectively. Although most mature amyloplasts in B73 endosperm contained only one starch granule as reported by Shannon and Garwood (1984), we observed some amyloplasts contained two starch granules (Fig. 4B-a, b). Fig. 4B-b shows an amyloplast in division containing two starch granules.

Although some amyloplasts at the subaleurone layer of GEMS-0067 endosperm contained only one spherical granule and they displayed normal growth rings and a hilum (Fig. 5A), the majority of amyloplasts contained two or more starch granules (Fig. 5B). Examples of features observed were two starch granules being initiated in one amyloplast, presumably at an early stage of granule development (Fig. 5C); starch granules almost fused (Fig. 5D); and two starch granules fused together forming an elongated starch granule (Fig. 5E). The inner growth rings were each centered around the two hila, but the outer growth rings were integrated into one granule. This elongated starch granule, consisting of two fused granules, agreed with the image of two Maltese-crosses observed in one starch granule (Fig. 2A-b).

Fig. 5F shows two connected starch granules and a third starch granule in the amyloplast protrusion. Three small granules were fused into one granule (Fig. 5G), showing one small granule with a hilum and growth rings, and the other two without hila or growth rings. This elongated starch granule consisted of three small granules displaying a birefringence pattern with one Maltese-cross at the head and weak to no birefringence in the remainder of the elongated granule (Fig. 2A-e). Fig. 5H shows an elongated starch granule formed from fusion of three small granules, each with a hilum and growth rings. This elongated granule represents the birefringence of the overlapping of Maltese-crosses in the starch granule shown in Fig. 2A-c, and the APTS-stained starch granules shown in Fig. 3c and f.

Fig. 5I shows four small starch granules, each with an individual hilum, fused together and displaying several layers of growth rings parallel to the boundary of the amyloplast. This granule is similar to the APTS-stained starch granules shown in Fig. 3b, d, and e. And in Fig. 5J, six starch granules, without hila and growth rings, were fused in one amylosplast to form an almost spherical starch granule. This granule would have no birefringence when viewed between crossed polarizers.

The TEM images suggest that elongated starch granules are formed from fusion of several small granules, each initiated early in the kernel development. These results support the different birefringence patterns observed using polarizing microscopy and APTS-staining patterns with CLSM for GEMS-0067 starch granules. These fused granules, however, were not observed with B73 normal maize starch.

*3.5. Proposed formation mechanism of elongated starch granules*

The multiple high-amylose maize starch granules (Fig. 5) appear to fail to separate and retard amyloplast division, resulting in elongated starch granules. Because the GEMS-0067 starch consists of ~85% amylose and the proportion of the elongated starch granules correlates with the amylose content of the starch (Jiang et al., 2009), it is plausible that the amylose molecules of an individual granule in the amyloplast interact and form anti-parallel double helices with amylose molecules of an adjacent granule. These double helices bind the two adjacent granules together and prevent amyloplast division. These fused granules have continuous outer layers, which consist of more amylose (Jiang et al., 2009) resulting from the increase in activity of granular-bound starch synthase at later stages of the kernel development (Sidebottom et al., 1998). The long-chain double helical crystallites formed from amylose molecules have melting temperatures above the boiling-water temperature, which retain the semicrystalline structure and, in turn, maintain the granular shape of the elongated starch granules after thermally stable $\alpha$-amylase hydrolysis at 95-100°C (Jiang et al., 2009). In normal maize starch granules, amylose molecules are separated by amylopectin molecules (Jane et al., 1992; Kasemsuwan & Jane, 1994) because of the low concentration of amylose (Li et al., 2007). And the branch chains of amylopectin molecules are not long enough to form stable anti-parallel double helices between two adjacent granules in the normal maize amyloplast. Thus, two starch granules separate along with amyloplast division, and each remains with a newly-formed amyloplast (Fig. 4).

A proposed model of elongated starch granule formation is shown in Fig. 6. Two starch granules, each with hilum and growth rings, are initiated in an amyloplast (Fig. 6A). Then two granules begin fusing by forming anti-parallel amylose double helices between two growing granules, which prevent the amyloplast division (Fig. 6B). The two granules, after

fusion, produce continuous outer layers (Fig. 6C). To the best of our knowledge, this mechanistic model is being proposed for the first time in this study, and assists the understanding of the formation of the elongated starch granules and RS formation in high-amylose maize starch.

## Acknowledgements

## References

AOAC (2003). Association of Official Analytical Chemists (AOAC) Official methods 991.43. Total, soluble, and insoluble dietary fiber in foods. In W. Horwithz. *Official methods of analysis of the AOAC international*. Gaithersburg, Maryland: AOAC International.

Behall, K. M., & Howe, J. C. (1996). Resistant starch as energy. *Journal of the American College of Nutrition, 15*, 248-254.

Behall, K. M., Scholfield, D. J., & Hallfrisch, J. G. (2006a). Barley [beta]-glucan reduces plasma glucose and insulin responses compared with resistant starch in men. *Nutrition Research, 26*, 644-650.

Behall, K. M., Scholfield, D. J., Hallfrisch, J. G., & Liljeberg-Elmstaahl, H. G. M.

(2006b). Consumption of both resistant starch and beta -glucan improves postprandial plasma glucose and insulin in women. *Diabetes Care, 29*, 976-981.

Boyer, C. D., Daniels, R. R., & Shannon, J. C. (1976). Abnormal starch granule formation in Zea-Mays-L endosperms possessing amylose-extender mutant. *Crop Science, 16*, 298-301.

Campbell, M. R., Jane, J., Pollak, L., Blanco, M., & O'Brien, A. (2007). Registration of maize germplasm line GEMS-0067. *Journal of Plant Registrations, 1*, 60-61.

Dronamraju, S. S., Coxhead, J. M., Kelly, S. B., Burn, J., & Mathers, J. C. (2009). Cell kinetics and gene expression changes in colorectal cancer patients given resistant starch: a randomised controlled trial. *Gut, 58*, 413-420.

Englyst, H. N., & Cummings, J. H. (1985). Digestion of the polysaccharides of some cereal food in the human small intestine. *American Journal of Clinical Nutrition, 42*, 778-787.

Englyst, H. N., & Macfarlane, G. T. (1986). Breakdown of resistant and readily digestible starch by human gut bacteria. *Journal of the Science of Food and Agriculture, 37*, 699-706.

French, D. (1984). Organization of starch granules. In R. L. Whistler, J. N. Bemiller, & E. F. Paschall. *Starch: Chemistry and Technology* (pp. 183-247). New York: Academic Press.

Glaring, M. A., Koch, C. B., & Blennow, A. (2006). Genotype-specific spatial distribution of starch molecules in the starch granule: a combined CLSM and SEM approach. *Biomacromolecules, 7*, 2310-2320.

Higgins, J. A., Higbee, D. R., Donahoo, W. T., Brown, I. L., Bell, M. L., & Bessesen, D.

H. (2004). Resistant starch consumption promotes lipid oxidation. *Nutrition & Metabolism, 1*, 8.

Horner, H. T., Healy, R. A., Ren, G., Fritz, D., Klyne, A., Seames, C., & Thornburg, R. W. (2007). Amyloplast to chromoplast conversion in developing ornamental tobacco floral nectaries provides sugar for nectar and antioxidants for protection. *American Journal of Botany, 94*, 12-24.

Jane, J., Xu, A., Radosavljevic, M., & Seib, P. A. (1992). Location of amylose in normal starch granules. I. Susceptibility of amylose and amylopectin to cross-linking reagents. *Cereal Chemistry, 69*, 405-409.

Jiang, H., Campbell, M., Blanco, M., & Jane, J. (2009). Characterization of maize amylose-extender (ae) mutant starches. Part II: Structures and properties of starch residues remaining after enzyme hydrolysis at boiling-water temperature. *Carbohydrate Polymers,* In press.

Kasemsuwan, T., & Jane, J. (1994). Location of amylose in normal starch granules. II. Locations of phosphodiester crosslinking revealed by phosphorus-31 nuclear magnetic resonance. *Cereal Chemistry, 71*, 282-287.

Li, L., Blanco, M., & Jane, J. (2007). Physicochemical properties of endosperm and pericarp starches during maize development. *Carbohydrate Polymers, 67*, 630-639.

Li, L., Jiang, H., Campbell, M., Blanco, M., & Jane, J. (2008). Characterization of maize amylose-extender (ae) mutant starches. Part I: Relationship between resistant starch contents and molecular structures. *Carbohydrate Polymers, 74*, 396-404.

Mercier, C., Charbonniere, R., Gallant, D., & Guilbot, A. (1970). Development of some

characteristics of starches extracted from normal corn and amylomaize grains during their formation. *Staerke, 22*, 9-16.

Morell, M. K., Samuel, M. S., & O'Shea, M. G. (1998). Analysis of starch structure using fluorophore-assisted carbohydrate electrophoresis. *Electrophoresis, 19*, 2603-2611.

O'Shea, M. G., Samuel, M. S., Konik, C. M., & Morell, M. K. (1998). Fluorophore-assisted carbohydrate electrophoresis (FACE) of oligosaccharides: efficiency of labelling and high-resolution separation. *Carbohydrate Research, 307*, 1-12.

Pawlak, D. B., Kushner, J. A., & Ludwig, D. S. (2004). Effects of dietary glycaemic index on adiposity, glucose homoeostasis, and plasma lipids in animals. *Lancet, 364*, 778-785.

Perera, C., Lu, Z., Sell, J., & Jane, J. (2001). Comparison of physicochemical properties and structures of sugary-2 cornstarch with normal and waxy cultivars. *Cereal Chemistry, 78*, 249-256.

Richardson, P. H., Jeffcoat, R., & Shi, Y.-C. (2000). High-amylose starches: From biosynthesis to their use as food ingredients. *MRS Bulletin, 25*, 20-24.

Robertson, M. D., Bickerton, A. S., Dennis, A. L., Vidal, H., & Frayn, K. N. (2005). Insulin-sensitizing effects of dietary resistant starch and effects on skeletal muscle and adipose tissue metabolism. *American Journal of Clinical Nutrition, 82*, 559-567.

Robertson, M. D., Currie, J. M., Morgan, L. M., Jewell, D. P., & Frayn, K. N. (2003). Prior short-term consumption of resistant starch enhances postprandial insulin sensitivity in healthy subjects. *Diabetologia, 46*, 659-665.

Robyt, J. F. (1998). Essentials of carbohydrate chemistry. New York: Springer-Verlag.

Shannon, J. C., & Garwood, D. L. (1984). Genetics and physiology of starch

development. In R. L. Whistler, J. N. Bemiller, & E. P. Paschall. *Starch: Chemistry and Technology* (pp. 25-79). New York: Academic Press.

Shi, Y.-C., & Jeffcoat, R. (2001). Structural features of resistant starch. In B. McCleary, & L. Prosky. *Advanced Dietary Fibre Technology* (pp. 430-439). Oxford, UK: Wiley-Blackwell.

Sidebottom, C., Kirkland, M., Strongitharm, B., & Jeffcoat, R. (1998). Characterization of the difference of starch branching enzyme activities in normal and low-amylopectin maize during kernel development. *Journal of Cereal Science, 27*, 279-287.

Van Munster, I. P., Tangerman, A., & Nagengast, F. M. (1994). Effect of resistant starch on colonic fermentation, bile acid metabolism, and mucosal proliferation. *Digestive Diseases and Sciences, 39*, 834-842.

Wolf, M. J., Seckinger, H. L., & Dimler, R. J. (1964). Microscopic characteristics of high-amylose corn starches. *Staerke, 16*, 377-382.

Wongsagonsup, R., Varavinit, S., & BeMiller, J. N. (2008). Increasing slowly digestible starch content of normal and waxy maize starches and properties of starch products. *Cereal Chemistry, 85*, 738-745.

Zhang, W., Wang, H., Zhang, Y., & Yang, Y. (2007). Effects of resistant starch on insulin resistance of type 2 mellitus patients. *Chinese J. Prev. Med., 41*, 101-104.
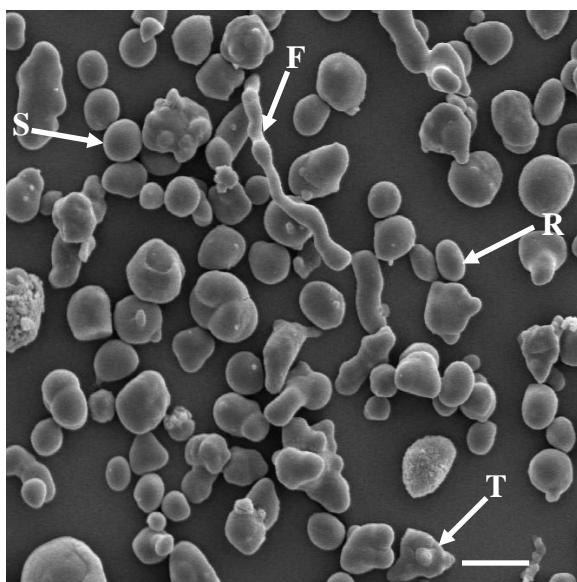
**Fig. 1**. Scanning electron microscope images of physiologically matured GEMS-0067 starch granules show spherical and elongated granules. Arrows indicate spherical (S), rod (R), filamentous (F), and triangular (T) starch granules. Bar = 10 μm.
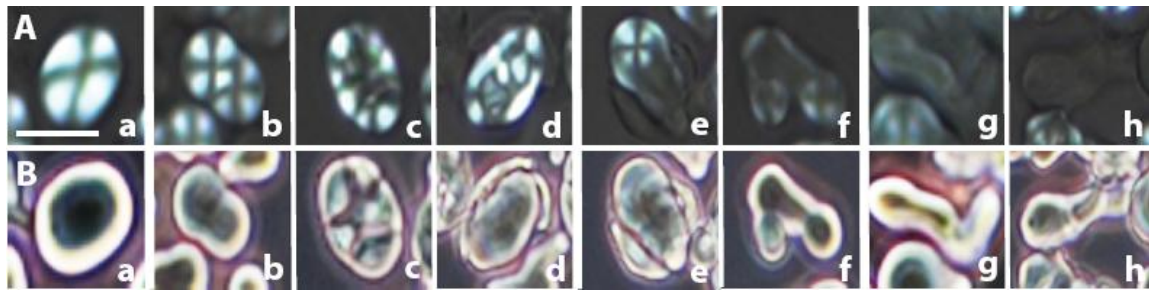
**Fig. 2**. Polarized (A) and phase-contrast (B) images of GEMS-0067 native starches. **a**: spherical granule displaying a single bright Maltese-cross; **b**, **c**, and **d**: type 1 birefringence pattern displaying overlapping of several Maltese-crosses; **e** and **f**: type 2 birefringence pattern consisting of one or more Maltese-crosses and weak to no birefringence for remainder of granule; **g** and **h**: type 3 birefringence pattern exhibiting weak birefringence along periphery of granule or no birefringence of granule. Bar = 10 μm for all figures.
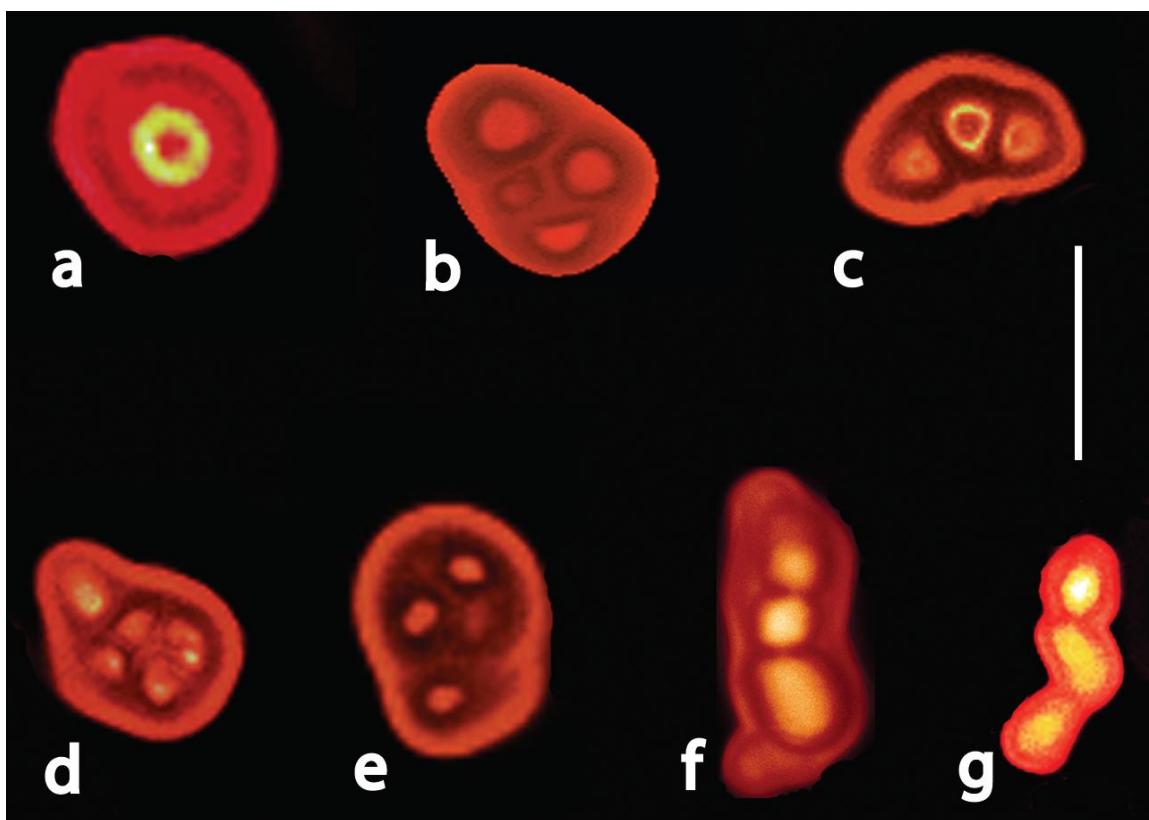
**Fig. 3**. Confocal laser scanning microscope images of GEMS-0067 starch granules. **a**: spherical granule with bright color in center of granule; **b**, **c**, **d**, **e**, **f**, and **g**: elongated granules with multiple regions differing in intensity of fluorescence. Bar = 10 μm.
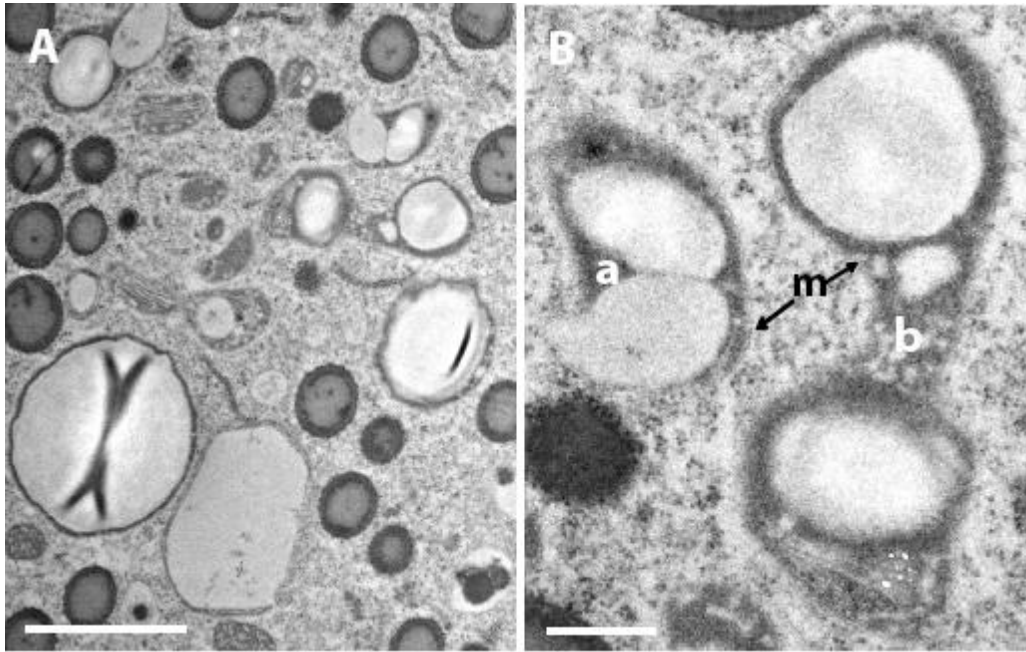
**Fig. 4**.Transmission electron microscope images of subaleurone layers of B73 (normal maize) endosperm tissue harvested on 20 DAP. **A**: overview; **B**: higher magnification of A. **a**: two starch granules initiated in one amyloplast; **b**: amyloplast in division containing two starch granules; **m**: membrane of amyloplast. Bars = 2 μm on A and 0.5 μm on B.
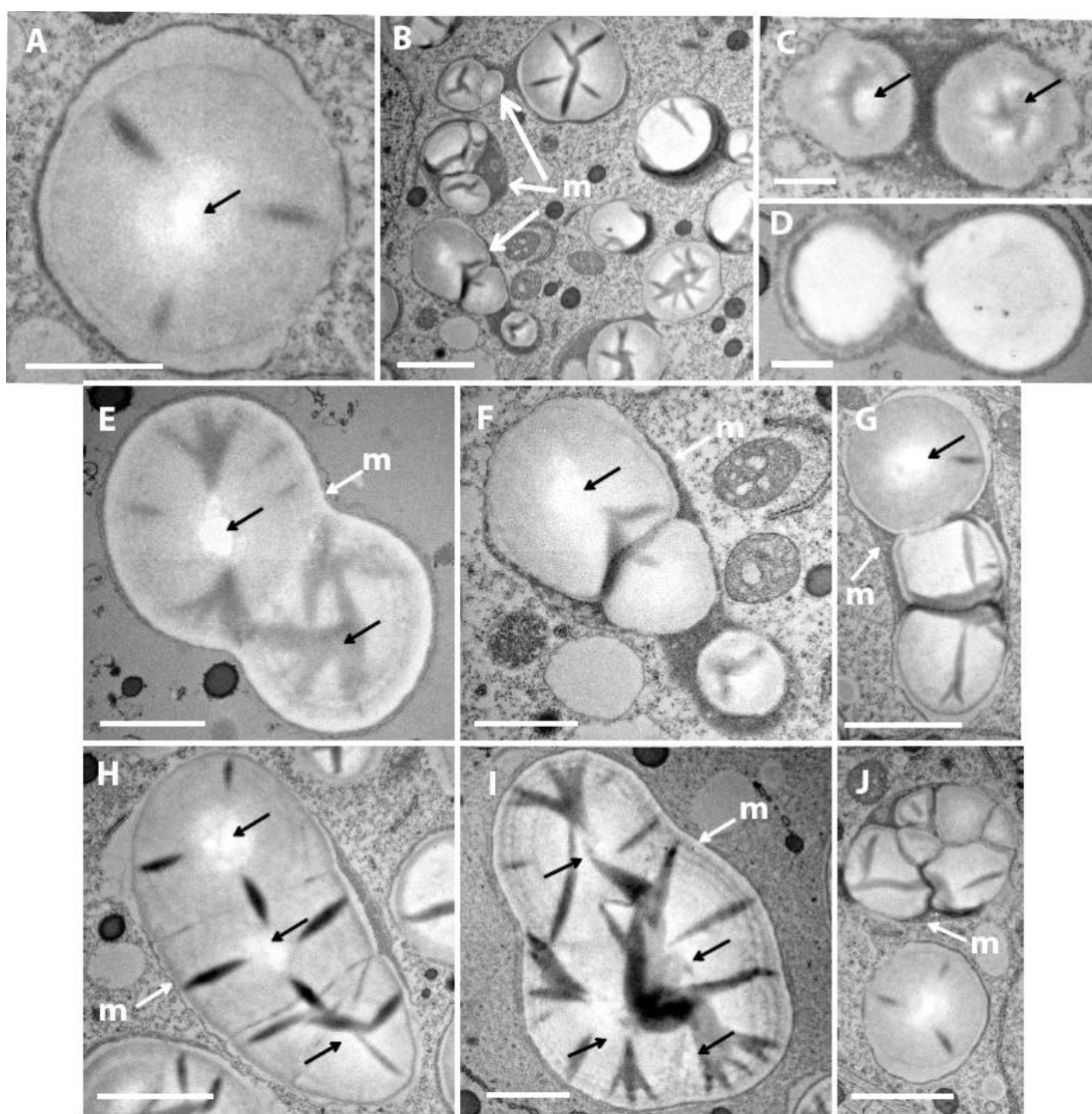
**Fig. 5**. Transmission electron microscope images of subaleurone layers of GEMS-0067 endosperm tissue harvested on 20 DAP. **A**: spherical starch granule with a hilum at center of granule and growth rings; **B**: overview of endosperm tissue; **C**: two starch granules initiated in one amyloplast at early stage of starch granule development; **D**: initial fusion of starch granules; **E**: two fused starch granules forming an elongated starch granule; **F**: two connected starch granules and a third starch granule in the amyloplast protrusion; **G**: three small granules fused into one granule, with one small granule at head showing hilum and growth rings, and the other two granules displaying no hilum or growth rings; **H**: elongated starch granule formed by fusion of three small granules, each with a hilum and growth rings; **I**: four small starch granules, each with an individual hilum, fused together and coated by several layers of growth rings parallel to boundary of amyloplast; **J**: six starch granules, without hila and growth rings, were fused in one amylosplast to form an almost spherical starch granule; **m**: membrane boundary of amyloplast. Black arrow indicates hilum. Bars = 2 µm on B, E, G, H, I and J; and 1 µm on A, C, D and E.

**Fig. 6.** Proposed model of elongated starch granule formation in amyloplast. **A**: two starch granules, each with hilum and growth rings, are initiated in amyloplast; **B**: two granules start fusion by amylose interaction forming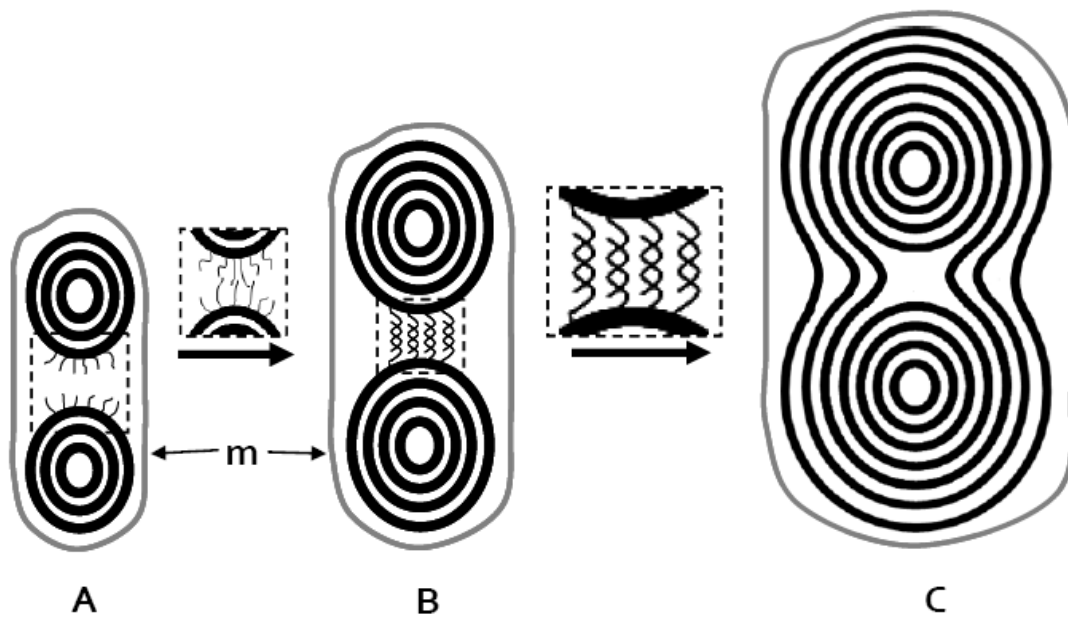 anti-parallel double helices between them, which prevent amyloplast division; **C**: fused granules have integrated outer layer growth rings; **m**: membrane boundary of amyloplast.

# CHAPTER 5. VARIATIONS IN STARCH PHYSICOCHEMICAL PROPERTIES FROM A GENERATION-MEANS ANALYSIS STUDY USING AMYLOMAIZE V AND VII PARENTS

Hongxin Jiang,[†] Jay-lin Jane,[†] Diana Acevedo,[‡] Andrew Green,[‡] George Shinn,[‡] Denyse

Schrenker,[‡] Sathaporn Srichuwong,[†] Mark Campbell,*[‡] and Yusheng Wu[§]

[†]Department of Food Science and Human Nutrition, Iowa State University, Ames, IA 50011,

USA;

[‡] Truman State University, Kirksville, MO 63501, USA

[§] Plant Science Department, South Dakota State University, Brookings, SD 57007, USA

* To whom correspondence should be addressed. Telephone: 660-785-4280. Fax: 660-785-

7604. E-mail: campbell@truman.edu

## Abstract

GEMS-0067 (PI 643420) maize line is a homozygous mutant of the recessive *amylose-extender* (*ae*) allele and an unknown number of high-amylose modifier (HAM) gene(s). GEMS-0067 produces starch with a ~25% higher resistant-starch (RS) content than maize *ae* single-mutant starches. The objective of this study was to understand how the HAM gene(s) affected the RS content and other properties of *ae*-background starches. Nine maize samples, including G/G, G/F1, G/H, F1/G, F1/F1, F1/H, H/G, H/F1, and H/H with HAM gene-dosage of 100%, 83.3%, 66.7%, 66.7%, 50%, 33.3%, 33.3%, 16.7%, and 0%, respectively, were produced from self- and inter-crosses of GEMS-0067 (G), H99*ae* (H), and GEMS-0067×H99*ae* (F1) in a generation-means analysis (GMA) study. RS contents of examined starches were 35.0, 29.5, 28.1, 32.0, 28.2, 29.4, 12.9, 18.4, and 15.7%, respectively, which

were significantly correlated with HAM gene-dosage (r = 0.81, *P* < 0.01). Amylose content, number of elongated starch granules, and conclusion gelatinization-temperature increased with the increase in HAM gene-dosage. X-ray diffraction study showed that the relative crystallinity (%) of starch granules decreased with the increase in HAM gene-dosage. The results suggested that the HAM gene-dosage was responsible for changes in starch molecular structure and organization of starch granules and, in turn, the RS formation in the maize *ae*-mutant starch.

**KEYWORDS: High-amylose maize; *ae*-mutant; resistant starch; amylose; starch physicochemical properties; high-amylose modifier gene**

**INTRODUCTION**

Normal (non-mutant) maize starch consists of two polysaccharides: amylose and amylopectin. Amylose molecules are essentially linear chains of $(1\rightarrow4)$-linked $\alpha$-D-glucopyranose; some amylose molecules possess a few branches. Amylopectin has highly branched structures consisting of $(\alpha1\rightarrow6)$ linked chains of $(1\rightarrow4)$-linked $\alpha$-D-glucopyranose (*1, 2*). In addition to amylose and amylopectin, high-amylose maize starch also contains intermediate components (IC) which are branched molecules having molecular weights similar to amylose (*3, 4*).

Starch is widely used for food and non-food applications, such as an energy source, thickeners, binders, films, and foams (*5*). In human digestive system, starch is digested predominantly in the small intestine by enzymes. Resistant starch (RS), however, resists enzymatic hydrolysis in the small intestine and passes to the large intestine where it is

subjected to bacterial fermentation (*6*). Studies have shown that RS provides many benefits

to human health, including prevention of colon cancer, lowering blood glucose, and

reduction of LDL-cholesterol (*7*). RS is classified into five types (*8-10*). The type I RS is the

physically inaccessible starch, resulting from entrapment in nondigestible plant tissue. The

type II RS is raw starch granules from potato, pea, or high-amylose maize starch, which has

the B- or C-type polymorphism. The type III RS is the retrograded amylose. The type IV RS

is the chemically modified starch. The type V RS is amylose-lipid complexed starch.

Normal maize starch consists of ~30% amylose (*11*). Commercial maize varieties

possessing high-amylose starch have been classified into amylomaize V, VI, and VII

reflecting amylose contents of 50, 60, and 70%, respectively (*12*). A high-amylose maize line,

GEMS-0067 (PI 643420), has been developed by USDA-ARS Germplasm Enhancement of

Maize (GEM) Project (*13*). Starches of GEMS-0067 lines consist of significantly larger

amylose/IC contents (86.1-89.3%) and RS contents (39.4-43.2%) than maize *amylose-

extender* (*ae*) single-mutant starches of H99*ae*, OH43*ae*, B89*ae*, and B84*ae* (66.5-74.6% and

11.5%-19.1%, respectively) (*14*). The GEMS-0067 line is a homozygous mutant of the

recessive *ae* gene and an unknown number of high-amylose modifier (HAM) gene(s). Wu et

al. (*15*) conducted a generation-means analysis (GMA) study using the GEMS-0067 line and

H99*ae* line in order to understand the effect of the HAM gene(s) on the amylose content of

the maize *ae*-mutant starch. It has been observed that the HAM gene(s) has an additive effect

rather than a dominance effect on the amylose content of starch when it is present in maize of

a homozygous *ae*-mutant background (*15*). There is no information, however, regarding the

impact of the HAM gene(s) on either RS content or other starch characteristics. Such

information could provide guidelines for maize breeders in the development of new

germplasms with increased grain yields and RS contents. This study aimed to understand

how HAM gene-dosage affected the RS content and other physicochemical properties of

maize *ae*-mutant starches obtained from the GMA study conducted by Wu et al. (*15*).


## MATERIALS AND METHODS

**Preparation of Maize Samples.** This study used a GMA model for traits under triploid

inheritance as described by Bogyo et al. (*16*). This model enables the estimates of the genetic

parameters of a greater contribution of the female parent. The generations, including G/G,

G/F1, G/H, F1/G, F1/F1, F1/H, H/G, H/F1, and H/H, were obtained from self- and inter-

crosses of GEMS-0067 (G), H99*ae* (H), and GEMS-0067×H99*ae* (F1). A diagram of

producing nine maize sample lines through crossing is shown in **Figure 1**. Pedigrees and

description of maize samples are given in **Table 1**. Plants were grown at the Truman State

University research farm near Kirksville, MO in summer of 2006 and established in a

randomized complete block design.

**Total Starch Determination.** A method using enzymatic hydrolysis, described by

McCleary et al. (*17*)  and Hall and Mertens (*18*) with modifications, was used to determine

the total starch content of the grain sample. The samples were ground using a Tecator sample

mill (Foss North America, Eden Prarie) to pass a screen with an opening of 1 mm. The

ground sample (0.1 g) was mixed with 1 mL of dimethyl sulfoxide (DMSO) and then

incubated in a water bath at 58°C for 24h. The starch dispersion was mixed with acetate

buffer (30 mL, 0.1 M, pH = 4.5), and then hydrolyzed using a thermally stable alpha-amylase

(0.1 mL, Spezyme® Xtra, Genencor, Rocherster, NY) at boiling-water temperature for 1h.

The hydrolyzate was further digested with glucoamylase (0.3 mL, G-Zyme® 480, Genencor,

Rocherster, NY) at 58°C for 2h. The glucose concentration (g/L) was determined using an

YSI 2700 Select Biochemistry monitoring system (Yellow Springs Instruments Inc, Yellow

Springs, OH). The total starch content of the sample was calculated as follows: %total starch

$= 100 \times 0.9 \times$ (total glucose released from starch)/ total dried weight of sample.

**Starch Isolation.** Starch was isolated from maize kernels using a wet-milling method in

presence of neutral proteases as described by Wittrock et al. (*19*).

**Determination of Amylose Content.** The amylose content of starch was determined

using an iodine-colorimetric method described by Wittrock et al. (*19*) and using Sepharose

CL-2B gel-permeation chromatography (GPC) (*20*) followed by a total carbohydrate

(phenol-sulfuric acid) assay (*21*).

**RS Content of Starch.** RS content of each starch sample was determined using the

AOAC Method 991.43 for total dietary fiber (*22*) as described by Li et al. (*14*).

**Scanning Electron Microscopy (SEM).** Starch was coated with gold-palladium (60:40).

Starch granules were viewed under a scanning electron microscope (JEOL JSM-6100) at 5.0

kV accelerating voltage.

**Light Microscopy.** Polarized and phase-contrast light micrographs of starch granules

were obtained using a light microscope (Zeiss Axioplan 2, Thornwood, NY) equipped with a

digital microscopy imaging system including an AxioCam MRC color camera and Axiovison

rel. 4.5 software. Images were analyzed for the number of starch granules displaying weak or

no birefringence and for the area, perimeter and circularity of starch granules using the online

program ImageJ from National Institute of Health (NIH), which is available by ftp at

zippy.nimh.nih.gov/ or http://rsb.info.nih.gov/nih-imageJ.

**X-Ray Diffraction and Starch Crystallinity.** Starch samples were equilibrated in a chamber at 100% relative humidity at 25°C for 24 hours. X-ray diffraction pattern and relative crystallinity of starch were determined using the method described by Ao & Jane (*23*).

**Thermal Properties of Starch.** Thermal properties of the starch were analyzed using a differential scanning calorimeter (DSC) (DSC-7, Perkin-Elmer, Norwalk, CT) (*24*). Starch (~6.0 mg, dry starch basis) was mixed with water (~18μL) in a stainless-steel pan, equilibrated at room temperature for 1 h, and then heated from 10 to 150°C at a rate of 10°C/min. A sealed empty stainless-steel pan was used as the reference. Onset ($T_o$), peak ($T_p$), and conclusion ($T_c$) gelatinization-temperatures and enthalpy change ($\Delta H$) of starch were analyzed by using the Pyris software (Perkin-Elmer, Norwalk, CT).

**Statistical Analysis.** Data were analyzed using SAS program (SAS 9.1).


## RESULTS AND DISCUSSION

**HAM Gene-Dosage of Maize Samples.** Maize endosperm is produced by fusion of two maternal nuclei and one paternal nucleus during fertilization resulting in a triploid tissue (*25*). Therefore, ears of G/G, G/H, H/G, and H/H had kernels with endosperms of a homogenous genotype bbb, Bbb, BBb, and BBB, respectively, in which b represented the HAM gene(s) (assuming a single locus) and B represented the wild type allele (**Table 1**). Each of other samples (G/F1, F1/G, F1/F1, F1/H, and H/F1) had endosperm genotypes with mixture of bbb, Bbb, BBb, or BBB because of segregation of alleles from the F1 gametes (**Table 1**). The HAM gene-dosage of endosperm was calculated as the total number of b divided by the sum of total numbers of B and b (**Table 1**). Consequently, the nine maize samples, G/G, G/F1,

G/H, F1/G, F1/F1, F1/H, H/G, H/F1, and H/H, had HAM gene-dosage levels of 100%,
83.3%, 66.7%, 66.7%, 50%, 33.3%, 33.3%, 16.7%, and 0%, respectively (**Table 1**).

The GEMS-0067 line has been demonstrated to be homozygous of *ae* and HAM gene(s),
whereas H99*ae* line is an *ae* single-mutant (*13*). The HAM gene(s) has an additive effect
rather than a dominance effect on the amylose content of maize *ae*-mutant starch (*15*).
Preliminary results showed that *sbeI* gene could be partially or entirely HAM gene(s) (*26*). It
is known that biosynthesis of the starch granule typically involves several enzymes including
ADP-glucose pyrophosphorylase, starch synthase, starch branching enzyme (SBE), and
starch debranching enzyme. The branched structure of amylopectin results from the activity
of SBEs. The SBEs catalyze the formation of ($\alpha1{\rightarrow}6$) glycosidic bonds by means of
cleavage within a linear chain and transfer of the free reducing end to the C6 of an adjacent
glucose unit. There are two major SBE isoforms in maize endosperm, SBEI and SBEII. The
SBEII is known to transfer shorter chains *in vitro*, whereas the SBEI transfers longer chains.
In maize endosperm, two closely related forms of SBEII (SBEIIa and SBEIIb) have been
reported. Mutation at the *sbeI* locus reduces enzyme activity of SBEI while mutation at *ae*
(*sbeIIb*) locus results in a decrease in the SBEIIb enzyme activity. The SBEIIb plays a major
role in biosynthesis of branch structures of amylopectin in normal-maize endosperm (*27, 28*).

**Amylose, RS, and Total Starch Contents.** Amylose contents of starches determined
using GPC followed by total carbohydrate (phenol-sulfuric) detection and using iodine-
colorimetric method are summarized in **Table 2**. The amylose content determined using GPC
followed by total carbohydrate determination, which includes both amylose and IC molecules,
increased from 68.9 to 88.2% as HAM gene-dosage increased (r = 0.98, $p < 0.001$). A similar
trend was also observed for the amylose content determined using iodine-colorimetric

method (**Table 2**). These results were in agreement with the result previously reported (*15*).

Amylose contents of maize *ae*-mutant starches are typically around 55% but can vary

significantly depending on the parental background genes (*12*). The effect of SBEIIb activity

on starch characteristics has been reported. Increasing doses of the recessive *ae* allele

decrease the enzyme activity of SBEIIb proportionally (*29*). Although an increase in amylose

content has been reported between *AeAeAe and Aeaeae* endosperm genotypes (*30*), there is

no significant difference between *AeAeAe* and *AeAeae*. Zuber et al. (*31*) reported amylose

contents up to 70.3%, which could be a result of modifying factors that were not allelic to *ae*.

Sidebottom et al. (*32*) reported that an amylomaize VII line contained an elevated amylose

content which could result from the losses of SBEIIb and SBEI enzyme activities. A low

amylopectin starch has been reported to have an even higher amylose level than the

amylomazie VII starch because of an additional loss of SBEIIa enzyme activity in the low

amylopectin maize line (*32*).

As shown in **Table 2**, the RS contents could be divided into two groups according to the

HAM gene-dosage. The first group had RS contents of 28.1-35.0%, which had G or F1 as the

female parent. Another group (RS 12.9-18.4%) had H as the female parent (**Table 2**). These

results along with endosperm genotypes of the samples (**Table 1**) suggested that two doses or

more of HAM gene(s) in the maize *ae*-mutant substantially increased RS content of the

starch. However, it was noted that one dose of HAM gene(s) had little effect on the RS

content.

Although the total starch content of maize *ae*-mutant sample did not show a clear trend

with the dosage of HAM gene(s), the lowest starch content (59.3%) was found in G/G with

homozygous HAM gene(s) (**Table 2**). The total starch contents (59.3-68.8%) of the maize

*ae*-mutants were less than that of normal maize (~72%) (*11*). It is known that the grain yields and total starch contents of maize *ae*-mutants were lower than that of the normal maize (*33*).

**Morphology of Starch Granules.** SEM images of starch granules of selected genotypes, G/G, G/H, H/G, and H/H are shown in **Figure 2**. Two types of starch granules, spherical and elongated granules, were observed for all starch samples, which were similar to the results previously reported (*34*). G/G starch contained a larger number of elongated granules than other starches (**Figure 2A-D**). When GEMS-0067 line was pollinated by H99*ae* line, some starch granules showed protrusions and began to have a less extreme rod shape (G/H, **Figure 2B**). When H99*ae* line was pollinated by GEMS-0067 line, some starch granules showed minor protrusions (H/G, **Figure 2C**) that were less pronounced than those found in G/H starch granules (**Figure 2B**). These results suggested that the HAM gene(s) affected the formation of elongated granules which could result from the increase in amylose content of the starch granules (**Table 2**). It has been reported that the proportion of elongated starch granules in maize *ae*-mutant starch increases with the increase in amylose content of the starch (*34*). The elongated starch granules in maize *ae*-mutant are developed by fusion of multiple granules through amylose interaction in the amyloplast at the early stage of the granule development (*35*).

The average circularity, area, and perimeter of starch granules are summarized in **Table 3**. The average area (r = -0.90, *p* < 0.01) and perimeter (r = -0.92, *p* < 0.001) of starch granules increased as the HAM gene-dosage decreased. Circularity of starch granules varied slightly between starches examined. However, the lowest value (0.76) was observed for the G/G starch in which the HAM gene(s) was fixed (**Table 3**). These findings confirmed that morphological properties of starch granules were influenced by the HAM gene-dosage.

Polarized and phase-contrast light micrographs of G/G starch granules are shown in **Figure 3**. The starch granules showed various birefringence patterns as previously reported (*35*), which included one Maltese-cross on a whole single granule, several Maltese-crosses overlapping in one granule, one single granule containing one or more Maltese-crosses and weak to no birefringence on the remainder of the granule, and granules showing weak or no birefringence. The starch granules that displayed weak or no birefringence were mostly elongated granules and were found in greater proportions for G/G and G/F1 starches (~27.1%) than other starches (6.0-13.5%) (**Table 3**). These results suggested that the increase in HAM gene-dosage resulted in changes in the birefringence patterns of the starch granules, indicating changes in molecular organization of the granules. It was noticed that three doses of HAM gene(s) in the endosperm of the maize *ae*-mutant played a major role in the proportion of starch granules that displayed weak or no birefringence pattern when viewed under a polarized light microscope. Because the increase of HAM gene-dosage in maize *ae*-mutant increased the amylose content of the starch (**Table 2**), the change in birefringence patterns of starch granules was a result of an increase in amylose content of starch granules.

**Crystallinity of Starches.** X-ray diffraction patterns of native starches of selected genotypes, G/G, G/H, H/G, and H/H are shown in **Figure 4**. Although the doses of HAM gene(s) decreased from 3, 2, 1 to 0 for the samples of G/G, G/H, H/G, and H/H, respectively, all the starches displayed B-type polymorph, indicating no effect of HAM gene-dosage on the starch polymorph of maize *ae*-mutant. The percentages of starch crystallinity increased from 16.3 to 23.7% with the decrease in the HAM gene-dosage (**Figure 4**) as well as the decrease in the amylose content (**Table 2**). This result was in agreement with previous report (*34*). The V-type X-ray diffraction pattern of amylose-lipid complex with 2θ peaks at 8°, 13°,

and 20° (*36*) was not observed for the starches, indicating no crystalline amylose-lipid complex present in the starch granules as previous reported (*14, 34*).

**Thermal Properties of Starches.** DSC thermograms of the nine maize starches are shown in **Figure 5**, and their thermal properties are summarized in **Table 4**. Broad thermal-transition peaks were observed for all the starch samples (**Figure 5**), which were in agreement with other observations of high-amylose starches (*14, 37*). The range of the thermal transition peak decreased when the HAM gene-dosage decreased (**Figure 5**).

Two endothermic peaks were observed for most starches except for G/G (**Figure 5**). The first peak ($T_{p1}$, 78.6-91.9°C; **Table 4**), corresponding to the melting of short-chain double-helical crystallites of mainly amylopectin molecules (*14, 34, 38*), decreased with an increase in HAM gene-dosage (**Figure 5**). The second peak ($T_{p2}$, ~99.4°C; **Table 4**), corresponding to the melting of long-chain double-helical crystallites of amylose/IC (*14, 38*) and the dissociation of amylose-lipid complexes (*14, 39*), increased with an increase in HAM gene-dosage (**Figure 5**). The conclusion gelatinization-temperatures were ~120.8°C for G/G, G/F1, G/H, F1/G, F1/F1, and F1/H starches, ~108.7°C for H/G and H/F1 starches, and 105.5°C for H/H starch (**Table 4**), which decreased with the decrease in HAM gene-dosage (r = 0.87, *p* < 0.01). These results supported that the HAM gene-dosage affected the molecular structures of maize *ae*-mutant starches, resulting in different gelatinization temperatures. It has been reported that the long-chain double-helical crystallites in maize *ae*-mutant starches have gelatinization temperatures above 100°C, retain semi-crystaline structures at 95-100°C, and are resistant to enzymatic hydrolysis at 95-100°C (*14, 34*). The lipids present in maize *ae*-mutant starches also reduce the enzyme digestibility of the starch granules (*34*). A decrease

in enthalpy change with the increase in HAM gene-dosage was also observed ($r = -0.83$, $p < 0.01$), which could result from the reduction in the starch crystallites (**Figure 4**) or the total double helices in starch granules.

**Relationship between HAM Gene-Dosage and Starch Physicochemical Properties.** The Pearson correlation coefficients between HAM gene-dosage and starch physicochemical properties are given in **Table 5**. The HAM gene-dosage positively correlated with amylose contents determined both using GPC and iodine-colorimetric methods ($r = 0.98$ and $0.96$, $p < 0.001$, respectively) (**Table 5**). A positive effect of HAM gene-dosage on RS content ($r = 0.81$, $p < 0.01$) and number of starch granules that displayed weak or no birefringence ($r = 0.83$, $p < 0.01$) was also observed. The HAM gene-dosage, however, showed negative correlation with some morphological properties of starch granules i.e. the average area ($r = -0.90$, $P < 0.01$) and perimeter ($r = -0.92$, $P < 0.001$).

The increase in HAM gene-dosage positively correlated with the peak gelatinization-temperature of the short-chain double-helical crystallites ($r = 0.84$, $P < 0.01$) (first peak, **Table 5**) and conclusion gelatinization-temperature ($r = 0.87$, $P < 0.01$), but negatively correlated with enthalpy change ($r = -0.83$, $p < 0.01$) (**Table 5**). It was a particular interest in the good correlation between conclusion gelatinization-temperature and RS content of the examined starches ($r = 0.94$, $p < 0.01$; **Table 5**). Because much of the recent interest in high-amylose maize has been focused on its RS content, the conclusion gelatinization-temperature could be potentially used as an indicator for estimation of RS content in high-amylose maize starch.

As listed in **Table 5**, the amylose content, like the HAM gene-dosage, also significantly correlated with RS content, number of starch granules that displayed weak or no

birefringence, the average area and perimeter of starch granules, and thermal properties including first peak and conclusion gelatinization-temperatures and enthalpy change. The results confirmed that the increase of HAM gene-dosage in the maize *ae*-mutant resulted in an increase in amylose content of the starch, leading to changes in molecular organization of the granule, granule morphology, starch thermal properties, and the RS content of the starch.

In conclusion, an increase of HAM gene-dosage in maize *ae*-mutant resulted in higher amylose content of the starch, which, in turn, significantly affected the molecular organization of the granule, granule morphology, starch crystallinity, and starch thermal properties. The increase of amylose content in maize *ae*-mutant starch contributed to the formation of long-chain double-helical crystallites and amylose-lipid complex resulting in RS formation in the starch. Two doses or more of HAM gene(s) in maize *ae*-mutant substantially increased the RS content of the starch, whereas one dose of HAM gene(s) had little effect on the RS content.

**LITERATURE CITED**

(1) Takeda, C.; Takeda, Y.; Hizukuri, S. Structure of amylomaize amylose. *Cereal Chem.* **1989,** 66 (1), 22-25.

(2) Takeda, Y.; Shitaozono, T.; Hizukuri, S. Molecular-structure of corn starch. *Starch/Starke* **1988,** 40 (2), 51-54.

(3) Baba, T.; Arai, Y. Structural features of amylomaize starch .3. Structural characterization of amylopectin and intermediate material in amylomaize starch granules. *Agr. Biol. Chem. Tokyo* **1984,** 48 (7), 1763-1775.

(4) Wang, Y. J.; White, P.; Pollak, L.; Jane, J. Amylopectin and intermediate materials in starches from mutant genotypes of the Oh43 inbred line. *Cereal Chem.* **1993,** 70 (5), 521-525.

(5) Richardson, P. H.; Jeffcoat, R.; Shi, Y.-C. High-amylose starches: From biosynthesis to their use as food ingredients. *MRS Bull.* **2000,** 25 (12), 20-24.

(6) Englyst, H. N.; Macfarlane, G. T. Breakdown of resistant and readily digestible starch by human gut bacteria. *J. Sci. Food. Agric.* **1986,** 37 (7), 699-706.

(7) Sajilata, M. G.; Singhal, R. S.; Kulkarni, P. R. Resistant starch - A review. *Compr. Rev. Food F.* **2006,** 5 (1), 1-17.

(8) Englyst, H. N.; Kingman, S. M.; Cummings, J. H. Classification and measurement of nutritionally important starch fractions. *Eur. J. Clin. Nutr.* **1992,** 46 Suppl 2, S33-50.

(9) Woo, K. S.; Seib, P. A. Cross-linked resistant starch: preparation and properties. *Cereal Chem.* **2002,** 79 (6), 819-825.

(10) Jane, J.; Hasjim, J.; Birt, D.; Zhao, Y. Resistant food starches and methods related thereto. *Patent No.* WO 2009023159, **2009**.

(11) Hasjim, J.; Srichuwong, S.; Scott, M. P.; Jane, J. Kernel Composition, Starch Structure, and Enzyme Digestibility of opaque-2 Maize and Quality Protein Maize. *J. Agric. Food Chem.* **2009,** 57 (5), 2049-2055.

(12) Vineyard, M. L.; Bear, R. P.; MacMasters, M. M.; Deatherage, W. L. Development of "amylomaize" - corn hybrides with high amylose starch: I. Genetic considerations. *Agron. J.* **1958,** 50, 595-598.

(13) Campbell, M. R.; Jane, J.; Pollak, L.; Blanco, M.; O'Brien, A. Registration of maize germplasm line GEMS-0067. *J. Plant Registra.* **2007,** 1, 60-61.

(14) Li, L.; Jiang, H.; Campbell, M.; Blanco, M.; Jane, J. Characterization of maize amylose-extender (*ae*) mutant starches: Part I. Relationship between resistant starch contents and molecular structures. *Carbohydr. Polym.* **2008,** 74 (3), 396-404.

(15) Wu, Y.; Campbell, M.; Yen, Y.; Wicks, Z., III; Ibrahim, A. M. H. Genetic analysis of high amylose content in maize (*Zea mays L.*) using a triploid endosperm model. *Euphytica* **2009,** 166 (2), 155-164.

(16) Bogyo, T. P.; Lance, R. C. M.; Chevalier, P.; Nilan, R. A. Genetic Models for Quantitatively Inherited Endosperm Characters. *Heredity* **1988,** 60, 61-67.

(17) McCleary, B. V.; Gibson, T. S.; Mugford, D. C. Measurement of total starch in cereal products by amyloglucosidase-alpha -amylase method: collaborative study. *J. AOAC Int.* **1997,** 80 (3), 571-579.

(18) Hall, M. B.; Mertens, D. R. Effect of sample processing procedures on measurement of starch in corn silage and corn grain. *J. Dairy Sci.* **2008,** 91 (12), 4830-4833.

(19) Wittrock, E.; Jiang, H.; Campbell, M.; Campbell, M.; Jane, J.; Anih, E.; Wang, Y.-J. A simplified isolation of high-amylose maize starch using neutral proteases. *Starch/Staerke* **2008,** 60 (11), 601-608.

(20) Jane, J.; Chen, J. F. Effect of amylose molecular size and amylopectin branch chain length on paste properties of starch. *Cereal Chem.* **1992,** 69 (1), 60-5.

(21) Dubois, M.; Gilles, K. A.; Hamilton, J. K.; Rebers, P. A.; Smith, F. Colorimetric method for determination of sugars and related substances. *Anal. Chem.* **1956,** 28, 350-6.

(22) Association of Official Analytical Chemists (AOAC) Official Method 991.43. Total, soluble, and insoluble dietary fiber in foods. In *Official methods of analysis of the AOAC international*, 17th ed. Rev.2 ed.; Horwithz, W., Ed. AOAC International: Gaithersburg, Maryland, **2003**.

(23) Ao, Z.; Jane, J. Characterization and modeling of the A- and B-granule starches of wheat, triticale, and barley. *Carbohydr. Polym.* **2007,** 67 (1), 46-55.

(24) Kasemsuwan, T.; Jane, J.; Schnable, P.; Stinard, P.; Robertson, D. Characterization of the dominant mutant amylose-extender (Ae1-5180) maize starch. *Cereal Chem.* **1995,** 72 (5), 457-64.

(25) Birchler, J. A. Dosage analysis of maize endosperm development. *Annu. Rev. Genet.* **1993,** 27, 181-204.

(26) Campbell, M.; Green, A.; Bell, J.; Jane, J.; Jiang, H.; Wu, Y. Germplasm Enhancement of Maize report **2007**, http://www.public.iastate.edu/~usda-gem/Public_Reports/Yr_2007 /GEMR_07_Campbell.pdf:.

(27) James, M. G.; Denyer, K.; Myers, A., M. Starch synthesis in the cereal endosperm. *Curr. Opin. Plant Biol.* **2003,** 6 (3), 215-22.

(28) Morell, M. K.; Myers, A. M. Towards the rational design of cereal starches. *Curr. Opin. Plant Biol.* **2005,** 8 (2), 204-10.

(29) Hedman, K. D.; Boyer, C. D. Gene dosage at the amylose-extender locus of maize: effects on the levels of starch branching enzymes. *Biochem. Genet.* **1982,** 20 (5-6), 483-492.

(30) Fergason, V. L.; Helm, J. L.; Zuber, M. S. Gene dosage effects at the *ae* locus on amylose content of corn endosperm. *J. Hered.* **1966,** 57, 90-94.

(31) Zuber, M. S.; Grogan, C. O.; Deatherage, W. L.; Hubbard, J. E.; Schulze, W. E.; MacMasters, M. M. Breeding high-amylose corn. *Agron. J.* **1958,** 50, 9-12.

(32) Sidebottom, C.; Kirkland, M.; Strongitharm, B.; Jeffcoat, R. Characterization of the difference of starch branching enzyme activities in normal and low-amylopectin maize during kernel development. *J. Cereal Sci.* **1998,** 27 (3), 279-287.

(33) Zuber, M. S.; Grogan, C. O.; Fergason, V. L.; Deatherage, W. L.; MacMasters, M. M. Some observed secondary effects of high-amylose genes in maize. *Cereal Chem.* **1960,** 37, 212-217.

(34) Jiang, H.; Campbell, M.; Blanco, M.; Jane, J. Characterization of maize amylose-extender (*ae*) mutant starches. Part II: Structures and properties of starch residues remaining after enzymatic hydrolysis at boiling-water temperature. *Carbohydr. Polym.* **2010,** 80 (1), 1-12.

(35) Jiang, H.; Horner, H. T.; Pepper, T. M.; Blanco, M.; Campbell, M.; Jane, J. Formation of elongated starch granules in high-amylose maize. *Carbohydr. Polym.* **2010,** 80 (2), 534-539.

(36) Zobel, H. F.; French, A. D.; Hinkle, M. E. X-ray diffraction of oriented amylose fibers. II. Structure of V-amyloses. *Biopolymers* **1967,** 5 (9), 837-845.

(37) Wang, Y. J.; White, P.; Pollak, L. Thermal and gelling properties of maize mutants from the Oh43-inbred line. *Cereal Chem.* **1992,** 69 (3), 328-334.

(38) Jiang, H.; Campbell, M.; Jane, J. Characterization of enzyme-resistant maize *ae*-mutant starches during kernel development. Annual Meeting of American Association of Cereal Chemists **2008**, Honolulu, Hawaii, U.S.A.

(39) Tufvesson, F.; Wahlgren, M.; Eliasson, A.-C. Formation of amylose-lipid complexes and effects of temperature treatment. Part 2. Fatty acids. *Starch/Staerke* **2003,** 55 (3-4), 138-149.

**Table 1.** Pedigrees and Description of Nine Maize Samples Derived from Self- and Inter-Crosses of GEMS-0067 (G), H99*ae* (H), and GEMS-0067×H99*ae* (F1)

| Sample | Breeding pathway | Pedigree | Endosperm genotype | HAM gene-dosage in endosperm[b] (%) |
|--------|------------------|----------|--------------------|-------------------------------------|
| G/G | P1 | GEMS-0067×GEMS-0067 | bbb[a] | 100 |
| G/F1 | BC1P1 | GEMS-0067×(GEMS-0067×H99*ae*) | Bbb, bbb | 83.3 |
| G/H | F1 | GEMS-0067×H99*ae* | Bbb | 66.7 |
| F1/G | BC1P1r | (GEMS-0067×H99*ae*)×GEMS-0067 | BBb, bbb | 66.7 |
| F1/F1 | F1/F1 | (GEMS-0067×H99*ae*)×(GEMS-0067×H99*ae*) | BBB, BBb, Bbb, bbb | 50 |
| F1/H | BC1P2r | (GEMS-0067×H99*ae*)×H99*ae* | BBB, Bbb | 33.3 |
| H/G | F1r | H99*ae*×GEMS-0067 | BBb | 33.3 |
| H/F1 | BC1P2 | H99*ae*×(GEMS-0067×H99*ae*) | BBB, BBb | 16.7 |
| H/H | P2 | H99*ae*×H99*ae* | BBB | 0 |

[a] b represents HAM gene(s) that was assuming a single locus, B represents wild type allele.

[b] %HAM gene-dosage = 100 × the total number of b/the sum of total numbers of B and b.

**Table 2.** Amylose and RS Contents of Native Maize Starches and Total Starch Contents of Grain Samples Derived from Self- and Inter-Crosses of GEMS-0067 (G), H99*ae* (H), and GEMS-0067×H99*ae* (F1)

| Sample | Amylose-GPC[a] (%) | Amylose-C[b] (%) | RS[c] (%) | Total starch (%) |
|---|---|---|---|---|
| G/G | $88.2 \pm 1.5$ | $69.9 \pm 0.0$ | $35.0 \pm 0.5$ | $59.3 \pm 1.5$ |
| G/F1 | $86.7 \pm 0.1$ | $68.3 \pm 0.6$ | $29.5 \pm 0.8$ | $63.4 \pm 0.6$ |
| G/H | $81.7 \pm 1.6$ | $64.9 \pm 0.4$ | $28.1 \pm 0.8$ | $65.1 \pm 0.7$ |
| F1/G | $84.0 \pm 0.1$ | $61.9 \pm 0.2$ | $32.0 \pm 1.4$ | $61.4 \pm 1.3$ |
| F1/F1 | $77.2 \pm 1.3$ | $63.1 \pm 0.5$ | $28.2 \pm 0.7$ | $62.5 \pm 1.0$ |
| F1/H | $74.7 \pm 0.4$ | $58.5 \pm 0.2$ | $29.4 \pm 0.7$ | $68.8 \pm 2.2$ |
| H/G | $77.9 \pm 0.8$ | $61.1 \pm 0.1$ | $12.9 \pm 0.2$ | $62.8 \pm 1.0$ |
| H/F1 | $72.8 \pm 0.2$ | $58.2 \pm 0.6$ | $18.4 \pm 1.3$ | $64.1 \pm 1.3$ |
| H/H | $68.9 \pm 1.6$ | $56.3 \pm 0.4$ | $15.7 \pm 0.2$ | $64.7 \pm 0.1$ |
| Linear[d] | ***[e] | *** | ** | NS |

[a] Amylose content of starch was determined using Sepharose CL-2B gel-permeation chromatography followed by total carbohydrate determination.

[b] Amylose content of starch was determined using iodine-colorimetric method.

[c] Resistant starch (RS) content of starch was determined using AOAC Method 991.43 for total dietary fiber.

[d] Linear relationship between HAM gene-dosage and contents of amylose, RS, and total starch.

[e] ***, $P < 0.001$; **, $P < 0.01$; *, $P < 0.05$; NS, not significant.

**Table 3.** Morphological Properties of Starch Granules Isolated from Kernels of Self- and Inter-Crossed Lines of GEMS-0067 (G), H99*ae* (H), and GEMS-0067×H99*ae* (F1)

| Sample | SG[a] (%) | Circularity[b] $4\pi(\text{area/perimeter}^2)$ | Area ($\mu m^2$) | Perimeter ($\mu m$) |
|---|---|---|---|---|
| G/G | $27.2 \pm 1.8$ | $0.76 \pm 0.005$ | $35.2 \pm 8.2$ | $24.1 \pm 0.3$ |
| G/F1 | $26.9 \pm 2.1$ | $0.81 \pm 0.003$ | $46.9 \pm 1.0$ | $26.4 \pm 0.3$ |
| G/H | $8.0 \pm 2.5$ | $0.80 \pm 0.003$ | $57.2 \pm 1.5$ | $29.5 \pm 0.4$ |
| F1/G | $13.5 \pm 3.5$ | $0.80 \pm 0.003$ | $55.7 \pm 1.5$ | $28.3 \pm 0.4$ |
| F1/F1 | $10.7 \pm 1.5$ | $0.81 \pm 0.003$ | $60.1 \pm 1.9$ | $29.1 \pm 0.5$ |
| F1/H | $6.1 \pm 1.8$ | $0.78 \pm 0.003$ | $64.5 \pm 1.6$ | $31.4 \pm 0.4$ |
| H/G | $9.7 \pm 1.0$ | $0.79 \pm 0.003$ | $60.1 \pm 1.6$ | $30.2 \pm 0.4$ |
| H/F1 | $8.0 \pm 2.0$ | $0.78 \pm 0.003$ | $68.9 \pm 1.9$ | $32.2 \pm 0.5$ |
| H/H | $6.0 \pm 1.5$ | $0.78 \pm 0.003$ | $64.5 \pm 1.8$ | $31.4 \pm 0.4$ |
| Linear[c] | **[d] | NS | ** | *** |

[a] Number of starch granules that displayed weak or no birefringence under a polarized-light microscope.

[b] A circularity value of 1.0 indicates a perfect circle. As the value approaches 0.0, it indicates an increasingly elongated polygon.

[c] Linear relationship between HAM gene-dosage and starch properties.

[d] ***, $P < 0.001$; **, $P < 0.01$; *, $P < 0.05$; NS, not significant.

**Table 4.** Thermal Properties of Nine Maize Starches Isolated from Kernels of Self- and Inter-Crossed Lines of GEMS-0067 (G), H99*ae* (H), and GEMS-0067×H99*ae* (F1)[a]

| Sample | Gelatinization | | | | |
|---|---|---|---|---|---|
| | $T_o$ (°C) | $T_{p1}$ (°C) | $T_{p2}$ (°C) | $T_c$ (°C) | $\Delta H$ (J/g) |
| G/G | 60.3 ± 0.4 | nd[b] | 99.7 ± 0.2 | 122.2 ± 0.2 | 7.8 ± 0.2 |
| G/F1 | 60.1 ± 0.4 | 91.9 ± 0.1 | 99.5 ± 0.4 | 123.0 ± 0.6 | 10.8 ± 0.9 |
| G/H | 60.3 ± 0.4 | 84.2 ± 0.2 | 99.1 ± 0.8 | 119.0 ± 0.3 | 13.7 ± 0.8 |
| F1/G | 60.3 ± 0.4 | 84.9 ± 0.2 | 99.0 ± 0.0 | 121.1 ± 2.1 | 9.3 ± 0.6 |
| F1/F1 | 59.6 ± 0.8 | 83.5 ± 0.7 | 99.7 ± 0.1 | 120.3 ± 0.4 | 14.4 ± 0.9 |
| F1/H | 59.9 ± 0.1 | 83.0 ± 0.0 | 99.8 ± 0.1 | 119.1 ± 0.1 | 13.3 ± 0.1 |
| H/G | 61.3 ± 0.4 | 82.5 ± 0.7 | 98.6 ± 0.1 | 108.9 ± 0.1 | 16.2 ± 0.8 |
| H/F1 | 60.8 ± 0.4 | 78.6 ± 1.7 | 99.1 ± 0.6 | 108.5 ± 0.7 | 15.5 ± 0.4 |
| H/H | 60.1 ± 0.1 | 81.1 ± 0.8 | 99.0 ± 0.3 | 105.5 ± 0.2 | 15.1 ± 0.8 |
| Linear[c] | NS[d] | ** | NS | ** | ** |

[a] $T_o$, $T_p$, $T_c$, and $\Delta H$ are onset temperature, peak temperature, conclusion temperature, and enthalpy change, respectively.
[b] nd = not detected.
[c] Linear relationship between HAM gene-dosage and starch thermal properties.
[d] ***, $P < 0.001$; **, $P < 0.01$; *, $P < 0.05$; NS, not significant.

**Table 5.** Pearson Correlation Coefficients ($r$) between HAM Gene-Dosage and Starch Physicochemical Properties

| | Amylose-GPC (%) | Amylose-C (%) | RS (%) | Total starch (%) | SG (%) | Circularity $4\pi(\text{area/perimeter}^2)$ | Area ($\mu m^2$) | Perimeter ($\mu m$) | $T_o$[e] (°C) | $T_{p1}$ (°C) | $T_{p2}$ (°C) | $T_c$ (°C) | $\Delta H$ (J/g) |
|---|---|---|---|---|---|---|---|---|---|---|---|---|---|
| HAM gene-dosage | 0.98 ***[f] | 0.96 *** | 0.81 ** | -0.55 | 0.83 ** | 0.12 | -0.90 ** | -0.92 *** | -0.18 | 0.84 ** | 0.41 | 0.87 ** | -0.83 ** |
| Amylose-GPC[a] (%) | 1 | 0.93 *** | 0.72 * | -0.59 | 0.84 ** | 0.14 | -0.88 ** | -0.91 ** | -0.03 | 0.83 * | 0.25 | 0.80 ** | -0.82 * |
| Amylose-C[b] (%) | | 1 | 0.70 * | -0.59 | 0.81 ** | 0.11 | -0.92 *** | -0.93 *** | -0.12 | 0.86 ** | 0.38 | 0.76 * | -0.70 * |
| RS[c] (%) | | | 1 | -0.24 | 0.59 | 0.07 | -0.65 | -0.69 * | -0.60 | 0.58 | 0.72 * | 0.94 ** | -0.84 ** |
| Total starch (%) | | | | 1 | -0.64 | -0.08 | 0.67 * | 0.72 * | -0.19 | -0.19 | 0.10 | -0.23 | 0.53 |
| SG[d] (%) | | | | | 1 | -0.05 | -0.92 *** | -0.93 *** | -0.08 | 0.90 ** | 0.38 | 0.61 | -0.78 * |
| Circularity $4\pi(\text{area/perimeter}^2)$ | | | | | | 1 | 0.17 | 0.04 | -0.26 | 0.74 | -0.09 | 0.30 | 0.16 |
| Area ($\mu m^2$) | | | | | | | 1 | 0.99 *** | 0.11 | -0.96 *** | -0.36 | -0.65 * | 0.84 ** |
| Perimeter ($\mu m$) | | | | | | | | 1 | 0.17 | -0.93 *** | -0.39 | -0.72 * | 0.85 ** |

[a] Amylose content of starch was determined using Sepharose CL-2B gel-permeation chromatography followed by total carbohydrate determination.
[b] Amylose content of starch was determined using iodine-colorimetric method.
[c] Resistant starch (RS) of starch was determined using AOAC Method 991.43 for total dietary fiber.
[d] Number of starch granules displayed weak or no birefringence under a polarized-light microscope.
[e] $T_o$, $T_p$, $T_c$, and $\Delta H$ are onset temperature, peak temperature, conclusion temperature, and enthalpy change, respectively.
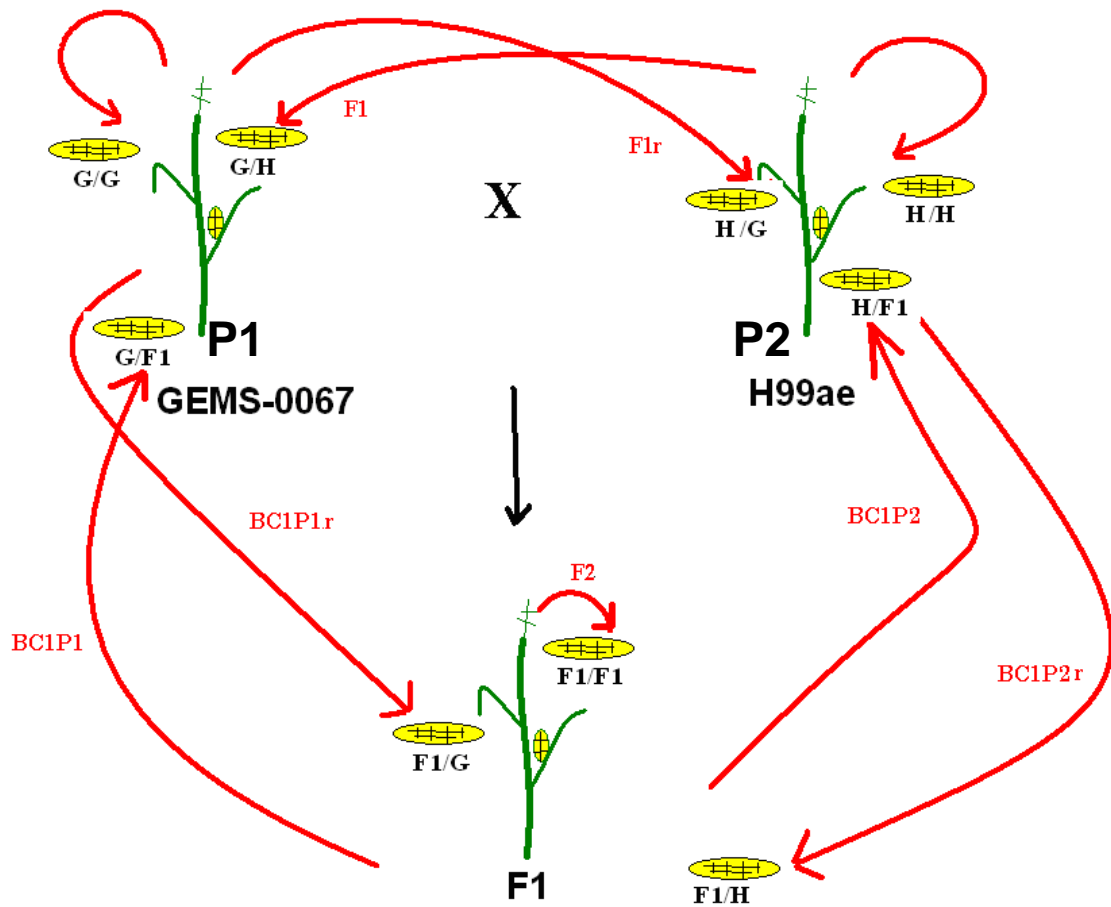[f] * $p < 0.05$, ** $p < 0.01$, *** $p < 0.001$

**Figure 1.** Nine maize samples derived from self- and inter-crosses of GEMS-0067 (G), H99*ae* (H), and GEMS-0067×H99*ae* (F1). G/G, GEMS-0067×GEMS-0067; G/F1, GEMS-0067×(GEMS-0067×H99*ae*); G/H, GEMS-0067×H99*ae*; F1/G, (GEMS-0067×H99*ae*)×GEMS-0067; F1/F1, (GEMS-0067×H99*ae*)×(GEMS-0067×H99*ae*); F1/H, (GEMS-0067×H99*ae*)×H99*ae*; H/G, H99*ae*×GEMS-0067; H/F1, H99*ae*×(GEMS-0067×H99*ae*); H/H, H99*ae*×H99*ae*; P1, parent 1; P2, parent 2; F1, first generation; BC1: first cycle of backcross.
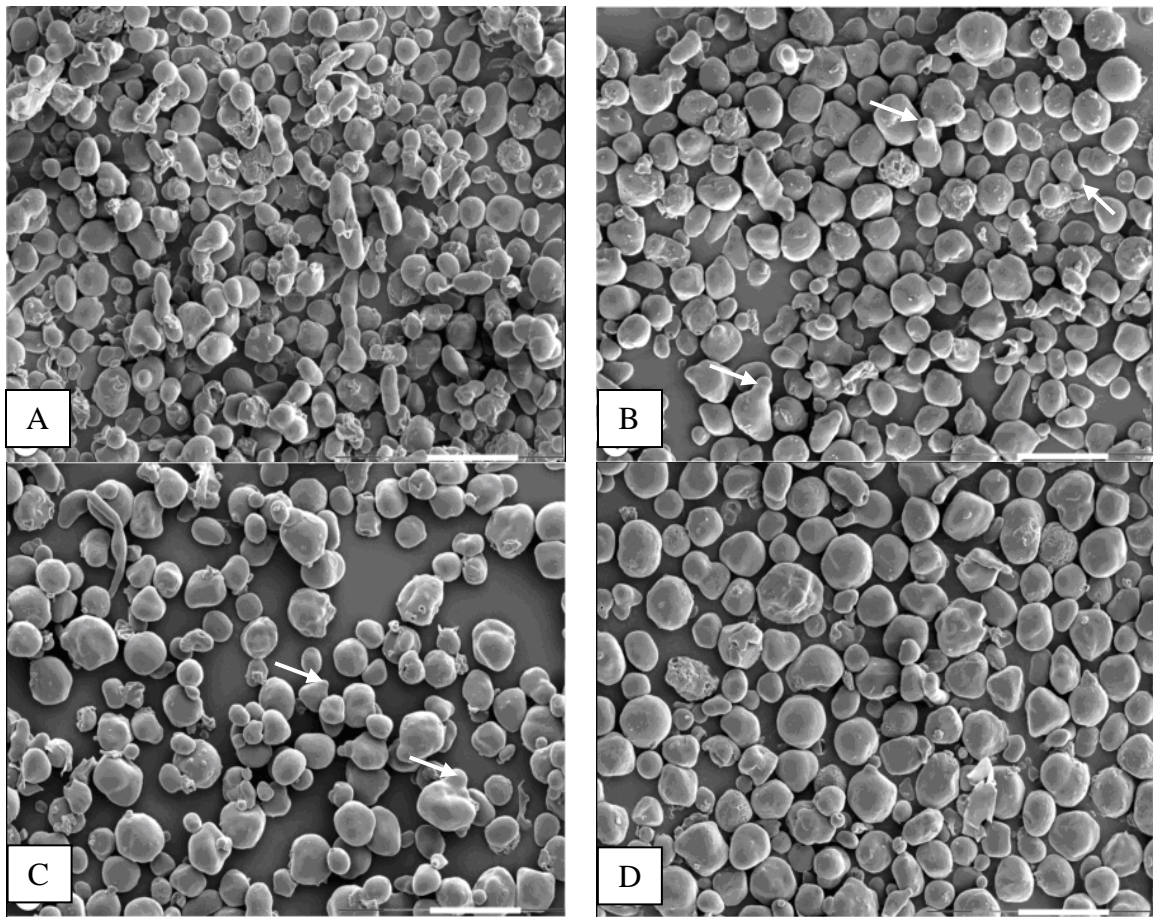
**Figure 2.** SEM images of starches isolated from maize endosperm homozygous for *ae* gene with decreasing doses of the HAM gene(s) from G/G (GEMS-0067). A, G/G; B, G/H, C, H/G; D, H/H. Arrow indicates protrusion. Scale bar = 20μm.
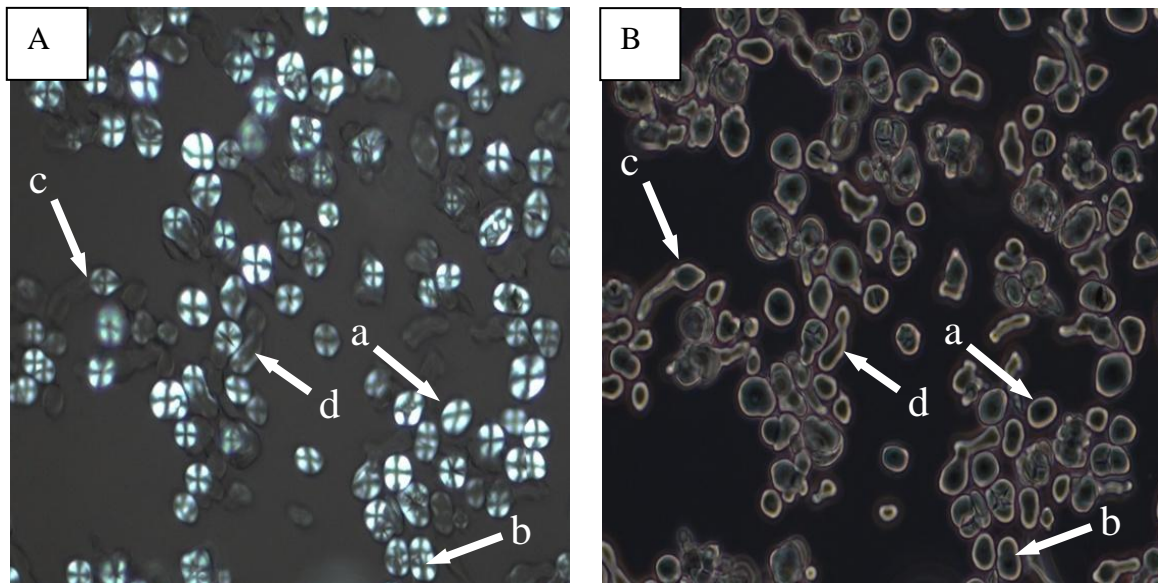
**Figure 3.** Polarized (A) and phase contrast (B) light micrographs of G/G (GEMS-0067) maize starch. Arrows indicate birefringence patterns of (a) one Maltese-cross on the whole granule, (b) Maltese-crosses overlapping in one granule, (c) one single granule containing one Maltese-cross and no birefringence on remainder of the granule, and (d) starch granule showing weak or no birefringence.
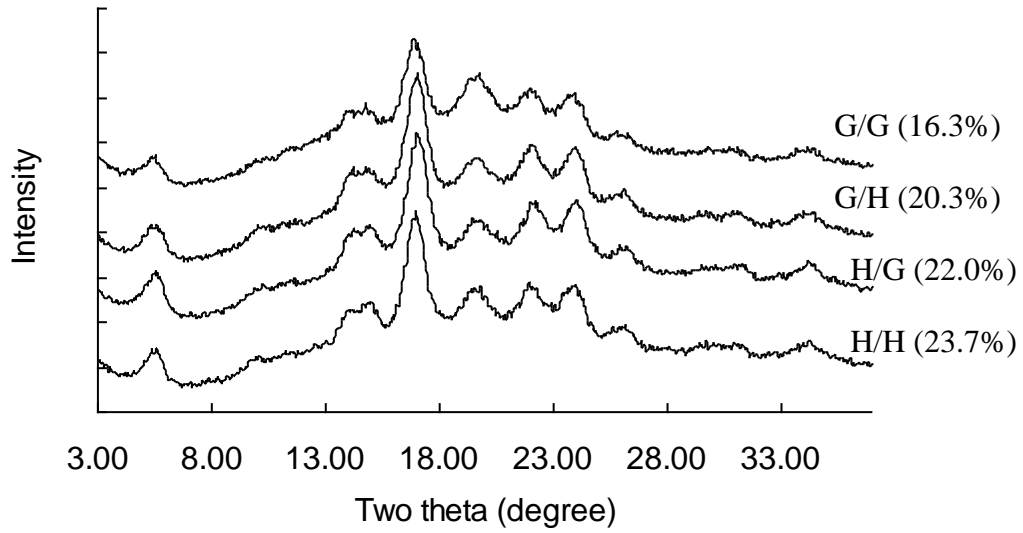
**Figure 4.** X-ray diffraction patterns of native maize starches isolated from kernels of self- and inter-crossed lines of GEMS-0067 (G) and H99*ae* (H). Percentage crystallinity is given in parentheses.
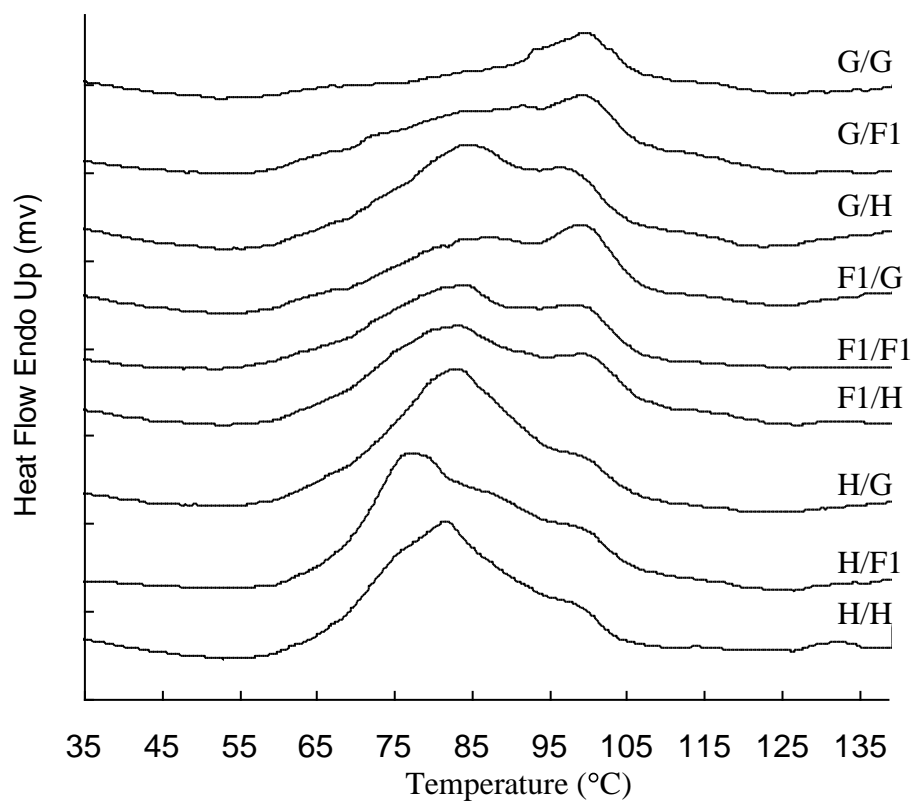
**Figure 5.** DSC gelatinization thermograms of native maize starches isolated from kernels of self- and inter-crossed lines of GEMS-0067 (G), H99*ae* (H), and GEMS-0067×H99*ae* (F1).

# CHAPTER 6. DOSAGE EFFECT OF HIGH-AMYLOSE MODIFIER (HAM) GENE ON THE STARCH STRUCTURE OF MAIZE AMYLOSE-EXTENDER (*ae*) MUTANT

A paper to be submitted to the *Journal of Cereal Science*

Hongxin Jiang [a], Mark Campbell [b], Jay-lin Jane [a,*]

[a] Department of Food Science and Human Nutrition, Iowa State University, Ames, Iowa 50011, USA

[b] Division of Science, Truman State University, Kirksville, MO 63501, USA

*Corresponding author.

2312 Food Sciences Building, Iowa State University, Ames, IA 50011, USA.

Tel.: +1 515 294 9892; Fax: +1 515 294 8181.

E-mail address: jjane@iastate.edu (J. Jane).

## ABSTRACT

The objective of this study was to understand how dosage of the high-amylose modifier (HAM) gene(s) affected the structure of endosperm starch of maize *ae*-mutant. Endosperms of G/G, G/H, H/G, and H/H with 3, 2, 1, and 0 doses of HAM gene(s) were produced by self- and inter-crossing of GEMS-0067 (G), a HAM-gene carrier, and H99*ae* (H), a maize *ae*-mutant. The endosperm starch was fractionated into amylopectin, amylose, and intermediate component (IC) of large and small molecular-weights using 1-butanol precipitation and gel-permeation chromatography. The content of amylopectin decreased from 31.1 to 11.8% with the increase in the dosage of HAM gene(s). The increase in the HAM gene dosage increased the branch chain-length of the small molecular-weight IC. The

HAM gene dosage had little effect on the branch chain-length distributions of amylopectin and large molecular-weight IC and on the molecular-weight of amylose.

**Keywords:** High-amylose maize starch; Amylose-extender mutant; High-amylose modifier gene; Starch structure; Resistant starch; Gene dosage

## 1. Introduction

Starch is the major energy reserve of green plants and widely exists in seeds, tubers, roots, stems, leaves, and fruits (Robyt, 1998). Starch is composed of amylopectin and amylose molecules in general. Amylopectin molecules consist of short chains of $\alpha1\rightarrow4$ linked D-glucopyranose units, which are connected by ($\alpha1\rightarrow6$) glycosidic branch linkages. Amylose molecules are primarily linear chains of ($\alpha1\rightarrow4$)-linked D-glucopyranose units; some amylose molecules possess a few branches (French, 1984; Hizukuri et al., 1981; Jane et al., 1999; Takeda et al., 1988). High-amylose maize starch also consists of intermediate components (IC) that have branched structures with molecular weights smaller than amylopectin but similar to amylose (Baba and Arai, 1984; Jiang et al., 2010a; Kasemsuwan et al., 1995; Klucinec and Thompson, 1998; Li et al., 2008; Wang et al., 1993).

Amylopectin molecules are synthesized through cooperative reactions of starch synthases, starch branching enzymes (SBEs), and starch debranching enzymes (James et al., 2003; Morell and Myers, 2005; Smith, 2001). SBEs include SBEI and SBEII; SBEII prefers to cleave and transfer shorter chains and catalyze the formation of $\alpha1\rightarrow6$ glycosidic bonds *in vitro*, whereas SBEI prefers to transfer longer chains (Guan and Preiss, 1993). There are two isoforms of SBEII, SBEIIa and SBEIIb, identified in maize endosperm. SBEIIb plays a major

role in biosynthesis of amylopectin molecules in maize endosperm (James et al., 2003).

Maize *ae*-mutant is deficient in enzyme activity of SBEIIb in the endosperm, which results in

starch having higher amylose content, larger amount of IC, and longer branch chain-length of

amylopectin than normal maize starch (Jane et al., 1999; Li et al., 2008; Shi and Seib, 1995;

Yuan et al., 1993).

A public high-amylose maize line registered as GEMS-0067 (PI 643420) has been

developed from USDA-ARS Germplasm Enhancement of Maize (GEM) Project by

selectively crossing the exotic line of GUAT209:S13 to a hybrid OH43*ae*×H99*ae* (Campbell

et al., 2007b). The GEMS-0067 maize line is a homozygous mutant of *ae* and HAM gene(s)

(Campbell et al., 2007b). Preliminary results showed that an *sbeI* allele was one of the HAM

gene(s) in the GEMS-0067 (Campbell et al., 2007a). Starch of the GEMS-0067 maize

consists of 39.4-43.2% resistant starch (RS) determined using the AOAC Method 991.43,

much greater than maize *ae* single-mutant starches of H99ae, OH43ae, B89ae, and B84ae

(11.5-19.1%) (Li et al., 2008). The RS content is attributed to long-chain double-helical

crystallites of amylose/IC, which maintain semi-crystalline structures at 95-100 °C and, thus,

are resistant to enzymatic hydrolysis (Jiang et al., 2010a; Li et al., 2008).

Jiang et al. (2010b) reported that the increase of HAM-gene dosage in the endosperm

of maize *ae*-mutant led to an increase in amylose content, formation of long-chain double-

helical crystallites, and changes in molecular organization of the granule, granule

morphology, starch crystallinity, and starch thermal properties. With two or more doses of

the HAM gene(s), the maize *ae*-mutant produces starch with substantially more RS. One

dose of HAM gene(s), however, had little effect on the RS content (Jiang et al., 2010b). In

this study, we aimed to understand how the HAM gene dosage in maize *ae*-mutant affected

the structures of amylopectin, IC, and amylose molecules.

## 2. Experimental

### 2.1. Materials

By self- and inter-crossing of GEMS-0067 (G) and H99*ae* (H), four maize samples,

G/G, G/H, H/G, and H/H, with 3, 2, 1, and 0 doses of HAM gene(s), respectively, were

produced. The experimental procedures for crossing and rationale using the triploid model

were previously described (Wu et al., 2009).The maize plants were grown in Kirksville, MO

in 2006. All the chemicals used for the study were reagent grade and purchased from Sigma-

Aldrich Chemical Co. (St. Louis, MO) or Fisher Scientific (Pittsburgh, PA). Crystalline

*Pseudomonas* isoamylase (EC 3.2.1.68) was purchased from Hayashibara Biochemical

Laboratories, Inc. (Okayama, Japan) and used for debranching amylopectin and IC molecules.

### 2.2. Starch isolation

Endosperm starch was isolated from maize kernels following the method of Li, et al.

(2008).

### 2.3. Fractionation of starch components

Starch was fractionated into amylose and a mixture of amylopectin and IC using

amylose-1-butanol precipitation method (Li et al., 2008; Schoch, 1942). Starch (2.0 g, dry

starch base) was wetted with deionized distilled-water (20.0 mL), dispersed in dimethyl

sulfoxide (DMSO) (180.0 mL) with mechanically stirring in a boiling-water bath for 1 h, mechanically stirred at room temperature for 16 h, precipitated with absolute ethanol (7 X), and collected by centrifugation. The collected amorphous starch was dissolved in hot deionized distilled-water (200.0 mL), mechanically stirred in a boiling-water bath for 30 min, mixed with 1-butanol (40.0 mL), and refluxed under mechanically stirring in a boiling-water bath for another 30 min. The refluxed starch-butanol dispersion was kept in a Duwar flask filled with boiling-water, properly sealed, and allowed to cool down gradually over ~30 h to reach room temperature. The amylose-1-butanol complex precipitated from the dispersion was collected by centrifugation (1000 g, 20 min). The amylopectin and IC molecules remained in the supernatant. The separated amylose and the mixture of amylopectin and IC were further purified by repeating the 1-butanol complex-formation procedure for at least 6 times. The purity of the amylose fraction and the mixture of amylopectin and IC were determined using Sepharose CL-2B gel-permeation chromatography (GPC) (Li et al. 2008) followed by total carbohydrate (phenol-sulfuric acid) (Dubois et al., 1956) and blue value (iodine staining) analyses (Juliano, 1971).

2.4. Amylopectin, IC, and amylose contents of starch

Amylopectin, amylose, and IC contents of starch were determined using Sepharose CL-2B GPC (Li et al. 2008) followed by total carbohydrate (phenol-sulfuric acid method) (Dubois et al., 1956) and blue value (iodine staining) analyses (Juliano, 1971). Whole starch or a mixture of amylopectin and IC (20 mg) was dispersed as described in 2.3. The dispersion (2.0 mL, 2 mg/mL) was injected into a Sepharose CL-2B GPC column (1.5 cm I.D. $\times$ 50 cm)

and eluted using an eluent containing sodium hydroxide (1 mM), sodium chloride (25 mM), and sodium azide (0.02%) at a flow rate of 0.7 mL/min in a descending mode. Fractions of 2.0 mL each were collected and analyzed for total carbohydrate (phenol-sulfuric acid method) and blue value (iodine staining) at 490 nm and 630 nm, respectively. The amylopectin, IC and amylose contents of starch were calculated using the method described by Li, et al. (2008).

2.5. Branch chain-length distributions of amylopectin and IC

Amylopectin and IC of different molecular-weights were separated using a Sepharose CL-2B column. The fractions within the amylopectin peak and within the IC peak of the large and small molecular-weights were combined and collected separately. Each of the combined fractions of amylopectin and IC of the large and small molecular-weights was concentrated using a rotary evaporator (Buchi/Brinkmann Rotavapor-R). The concentrated sample was precipitated with absolute ethanol (7 X).

The precipitated amylopectin and IC of large and small molecular-weights were dispersed as described in 2.3, debranched, and labeled with 8-aminopyrene-1,3,6-trisulfonic acid following the method of Morell et al. (1998) modified by Jiang et al. (2010a). Branch chain-length distributions of amylopectin and IC of large and small molecular-weights were determined using a fluorophore-assisted capillary electrophoresis (FACE) (P/ACE MDQ, Beckman Coulter, Fullerton, CA) following the method of Morell et al. (1998) modified by Jiang et al. (2010a)

2.6. Molecular-size distribution of amylose

Molecular-size distributions of amylose, before and after the debranching reaction, were determined using high-performance size-exclusion chromatography (HPSEC), following the method of Jiang et al. (2010a) with modifications. Shodex SB-804 and SB-803 analytical columns with a Shodex OH pak SB-G guard column (Showa Denko K.K., Tokyo, Japan) were used to analyze the molecular-size distribution of amylose. Preparation of amylose dispersion for determination of molecular-size distribution was conducted using the same procedure as described in 2.3. The amylose molecules were debranched following the method of Li et al.(2008). The debranched amylose was precipitated using absolute ethanol (20 X). The collected debranched-amylose was dispersed in 90% DMSO in a boiling-water bath for 1h, mechanically stirred at room temperature for 16 h, precipitated with absolute ethanol (20 X), collected, and dispersed with hot water in a boiling-water bath for 30 min. The dispersed debranched-amylose (100 μl, 2 mg/mL) was filtered through a membrane (pore size of 5.0 μm) and injected into the HPSEC column. Maltose, maltotriose, maltotetraose, maltohepaose, and pullulan standards (P-5, P10, P20, P50, P100, P200, and P400, Showa Denko K.K., Tokyo, Japan) were used as references for the determination of molecular size of amylose.

**3. Results and discussion**

3.1. Contents of amylopectin, amylose, and IC

Sepharose CL-2B gel-permeation chromatograms of the starches isolated from the kernels of the four crossed plants differing in HAM-gene dosage are shown in Fig.1. All the

GPC profiles of the starches showed two peaks. The first peak (fractions 11-18) was amylopectin molecules, and the second peak (fractions 19-45) was a mixture of amylose and IC (Fig. 1).

The amylopectin contents of the starches, calculated on the basis of the total carbohydrate shown in the peaks of GPC (Fig. 1), are summarized in Table 1. The amylopectin contents of the starches increased from 11.8 to 31.1% with the decrease in HAM gene doses from 3 to 0 (Table 1), which were negatively correlated with RS contents (r = -0.83, $p < 0.05$). This result confirmed previous reported result that amylose/IC contribute to the RS formation in maize *ae*-mutant starch (Jiang et al., 2010a). Although the G/H starch had 3.8% of a moderate decrease in the amylopectin content from the H/G starch (Table 1), the G/H starch consisted of 28.1% RS, which was substantially greater than the H/G starch (12.9%) (Jiang et al., 2010b).

It was intriguing to find out how the HAM gene dosage in the maize *ae*-mutant altered the structures of amylose and IC in addition to their contents and resulted in a substantial increase in the RS content. After the amylose molecules were removed by precipitation using 1-butanol, the mixture of the amylopectin and IC was further separated using GPC (Fig. 2). The removal of amylose molecules was confirmed by the ratio of the blue value to the total carbohydrate in Fractions 19-45 (Fig. 2). The amylopectin molecules were eluted in the peak between fractions 11 and 18. The large molecular-weight IC was collected from fractions 19 to 30, and the small molecular-weight IC was collected from fractions 31 to 45 (Li et al., 2008). The contents of amylose, large molecular-weight IC, and small molecular-weight IC, calculated on the basis of the total carbohydrate shown in the peaks of GPC (Figs. 1-2) as described by Li et al. (2008), are summarized in Table 1. The

G/G starch had more amylose (63.7%), less the small molecular-weight IC (16.8%) than the

G/H starch (54.2% and 19.9%, respectively) (Table 1), but similar content of the large

molecular-weight IC for the G/G and G/H starches (7.5% and 7.5%, respectively) (Table 1).

These results suggested that 3 doses of HAM gene in G/G maize endosperm increased the

amylose content of starch. The greater RS content of the G/G starch (35.0%) than the G/H

starch (28.1%) (Jiang et al., 2010b) was attributed to the larger amylose-content of the native

maize *ae*-mutant starch. It has been reported that amylose, the major component of the maize

*ae*-mutant starch, formed double-helical crystallites having gelatinization temperature above

100 °C, which were resistant to enzymatic hydrolysis at hydrolysis temperature of 95-100 °C

(Jiang et al., 2010a; Jiang et al., 2010c).

The amylose and large molecular-weight IC contents of G/H and H/G starches (2 and

1 of HAM gene dosage, respectively) were similar (54.2 and 55.8 %, and 7.5 and 7.5%,

respectively). Thus, the greater RS content of the G/H starch (28.1%) than the H/G starch

(12.9%) (Jiang et al., 2010b) could be attributed to the large content of small molecular-

weight of G/H (19.9%) than H/G (14.6%). This result suggested that 2 doses of HAM gene in

G/H maize increased the content of small molecular-weight IC, which formed long-chain

double-helical crystallites and were resistant to enzymatic hydrolysis at 95-100°C (Jiang et

al., 2010a).

*3.2. Branch chain-length distributions of amylopectins*

Branch chain-length distributions of amylopectins determined using FACE are shown

in Fig. 3. The branch chain-length profiles of the amylopectins showed bimodal distributions

with the peak chain-lengths at DP 14-15 and DP 46-49 (Fig. 3). Percentage branch-chains of

amyloepctins are summarized in Table 2. Although G/G amylopectin had slightly more short

chains of DP ≤ 12 than other amylopectins, no distinguishable differences between

amylopectins were observed for percentages of branch chains of DP 13-24, DP 25-36, and

DP ≥ 37 (Table 2). Average branch chain-lengths of amylopectins were similar (DP 26.2-

27.1) (Table 2). These results suggested that the HAM gene dosage had little effect on the

branch chain-length of amylopectin of maize *ae*-mutant starch.

*3.3. Branch chain-length distributions of large molecular-weight IC*

Branch chain-length distributions of large molecular-weight IC determined using

FACE are shown in Fig. 4. The branch chain-length profiles of the large molecular-weight IC

also showed bimodal distributions (Fig. 4), similar to that of the amylopectins (Fig. 3). The

large molecular-weight IC had average branch chain-lengths ranging from 27.3-27.9 (Table

3), which were slightly longer than the amylopectin counterparts (26.2-27.1) (Table 2). All

the large molecular-weight IC had similar percentages of branch-chains of DP ≤ 12, DP 13-

24, DP 25-36, and DP ≥ 37 (Table 3). These results suggested that HAM gene dosage also

had little effect on the branch chain-length of the large molecular-weight IC of the *ae*-mutant

maize starch. The similarity of chain length between the large molecular-weight IC and

amylopectin indicated that the large molecular-weight IC had little or no contribution to the

RS formation in maize *ae*-mutant starch.

*3.4. Branch chain-length distributions of small molecular-weight IC*

Branch chain-length distributions of the small molecular-weight IC determined using

FACE are given in Fig. 5. The branch chain-length profiles of the small molecular-weight IC

showed a well-defined peak at chain-length DP 15-17 and a shoulder-like peak for the chain-lengths DP ≥37 (Fig. 5). As the HAM-gene doses increased from 0 to 3, the percentages of branch-chains of DP ≥37 were 31.5, 29.1, 37.2, and 43.7% and the average branch chain-lengths were DP 30.8, 29.1, 32.6, and 35.4 for the H/H, H/G, G/H, and G/G, respectively (Table 4). These results suggested that the increase in HAM gene dosage increased the branch-chain length of the small molecular-weight IC of the maize *ae*-mutant starch. The large proportions of long branch-chains (DP ≥37; table 4) indicated that the small molecular-weight IC could prompt formation of long-chain double-helical crystallites, which could have gelatinization temperatures above 100°C and were resistant to enzymatic hydrolysis at 95-100°C (Jiang et al., 2010a).

### 3.5. Molecular structure of amylose

After amylose was precipitated from the dispersed whole starch using normal-butanol, the purity of amylose was examined using GPC (Fig. 6). The amylose was highly purified as indicated by very small amount of amylopectin (0.2-1.4%, Fig. 6) between fractions 11 and 18 and indicated by the ratio of the blue value to the total carbohydrate.

High-performance size-exclusion chromatograms of amylose, before and after isoamylase-debranching, are shown in Fig. 7. The molecular sizes of amyloses are summarized in Table 5. Although the G/G starch consisted of 63.7% amylose larger than the G/H (54.2%), H/G (55.8%), and H/H (42.1%) starches, all the amyloses showed similar molecular-size distributions with average molecular-sizes of DP 731-817 (Table 5). This result was in agreement with the molecular-sizes of amyloses isolated from high-amylose maize starches reported by Takeda et al. (1989).

Three peaks were observed on the chromatograms of amyloses (Fig. 7), including a minor peak (eluted between 25-32 min) with peak molecular-sizes at DP 16502-17699, one major peak with peak molecular-sizes at DP 1018-1160 and a shoulder-like peak with peak molecular-sizes at DP ~ 472 (Eluted at ~40 min) (Figs. 7A-D). After debranching reaction, the molecular-size distributions of amyloses were shifted (Figs. 7A-D) and the average molecular sizes of debranched amyloses ranged from 417 to 487 (Table 5). These results indicated that some amylose molecules had branched structures, which were in agreement with previous results reported by Takeda et al. (1989). A slight shoulder (Eluted at ~45min, DP ~105) was observed for the debranched G/G amylose (Fig. 7A), but not for G/H, H/G, H/H amylose (Figs. 7B-7D). These results indicated that the HAM gene dosage in the maize *ae*-mutant had little effect on the amylose structure.

**Conclusion**

The increase in HAM gene dosage in the endosperm of *ae*-mutant maize had little effect on the branch chain-length of the amylopectin and large molecular-weight IC, but increased branch chain-length of the small molecular-weight IC and increased contents of amylose and the small molecular-weight IC. Two doses of HAM gene(s) in the endosperm of *ae*-mutant maize increased the content of small molecular-weight IC of the starch, whereas three doses of HAM gene(s) increased amylose content. The HAM gene dosage also had little effect on the structure of amylose of the maize *ae*-mutant starch. The RS content of maize *ae*-mutant starch was mainly contributed by amylose and the small molecular-weight IC.

## References

Baba, T., Arai, Y., 1984. Structural features of amylomaize starch .3. Structural
characterization of amylopectin and intermediate material in amylomaize starch
granules. Agricultural and Biological Chemistry 48, 1763-1775.

Campbell, M., Green, A., Bell, J., Jane, J., Jiang, H., Wu, Y., 2007a. Germplasm
Enhancement of Maize report http://www.public.iastate.edu/~usda-
gem/Public_Reports/Yr_2007/GEMR_07_Campbell.pdf.

Campbell, M.R., Jane, J., Pollak, L., Blanco, M., O'Brien, A., 2007b. Registration of
maize germplasm line GEMS-0067. Journal of Plant Registrations 1, 60-61.

Dubois, M., Gilles, K.A., Hamilton, J.K., Rebers, P.A., Smith, F., 1956. Colorimetric
method for determination of sugars and related substances. Analytical Chemistry 28,
350-6.

French, D., 1984. Organization of starch granules. In: Whistler, R.L., Bemiller, J.N.,
Paschall, E.F. (Eds.), Starch: Chemistry and Technology. Academic Press, New York,
pp. 183-247.

Guan, H.P., Preiss, J., 1993. Differentiation of the properties of the branching isoenzymes
from maize (Zea mays). Plant Physiology 102, 1269-73.

Hizukuri, S., Takeda, Y., Yasuda, M., Suzuki, A., 1981. Multibranched nature of amylose
and the action of debranching enzymes. Carbohydrate Research 94, 205-13.

James, M.G., Denyer, K., Myers, A.M., 2003. Starch synthesis in the cereal endosperm.
Current Opinion in Plant Biology 6, 215-222.

Jane, J., Chen, Y.Y., Lee, L.F., McPherson, A.E., Wong, K.S., Radosavljevic, M.,
Kasemsuwan, T., 1999. Effects of amylopectin branch chain length and amylose content on

the gelatinization and pasting properties of starch. Cereal Chemistry 76, 629-637.

Jiang, H., Campbell, M., Blanco, M., Jane, J., 2010a. Characterization of maize amylose-extender (*ae*) mutant starches. Part II: Structures and properties of starch residues remaining after enzymatic hydrolysis at boiling-water temperature. Carbohydrate Polymers 80, 1-12.

Jiang, H., Jane, J., Acevedo, D., Green, A., Shinn, G., Schrenker, D., Srichuwong, S., Campbell, M., Wu, Y., 2010b. Variations in starch physicochemical properties from a generation-means analysis study using amylomaize V and VII parents. Journal of Agricultural and Food Chemistry, Submitted.

Jiang, H., Srichuwong, S., Campbell, M., Jane, J., 2010c. Characterization of maize amylose-extender (*ae*) mutant starches. Part III: Structures and properties of the Naegeli dextrins. Carbohydrate Polymers, Submitted.

Juliano, B.O., 1971. Asimplified assay for milled-rice amylose. Cereal Science Today 16, 334-340.

Kasemsuwan, T., Jane, J., Schnable, P., Stinard, P., Robertson, D., 1995. Characterization of the dominant mutant amylose-extender (Ae1-5180) maize starch. Cereal Chemistry 72, 457-64.

Klucinec, J.D., Thompson, D.B., 1998. Fractionation of high-amylose maize starches by differential alcohol precipitation and chromatography of the fractions. Cereal Chemistry 75, 887-896.

Li, L., Jiang, H., Campbell, M., Blanco, M., Jane, J., 2008. Characterization of maize amylose-extender (*ae*) mutant starches: Part I. Relationship between resistant starch contents and molecular structures. Carbohydrate Polymers 74, 396-404.

Morell, M.K., Myers, A.M., 2005. Towards the rational design of cereal starches. Current opinion in plant biology 8, 204-10.

Robyt, J.F., 1998. Essentials of Carbohydrate Chemistry. Springer-Verlag, New York.

Schoch, T.J., 1942. Fractionation of starch by selective precipitation with butanol. Journal of the American Chemical Society 64, 2957-61.

Shi, Y.-C., Seib, P.A., 1995. Fine structure of maize starches from four wx-containing genotypes of the W64A inbred line in relation to gelatinization and retrogradation. Carbohydrate Polymers 26, 141-7.

Smith, A.M., 2001. The Biosynthesis of Starch Granules. Biomacromolecules 2, 335-341.

Takeda, C., Takeda, Y., Hizukuri, S., 1989. Structure of Amylomaize Amylose. Cereal Chemistry 66, 22-25.

Takeda, Y., Shitaozono, T., Hizukuri, S., 1988. Molecular-Structure of Corn Starch. Starch-Starke 40, 51-54.

Wang, Y.J., White, P., Pollak, L., Jane, J., 1993. Amylopectin and intermediate materials in starches from mutant genotypes of the Oh43 inbred line. Cereal Chemistry 70, 521-5.

Wu, Y., Campbell, M., Yen, Y., Wicks, Z., III, Ibrahim, A.M.H., 2009. Genetic analysis of high amylose content in maize (*Zea mays L.*) using a triploid endosperm model. Euphytica 166, 155-164.

Yuan, R.C., Thompson, D.B., Boyer, C.D., 1993. Fine structure of amylopectin in relation to gelatinization and retrogradation behavior of maize starches from three wx-containing genotypes in two inbred lines. Cereal Chemistry 70, 81-9.

**Table 1** Amylopectin, amylose, and intermediate component (IC) contents of starches isolated from kernels of self- and inter-crossed lines of GEMS-0067 (G) and H99*ae* (H)

| Sample | Amylopectin[a] (%) | Amylose (%) | IC | |
|---|---|---|---|---|
| | | | Large[b] (%) | Small[b] (%) |
| G/G | $11.8 \pm 1.5$ | $63.7 \pm 1.8$ | $7.8 \pm 0.6$ | $16.8 \pm 1.2$ |
| G/H | $18.3 \pm 1.6$ | $54.2 \pm 0.6$ | $7.5 \pm 1.2$ | $19.9 \pm 1.9$ |
| H/G | $22.1 \pm 0.8$ | $55.8 \pm 0.6$ | $7.5 \pm 0.0$ | $14.6 \pm 0.6$ |
| H/H | $31.1 \pm 1.6$ | $42.1 \pm 1.9$ | $14.9 \pm 1.4$ | $11.8 \pm 0.5$ |

[a] Amylopectin, amylose, and IC contents were determined using 1-butanol precipitation method and Sepharose Cl-2B gel-permeation chromatography followed by total carbohydrate determination.

[b] Large molecular-weight IC molecules were in fractions 19 to 30 (see Fig. 2); Small molecular-weight IC molecules were in fractions 31 to 45 (see Fig. 2).

**Table 2** Molar-based branch-chain-length distributions of amylopectins separated from starches of self- and inter-crossed lines of GEMS-0067 (G) and H99*ae* (H)[a, b]

| Sample | Average CL[c] (DP) | DP≤12 (%) | DP13-24 (%) | DP25-36 (%) | DP≥37 (%) |
|---|---|---|---|---|---|
| G/G | 26.2 | 16.2 ± 0.0 | 46.3 ± 0.5 | 13.5 ± 0.5 | 23.9 ± 1.1 |
| G/H | 26.3 | 13.6 ± 0.5 | 48.3 ± 0.5 | 14.7 ± 0.7 | 23.4 ± 0.3 |
| H/G | 26.9 | 13.7 ± 0.0 | 46.9 ± 0.3 | 14.7 ± 0.5 | 24.7 ± 0.9 |
| H/H | 27.1 | 13.2 ± 0.1 | 47.0 ± 0.7 | 14.9 ± 0.2 | 25.0 ± 1.0 |

[a] Branch chain-length distribution of amylopectin was determined using a fluorophore-assisted capillary-electrophoresis.

[b] The amylopectin was collected from GPC fractions 11-18 (see Fig. 2).

[c] CL = chain length; DP = degree of polymerization.

**Table 3** Molar-based branch-chain-length distributions of the large molecular-weight IC separated from starches of self- and inter-crossed lines of GEMS-0067 (G) and H99*ae* (H)[a, b]

| Sample | Average CL[c] (DP) | DP≤12 (%) | DP13-24 (%) | DP25-36 (%) | DP≥37 (%) |
|--------|--------------------|-----------|-------------|-------------|-----------|
| G/G | 27.6 | 12.0 ± 0.0 | 45.3 ± 0.1 | 17.8 ± 0.3 | 24.9 ± 0.2 |
| G/H | 27.3 | 12.3 ± 0.2 | 46.7 ± 1.0 | 16.3 ± 1.1 | 24.7 ± 0.1 |
| H/G | 27.9 | 11.4 ± 0.1 | 45.3 ± 0.2 | 17.6 ± 0.2 | 25.7 ± 0.6 |
| H/H | 27.6 | 11.2 ± 0.1 | 45.7 ± 0.1 | 17.4 ± 0.6 | 25.7 ± 0.8 |

[a] Branch chain-length distribution of the large molecular-weight IC was determined a fluorophore-assisted capillary-electrophoresis.

[b] The large molecular-weight IC was collected from GPC fractions 19-30 (see Fig. 2).

[c] CL = chain length; DP = degree of polymerization.

**Table 4** Molar-based branch-chain-length distributions of the small molecular-weight IC separated from starches of self- and inter-crossed lines of GEMS-0067 (G) and H99*ae* (H)[a, b]

| Sample | Average CL[c] (DP) | DP≤12 (%) | DP13-24 (%) | DP25-36 (%) | DP≥37 (%) |
|--------|--------------------|-----------|-------------|-------------|-----------|
| G/G | 35.4 | $7.2 \pm 0.3$ | $28.2 \pm 0.2$ | $20.8 \pm 0.1$ | $43.7 \pm 0.3$ |
| G/H | 32.6 | $7.1 \pm 1.0$ | $33.6 \pm 0.6$ | $22.1 \pm 0.1$ | $37.2 \pm 0.3$ |
| H/G | 29.1 | $10.3 \pm 0.1$ | $41.2 \pm 0.4$ | $20.3 \pm 0.2$ | $29.1 \pm 0.1$ |
| H/H | 30.8 | $7.1 \pm 0.3$ | $38.5 \pm 0.0$ | $23.0 \pm 0.0$ | $31.5 \pm 0.3$ |

[a] The branch chain-length distribution of the small molecular-weight IC was determined a fluorophore-assisted capillary-electrophoresis.

[b] The small molecular-weight IC was collected from GPC fractions 31-45 (see Fig. 2).

[c] CL = chain length; DP = degree of polymerization.

**Table 5** Average molecular-weights of amyloses separated from starches of self- and inter-crossed lines of GEMS-0067 (G) and H99*ae* (H)

| Sample | Before debranching (DP[a]) | After debranching (DP) |
|--------|---------------------------|------------------------|
| G/G | $817 \pm 0$ | $452 \pm 1$ |
| G/H | $731 \pm 8$ | $445 \pm 10$ |
| H/G | $795 \pm 1$ | $487 \pm 7$ |
| H/H | $756 \pm 2$ | $417 \pm 1$ |

[a] DP = degree of polymerization
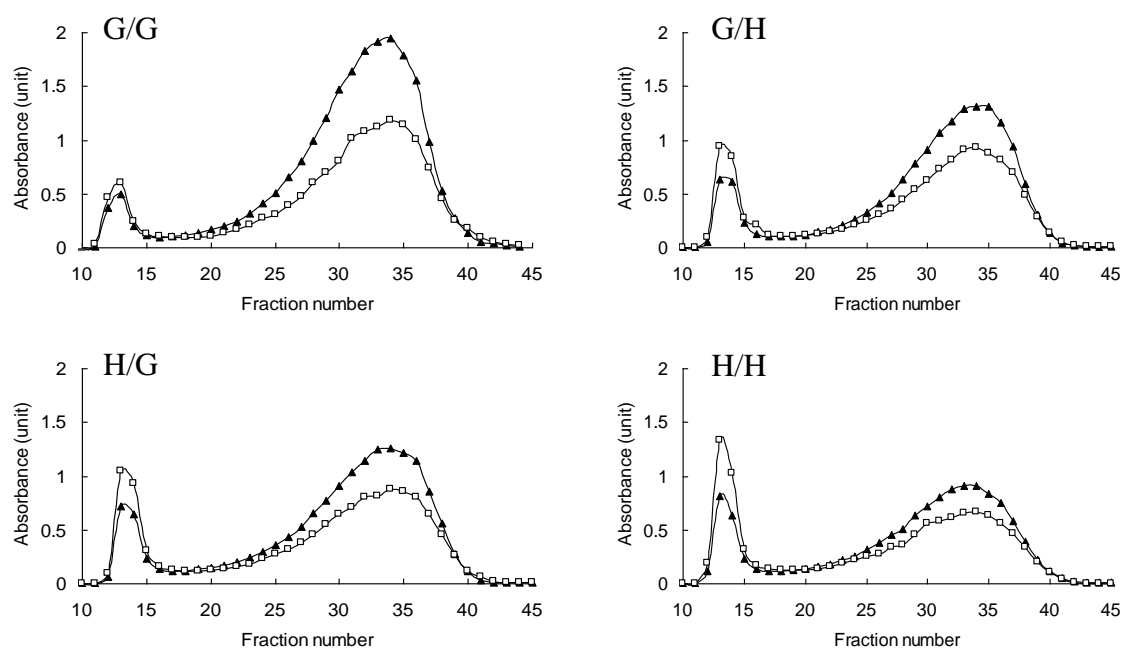
**Fig. 1.** Sepharose CL-2B gel-permeation profiles of the whole starches isolated from kernels of self- and inter-crossed lines of GEMS-0067 (G) and H99*ae* (H). ▲, blue value; ▫, total carbohydrate.
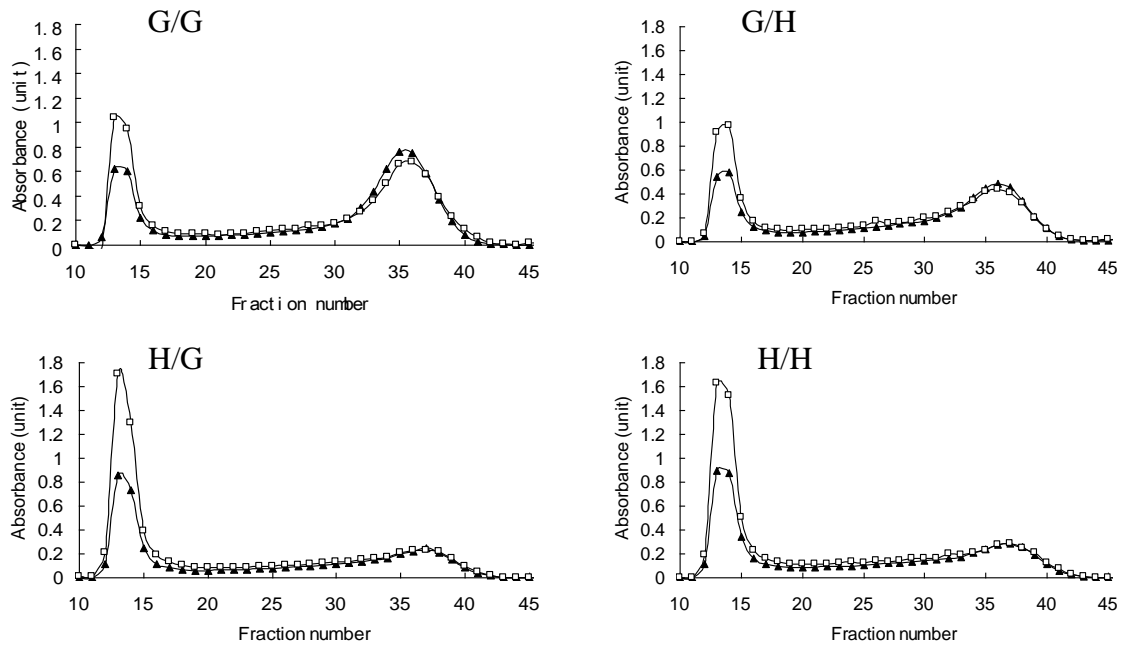
**Fig. 2.** Sepharose CL-2B gel-permeation profiles of amylopectin/IC mixtures separated from starches of self- and inter-crossed lines of GEMS-0067 (G) and H99*ae* (H). ▲, blue value; □, total carbohydrate.
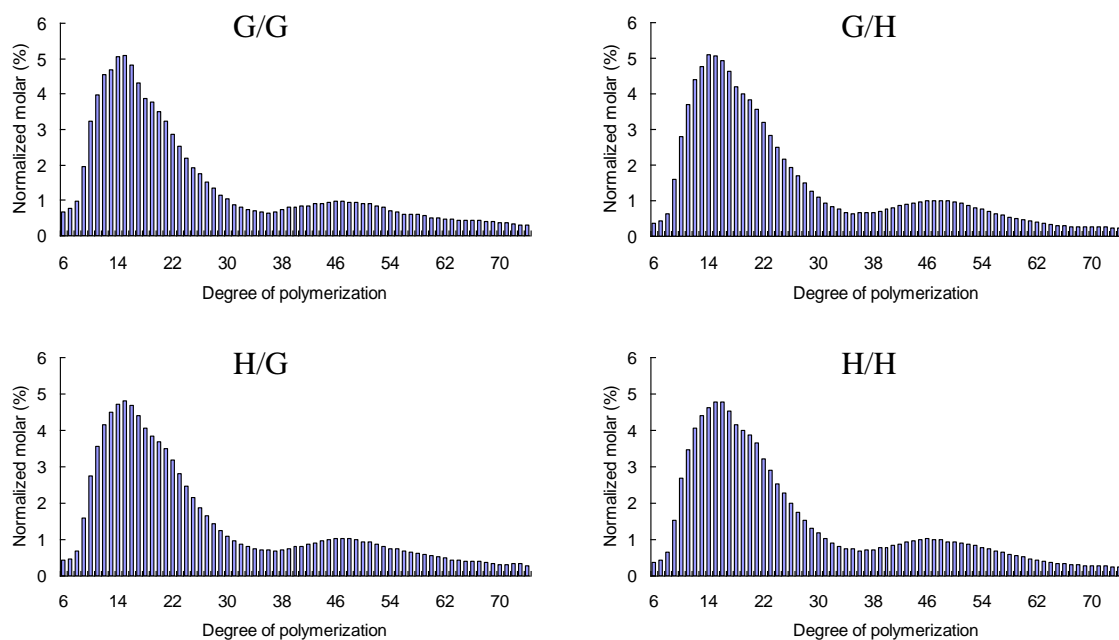
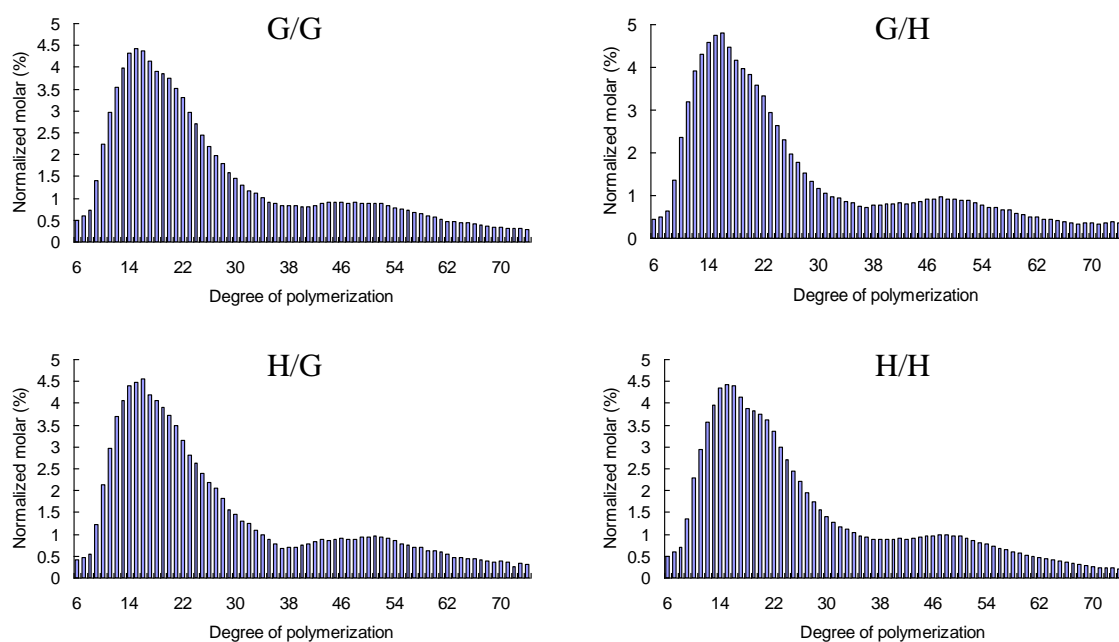**Fig. 3.** Branch chain-length distributions of amylopectins separated from starches of self- and inter-crossed lines of GEMS-0067 (G) and H99*ae* (H). A fluorophore-assisted capillary-electrophoresis was used for the analysis. The amylopectin was collected from GPC fractions 11-18 (see Fig. 2).

**Fig. 4.** Branch chain-length distributions of the large molecular-weight IC separated from starches of self- and inter-crossed lines of GEMS-0067 (G) and H99*ae* (H). A fluorophore-assisted capillary-electrophoresis was used for the analysis. The large molecular-weight IC was collected from GPC fractions19-30 (see Fig. 2).
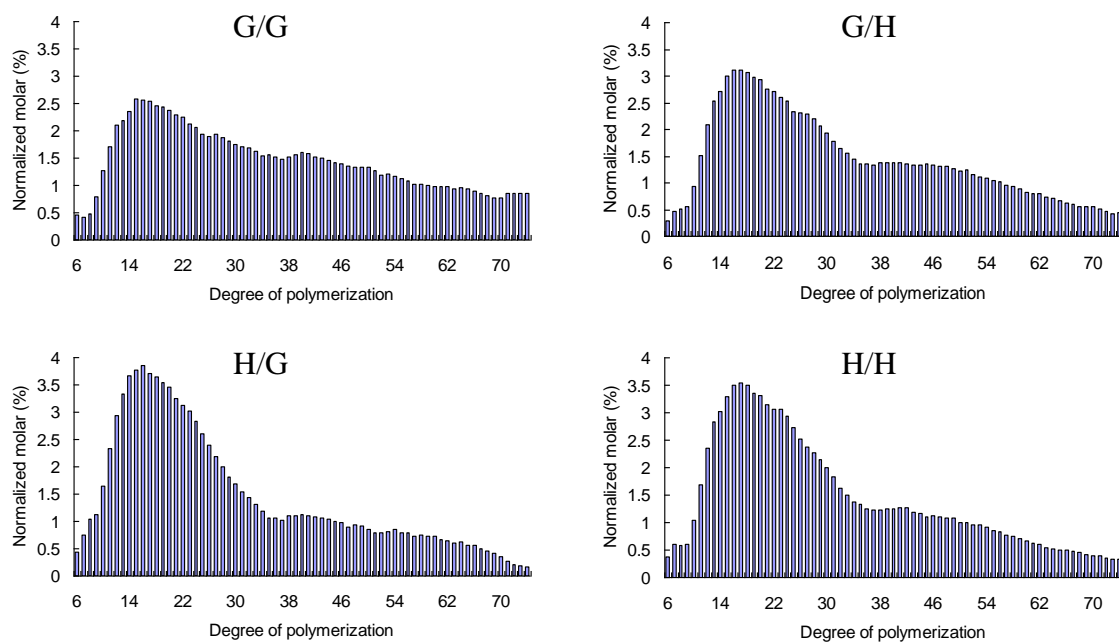
**Fig. 5.** Branch chain-length distributions of the small molecular-weight IC separated from starches of self- and inter-crossed lines of GEMS-0067 (G) and H99*ae* (H). A fluorophore-assisted capillary-electrophoresis was used for the analysis. The small molecular-weight IC was collected from GPC fractions 31-45 (see Fig. 2).
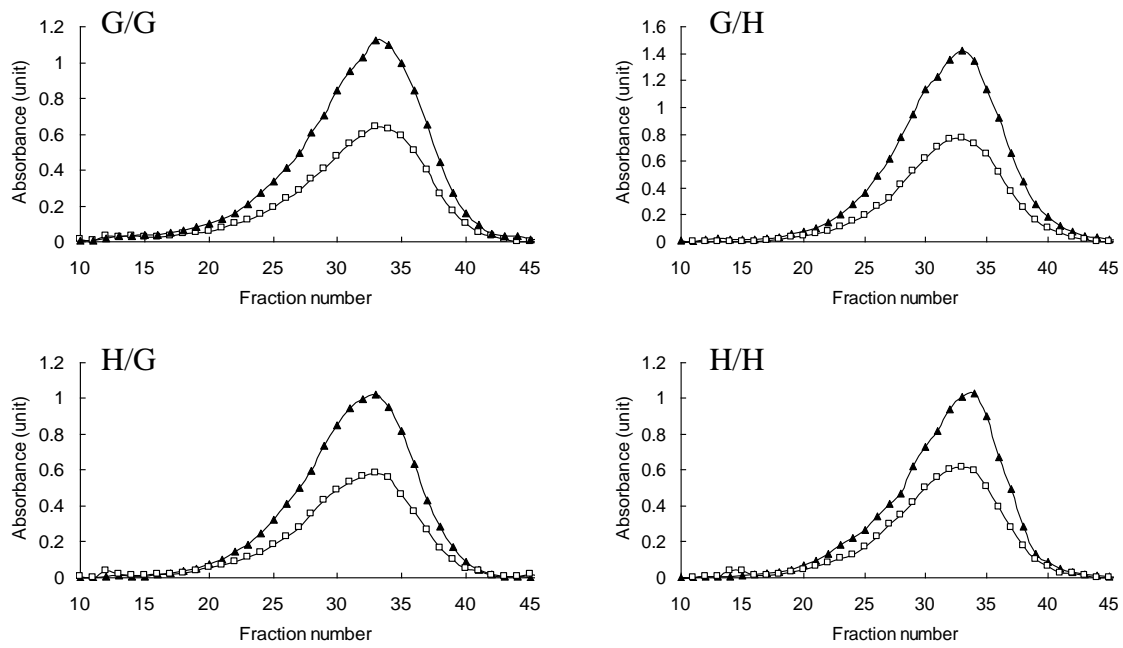
**Fig. 6.** Sepharose CL-2B gel-permeation profiles of amyloses separated from starches of self- and inter-crossed lines of GEMS-0067 (G) and H99*ae* (H). ──▲──, blue value; ──□──, total carbohydrate.
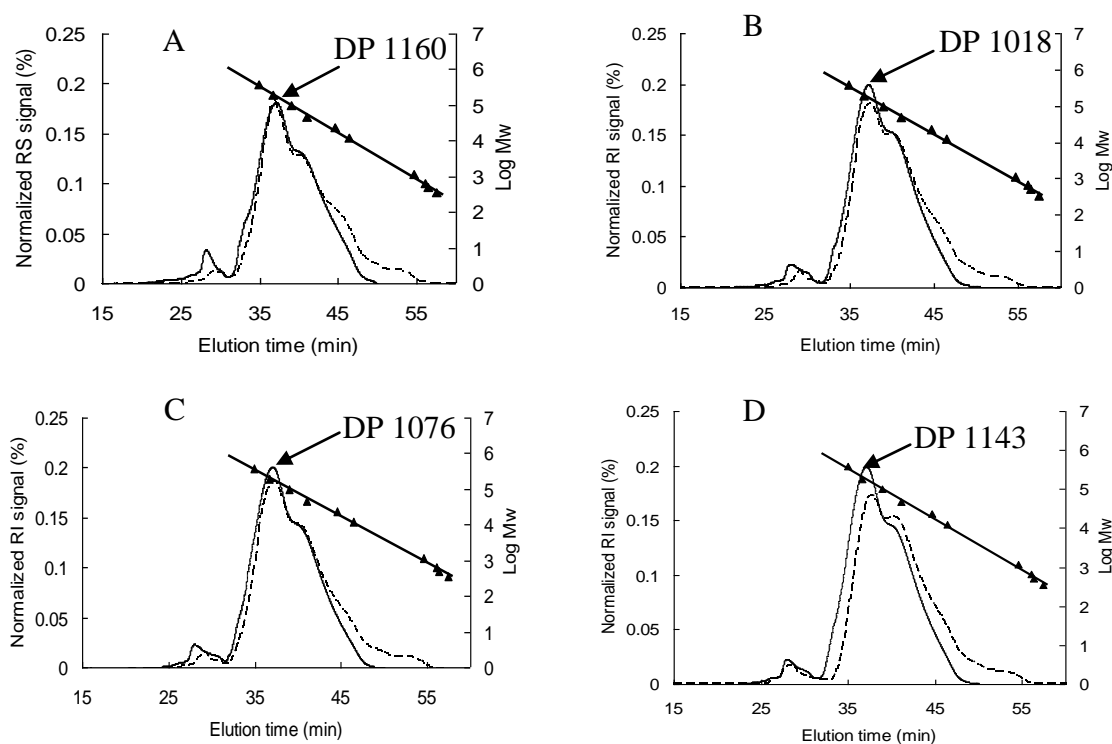
**Fig. 7.** Molecular-weight distributions of amyloses separated from starches of self- and inter-crossed lines of GEMS-0067 (G) and H99*ae* (H). The separation was conducted using Shodex SB-804 and SB-803 analytical columns (Showa Denko K.K., Tokyo, Japan). A, G/G; B, G/H; C, H/G; and D, H/H. Solid line, before isoamylase-debranching; dashed line, after isoamylase-debranching; and linear line, a standard curve with molecular sizes of DP 2, 3, 4, 7, 75, 141, 292, 617, 1148, and 2346.

## GENERAL CONCLUSIONS

The elongated starch granules and the outer layer of the spherical starch granules were more resistant to enzymatic hydrolysis at 95-100°C and remained in the RS residues. The RS residues displayed the B-type polymorph and had gelatinization temperatures above 100°C. The RS residues consisted of two major components: large molecules (average DP 840-951) of mostly partially-preserved amylose and IC molecules, and small molecules (average DP 59-74) of mostly linear chains resulting from enzymatic hydrolysis of semi-crystalline amylose, IC, and amylopectin molecules at 95-100°C. The RS residues were mainly attributed to the long-chain double-helical crystallites of amylose/IC molecules present in the native maize *ae*-mutant starches, which had gelatinization-temperatures above 100°C. The long-chain double helical crystallites retained the semi-crystalline structures at 95-100°C and were resistant to the enzymatic hydrolysis. Lipids present in the granule also protected starch from enzymatic hydrolysis at 95-100°C.

Naegeli dextrins of the maize *ae*-mutant starches displayed the B-type polymorph and had highly crystalline structures of double helices. The Naegeli dextrins consisted of essentially linear molecules and showed unimodal molecular-size distributions with the peak molecular-size at DP 16. The average chain-lengths of the double helices of the Naegeli dextrins were between DP 23.8 and 27.5, much longer than normal and *ae-waxy* starch counterparts. The Naegeli dextrins displayed similar gelatinization-temperatures of 45.1-51.4$^{\circ}$C, 113.9-122.2$^{\circ}$C, and 148.0-160.0$^{\circ}$C for $T_o$, $T_p$, and $T_c$, respectively. These results supported the presence of amylose double-helical crystallites in the native maize *ae*-mutant starches, which were resistant to enzymatic hydrolysis at 95-100°C.

The RS content of the GEMS-0067 starch increased with kernel maturation and the increase in amylose/IC content of the starch. The increase in the amylose/IC content during kernel development led to the formation of the long-chain double-helical crystallites and resulted in the increase in the RS content of the starch. The increase in the lipid content of the GEMS-0067 starch also reduced enzyme digestibility of the starch. The elongated starch granules of GEMS-0067 were formed through fusion of small granules in the amyloplast during the granule development.

An increase of HAM gene-dosage in maize *ae*-mutant resulted in higher amylose/IC content of the starch and significantly affected the molecular organization in the granule, granule morphology, starch crystallinity, and starch thermal properties. Two doses of HAM gene or more in maize *ae*-mutant substantially increased the RS content of the starch, whereas one dose of HAM gene had little effect on the RS content. The increase in HAM gene dosage in the endosperm of *ae*-mutant maize had little effect on the branch chain-length of the amylopectin and large molecular-weight IC, but increased branch chain-length of the small molecular-weight IC. The HAM gene dosage also had little effect on the structure of amylose of the maize *ae*-mutant starch. The RS content of maize *ae*-mutant starch was mainly contributed by amylose and the small molecular-weight IC.

## ACKNOWLEDGEMENTS

First and foremost, I would like to express my deepest gratitude to my major professor, Dr. Jay-lin Jane, for his academic advice, affectionate encouragement, extreme patience and tireless effort throughout my research and preparation of this dissertation.

I would also like to thank my committee members Dr. Michael Blanco, Dr. Buddhi Lamsal, Dr. Paul Scott, and Dr. Tong Wang for their valuable advice, precious guidance, and constant help. Your kindness and contribution will be forever remembered.

Many thanks go to USDA-ARS Germplasm Enhancement of Maize Project for the financial support of this research, Dr. Mark Campbell for sending me the interesting maize samples, Dr. Harry T. Horner, Tracey M. Pepper, Mr. Randall Den Adel of the Microscopy and NanoImaging Facility for helping with the light, scanning electron, transmission electron microscopy studies, Dr. P. White for partially being my POS committee member, Ms. Margie Carter for the assistance with confocal laser scanning microscopy, Dr. Schlorholtz for his help on X-ray analysis, Dr. Kan Wang for the use of speed vacuum.

Heartfelt thanks are due to lab members Yongfeng Ai, Dr. Shuangkui Du, Mr. Vicente Espinosa, Dr. Jovin Hasjim, Dr. Qiang Huang, Dr. Janusz Kapusniak, Dr. Li Li, Dr. Amy Lin, Jelena Medic, Dr. Bruce Min, Dr. Jin Hee Park, Dr. Jongtae Park, Stephen Setiawan, Dr. Sathaporn Srichuwong, Dr. Kook Wongsagonsup, Dr. Qinjie Sun, Dr. Thais, Mr. Julian de la Rosa for their help and enthusiasm on the research and discussion. I am grateful to the faculty, staff, my colleagues in the Department of Food Science and Human Nutrition.

Finally, special acknowledgments go to my parents, parents-in-law, brothers and sisters, relatives, and friends for their unconditional love and everlasting support. Last but not

the least, my sincere thanks and appreciations go to my dear wife, Yaping Feng, and My

kids, Alan and Alice Jiang, for their contributions and understanding to the author.